MAMESTRA CONFIGURATA NUCLEOPOLYHEDROVIRUS (MacoNPV): POTENTIAL CHITIN-BINDING PROTEINS AND THEIR ROLE IN ORAL INFECTIVITY

A thesis submitted to the College of
Graduate Studies and Research
in partial fulfillment of the requirements
for the degree of Master of Science
in the Department of Biology
University of Saskatchewan
Saskatoon

By
Amy Lynn Noakes

PERMISSION TO USE

In presenting this thesis/dissertation in partial fulfillment of the requirements for a Postgraduate degree from the University of Saskatchewan, I agree that the Libraries of this University may make it freely available for inspection. I further agree that permission for copying of this thesis/dissertation in any manner, in whole or in part, for scholarly purposes may be granted by the professor or professors who supervised my thesis/dissertation work or, in their absence, by the Head of the Department or the Dean of the College in which my thesis work was done. It is understood that any copying or publication or use of this thesis/dissertation or parts thereof for financial gain shall not be allowed without my written permission. It is also understood that due recognition shall be given to me and to the University of Saskatchewan in any scholarly use which may be made of any material in my thesis/dissertation.

DISCLAIMER

Reference in this thesis/dissertation to any specific commercial products, process, or service by trade name, trademark, manufacturer, or otherwise, does not constitute or imply its endorsement, recommendation, or favouring by the University of Saskatchewan. The views and opinions of the author expressed herein do not state or reflect those of the University of Saskatchewan, and shall not be used for advertising or product endorsement purposes.

Requests for permission to copy or to make other uses of materials in this thesis/dissertation in whole or part should be addressed to:

Head of the Department of Biology
University of Saskatchewan
112 Science Place
Saskatoon, Saskatchewan S7N 5E2
Canada

OR

Dean
College of Graduate Studies and Research
University of Saskatchewan
107 Administration Place
Saskatoon, Saskatchewan S7N 5A2
Canada

ABSTRACT

The bertha armyworm (*Mamestra configurata*) is a major pest of canola and other oilseed crops. A promising control agent for this species is the baculovirus *Mamestra configurata nucleopolyhedrovirus* (MacoNPV). Baculoviruses are insect-specific viruses. Infections initiate in the host midgut following ingestion of virus particles called occlusion bodies. For a productive infection to occur, the occlusion bodies must dissolve to release the infectious occlusion-derived virions. These virions must pass through the peritrophic matrix, a protein-chitin meshwork that lines the midgut of most insects and provides protection against abrasion and pathogen invasion. The mechanism by which the baculovirus virions transit the peritrophic matrix is unknown. Following the initial infection of midgut cells, a second virion phenotype, the budded virus, is released from infected cells and establishes a systemic infection within the insect.

The 11K group of genes, which are conserved among baculovirus species and other insect-infecting viruses, encode proteins with a predicted chitin-binding domain. The degree of conservation of these genes among insect-infecting viruses suggests that they may play a role in insect infectivity. It is possible that the gene products could be involved in an interaction between the baculovirus occlusion-derived virions and the peritrophic matrix or the chitin-secreting cells of the midgut epithelium, and therefore may be involved in initial oral infectivity.

The two 11K genes from MacoNPV (ORF 118 and ORF 164), and their homologues in a second species of baculovirus, *Autographa californica multiple nucleopolyhedrovirus* (AcMNPV [ORF145 and ORF150]) were expressed in a baculovirus expression system. The ability of the proteins, Maco118, Maco164, Ac145, and Ac150, to bind to chitin was assessed *in vitro* using chitin-coated beads. Each of the four proteins binds to chitin, and hydrophobic interactions mediate the binding. Other binding mechanisms are likely involved, but were not determined in this project.

To determine the function of these proteins, a series of gene knockout and repair constructs was produced for AcMNPV ORF 145 and ORF 150 using an established bacmid system. An analysis of the knockout and repair constructs using quantitative real-time polymerase chain reaction showed that deletion of either ORF 145 or ORF 150 had no effect on the rate of budded virus production or viral DNA replication. Oral and injection bioassays were performed in *Trichoplusia ni* larvae to determine if there were differences in infectivity between the knockout,

repair, and wild type constructs. Injection assays, in which budded virus from each construct was injected directly into the insect haemocoel, therefore bypassing the midgut and peritrophic matrix, indicated that there was no statistical difference in infectivity between the knockout, repair, and wild type constructs at a dose of 15 $TCID_{50}$ U per larva. Oral bioassays, in which larvae were fed occlusion bodies from each virus construct, indicated that there was no statistical difference in mortality rates between the knockout, repair, and wild type constructs.

The results from this study indicate that although the baculovirus 11K genes are highly conserved among baculovirus species, and the 11K gene products from MacoNPV and AcMNPV interact with chitin, they are not required for oral infectivity in *T. ni* larvae, and likely serve another function in the baculovirus infection cycle.

ACKNOWLEDGEMENTS

I would first like to thank my supervisor, Dr. Martin Erlandson for his support during my time as a student in his lab. I greatly appreciate the patience, guidance, and encouragement you have given me over the past few years. It has truly been a pleasure working with you Martin.

I would also like to thank my committee members, Drs. Cedric Gillott and Dwayne Hegedus for their thoughtful questions and comments both on my research progress and during the preparation of this thesis. I would also like to extend my gratitude to Dr. Janet Hill for serving as external examiner for my thesis defence.

I am grateful to my collaborators at AAFC (Summerland, BC), Dr. David Theilmann and Les Willis for their help in the design and creation of the knockout constructs, as well as for providing many of the cell lines and plasmids required for the production of the knockouts.

I would like to thank all of my lab mates, current and former, especially Dr. Ruwandi Andrahennadi for her assistance with insect rearing and Doug Baldwin, Stephanie Harris, and Diney Bekkaoui for their assistance with northern blots. I would also like to thank Jennifer Holowachuk, Edyta Sieminska, Leora Lee, and Brynn Mistafa for their help setting up bioassays. Thank you to Cathy Coutu for her assistance with protein modelling and to Larry Grenko and Larry Mann for their help with statistical analysis of the bioassay data. Thank you to Edyta Sieminska for providing the MsOSP-HA-tagged protein and for performing the MsOSP chitin-binding assays.

I would not have been able to complete this research without the help of generous funding sources. Thank you to the Entomological Society of Saskatchewan for the Arthur R. Brooks Scholarship; to the University of Saskatchewan for the Harvey Graduate Scholarship, the R. Jan F. Smith Memorial Scholarship, and the College of Graduate Studies and Research travel award; and to Agriculture and Agri-Food Canada for their financial assistance through the Research Affiliate Program.

To the faculty, staff and students in the Department of Biology at the U of S, thank you for all of your help and friendship during my time in Saskatoon. You have made my time in Saskatoon very enjoyable.

Finally, I would like to thank my parents, Don and Olga, my sister Megan, and my partner Paul for all of their support, not only during my time at the University of Saskatchewan, but throughout my life. Love you all, and thank you.

TABLE OF CONTENTS

LIST OF FIGURES

LIST OF TABLES

LIST OF ABBREVIATIONS

AAFC……Agriculture and Agri-Food Canada

AcMNPV…….. *Autographa californica multiple nucleopolyhedrovirus*

Amp……..…Ampicillin

ANCOVA……..……Analysis of covariance

ANOVA……Analysis of variance

β-ME……..β-mercaptoethanol (2-mercaptoethanol)

BSA……...Bovine serum albumin

BV…….……Budded virus

CAT…….**....**Chloramphenicol acetyltransferase

CBD……..…….Chitin-binding domain

Chl…….**...**……...Chloramphenicol

CIP……..Calf intestinal phosphatase

c-MYC…….Epitope tag derived from the myc family of transcription factors

cv……..…Cultivar

DE……...…Delayed early gene

DEPC……. Diethylpyrocarbonate

DMSO…….Dimethyl sulfoxide

DTT**…**……..Dithiothreitol

EDTA……. Ethylenediaminetetraacetic acid

EFP…….….Envelope fusion protein

FBS……....Foetal bovine serum

Freq pat……PROSITE patterns frequent match producers database

Gen.……Gentamycin

GFP……...Green fluorescent protein

GIM……..Grace's Insect Medium

GlcNAc……..β–(1,4)-N-acetyl-D-glucosamine

GOI……...Gene of interest

GSP……...Gene specific primer

GV…….Granulovirus

HA…….…… Human influenza hemagglutinin epitope tag

HearNPV…….. *Helicoverpa armigera single nucleocapsid nucleopolyhedrovirus*

HF……..High fidelity

hpi……...…..Hours post-infection

hr…..……..……..….Homologous regions

HRP……..Horseradish peroxidase

IE……....Immediate early gene

INR……...Initiation motif

IPM……...Integrated pest management

IPS……Insect production services

IPTG……Isopropyl β-D-1-thiogalactopyranoside

Kan..……Kanamycin

LB……..Luria-Bertani media

LEF……..…...Late expression factor

LSD……....Least significant difference

MacoNPV……...*Mamestra configurata nucleopolyhedrovirus*

MOI…….Multiplicity of infection

MNPV……..Multiple nucleopolyhedrovirus

NCBI……..……National Centre for Biotechnology Information

NPV……Nucleopolyhedrovirus

OB…….……Occlusion body

ODV…….…...Occlusion-derived virus

ORF……..……..Open reading frame

ORI……..……..Origin of replication

P1 (P2, P3)……..Serial passages of budded virus or occlusion body stocks

PAGE…….....Polyacrylamide gel electrophoresis

PBI……..National Research Council Plant Biotechnology Institute

PBS…….…..Phosphate buffered saline

PBS-T……...Phosphate buffered saline with 0.05% Tween-20

Pfam……...Protein families database

Pfam Fs……...Protein families hidden Markov models local models database

Pfam Is……...…….Protein families hidden Markov models global models database

PIF……...…..*Per oral/per os* infectivity factor

PM…….……Peritrophic matrix

Polh……...Polyhedrin

prf……...PROSITE profiles database

PROC GLM……...…….General linear model procedure

qPCR……...Quantitative polymerase chain reaction

RACE…….Rapid amplification of cDNA ends

Rep……..Replicate

RT……...…..Room temperature

RT-PCR……....Reverse transcriptase polymerase chain reaction

SDS…….…….Sodium dodecyl sulfate

Sf9……..*Spodoptera frugiperda* cell line derived from parental strain IPLB-SF21 AE2

SNPV……...Single nucleopolyhedrovirus

SpliNPV…….. *Spodoptera littoralis nucleopolyhedrovirus*

SOC……..Super optimal broth with catabolite repression

SSC……...…….....Saline-sodium citrate

TAE……..Tris acetate ethylenediaminetetraacetic acid

TAP……...Tobacco acid pyrophosphatase

$TCID_{50}$……..…..Tissue culture infectious dose 50%

TE……..Tris/ethylenediaminetetraacetic acid buffer

Tet……..Tetracycline

TMH……....Transmembrane helix

TnHi5…….**...**Cell line derived from *Trichoplusia ni* ovarian tissue, parental strain BTI-TN-5B1-4

UTR……...……..Un-translated Region

WGA…….Wheat-germ agglutinin

wt……**...**…….……Wild type

X-Gal……..5-bromo-4-chloro-indolyl-β-D-galactopyranoside

YENB…….……Yeast extract nutrient broth media

Zeo……..Zeocin

1. GENERAL INTRODUCTION

1.1. Importance of the Canadian agriculture industry

The agriculture industry accounts for approximately 8% of the Canadian gross domestic product and employs approximately two million people (1). Canada is both a major importer and exporter of agricultural products, with annual imports and exports reaching $20.4 billion and $26.5 billion respectively (1). Grains, oilseeds, and grain and oilseed products account for roughly a third of Canada's agricultural exports, or approximately $8.8 billion annually (1). Oilseed crops are grown for the oil produced within their seeds (2, 3). Oilseed crops such as canola (*Brassica napus*), flax (*Linum usitatissimum*), and mustard (*Brassica juncea*), are grown on the Canadian prairies in the provinces of Alberta, Manitoba, and in particular, Saskatchewan (3). Because these crops, especially canola, have such a large impact on Canadian agriculture and the Canadian economy, a significant amount of research has focused on how to maximize production, in particular mitigating crop losses due to insect pests.

1.2. Influence of insects on the agriculture industry

Insects have several impacts on the agriculture industry (4, 5). Some species pollinate crops, while other species enhance decomposition and nutrient cycling in the soil (4-6). Predatory or parasitic insects provide arthropod pest control (4-6). A recent study estimated that the annual economic value of insect services is $57 billion (US) (4). However, in spite of these benefits, insects also cause substantial damage to and fouling of agricultural crops, forest products, and manufactured and stored goods (5, 7). Annually, nearly 3 million tons of pesticides, worth an estimated $40 billion (US), are applied to commercial crops worldwide to reduce these losses (7).

1.3. Pest management strategies

Traditionally, chemical pesticides have been used to control pest populations (7, 8). Although chemical pesticides are convenient to use, they have several limitations. They are costly to develop and apply, and the length of time that they are effective is often quite short due to the development of resistance in the target species (7, 9). Furthermore, chemical pesticides can have a large impact on the environment. Pesticides can enter water supplies, and humans, wild and domesticated animals incur health problems by consuming tainted foodstuffs (7, 9-12). Recently,

there has been much concern about these issues, which has spurred demand for the development of more environmentally benign control strategies.

A current trend in pest management is the adoption of more comprehensive approaches, such as integrated pest management (IPM). IPM systems rely on the concurrent use of multiple control strategies including habitat management, crop rotation, resistant crop varieties, chemical insecticides, and biological control agents (13). By reducing reliance on chemical insecticides and by targeting multiple physiological pathways in the pest, IPM systems reduce the likelihood of the development of resistance to a control agent (13, 14). The decreased dependence on chemical insecticides also reduces the environmental impact of insect control (13, 14). Biological control is an especially promising component of IPM as the agents are typically highly specific to target insects, thus having low or no toxicity to humans and non-target species (15).

1.4. Biological control agents

Biological control agents are naturally occurring "enemies" of a particular insect species (8). Biological control agents encompass a broad spectrum of organisms including parasitic and predatory insects, bacteria, fungi, nematodes, protozoa, and viruses, as well as natural products produced by these organisms (16). The goal of biological control is to produce and apply these natural antagonists to reduce the population of a pest species to a level at which the pest no longer causes significant economic damage (8). Ideally, biological control agents should be cost effective, with low environmental and non-target species impact, and should preferably be self-sustaining in the environment (14).

For a microbial biological control agent to be registered, it needs to undergo rigorous testing to demonstrate its efficacy against the target species and its safety for use near non-target organisms and in the environment (17). The first step in the development of a biological control agent is to gain an understanding of the biology of the control agent, including determining its host range (17). Biological control agents are selected based on their degree of specificity towards a single or small group of closely related target species (17). Many factors affect host range and it is possible that host cell components, such as membrane proteins and transcriptional and DNA replicative enzymes, may affect the ability of viral biological control agents to infect and replicate in a particular host (18).

1.5. Economically significant pests in Saskatchewan with the potential to be managed with biological control agents

The bertha armyworm (*Mamestra configurata*) is a sporadic, but significant, pest of canola and other oilseed crops (Figure 1) (19). In outbreak years, this species can cause tens of millions of dollars in crop losses, as well as cost farmers upwards of $10 million in pesticide application (19).

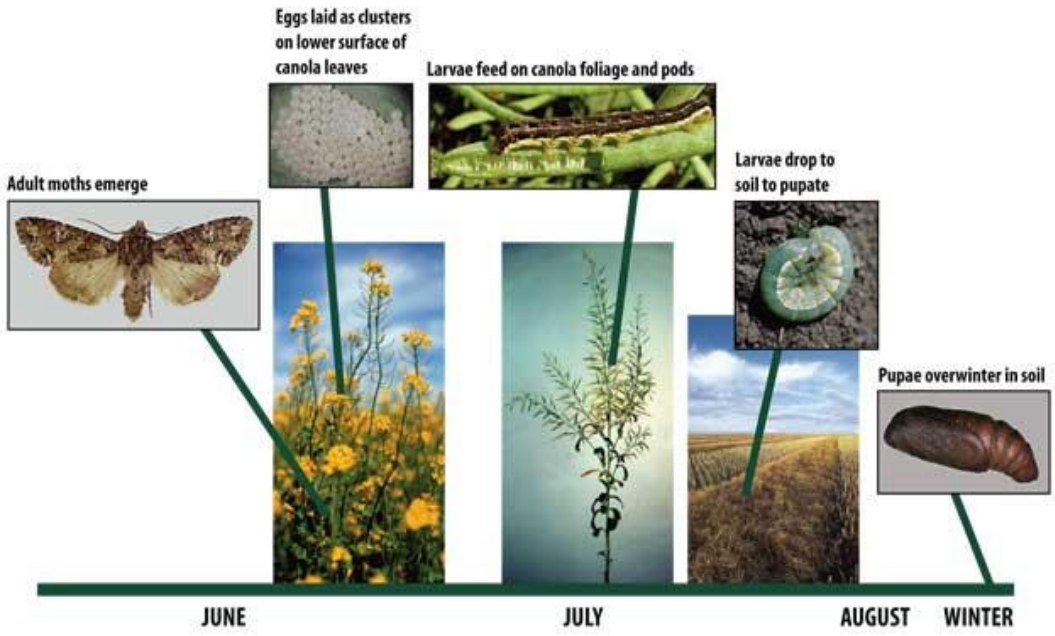

Figure 1. The life cycle of the bertha armyworm, a climbing cutworm.
Reprinted from (20) with permission from North Dakota State University.

The bertha armyworm is a noctuid lepidopteran (19). It completes six larval stages during the summer, overwinters as a pupa, then emerges as an adult the following summer (19). Although all larval instars can cause crop damage, up to 80% of the damage is caused by the 5th and 6th instar larvae (19). The larger larvae consume leaf tissue and damage stems and seed pods (19). Current management strategies for the bertha armyworm include aerial application of broad-spectrum chemical pesticides (19). These pesticides are not specific to this pest and can cause unwanted harm to beneficial insects (21).

A virus that infects the bertha armyworm, *Mamestra configurata nucleopolyhedrovirus* (MacoNPV), was identified (22, 23). Although there is still much work to do to fully characterize this virus, MacoNPV has the potential to be used as a biological control agent to control bertha armyworm outbreaks (22, 23).

2. LITERATURE REVIEW

2.1. The insect alimentary canal

The insect alimentary canal is a continuous tube running from the mouth of the insect to the anus (5, 24). It functions as a conduit for food to travel through the insect and as a site for digestion and absorption of nutrients and water (5, 24). The alimentary canal is divided into three regions: the foregut, midgut, and hindgut (5, 24).

The foregut is formed by an invagination of the ectoderm during embryogenesis, and is lined with a layer of cuticle (5, 24, 25). Peristaltic contractions of the muscles surrounding the foregut assist with the movement of the food bolus from the foregut into the midgut (26, 27).

The midgut is of endodermal origin, and is not lined with cuticle (5, 24, 25). The midgut is lined with epithelial cells, which are one cell layer thick and rest on a basal lamina (26, 27). Four cell types are present in the midgut epithelium: endocrine cells, regenerative cells, goblet cells, and columnar cells (26, 27). The endocrine cells secrete compounds which relay information from the midgut to other cells within the insect (25). The regenerative stem cells replenish the other cell types (26, 28). Goblet cells regulate potassium levels within the midgut and haemolymph (25, 26, 29). The most abundant cell type, the columnar cells, possess many microvilli which increase the surface area available for absorption of nutrients and for secretion of digestive enzymes (26, 27).

In most insects, the midgut is lined with a selectively permeable, acellular, cylindrical structure called the peritrophic matrix (PM) (5, 24-27). The PM consists of a highly ordered meshwork of chitin fibrils (a polymer of β–(1,4)-N-acetyl-D-glucosamine [GlcNAc]), along with other carbohydrates and a variety of structural and enzymatic proteins (30, 31). The structure and function of the PM are discussed in Section 2.2.

Most digestion of carbohydrates, lipids, and proteins, and the absorption of the resulting nutrients occurs in the midgut (5). Any material that is not absorbed in the midgut, moves into the hindgut for further processing or defecation (5).

The hindgut, like the foregut, is of ectodermal origin and lined with cuticle (5, 24, 25). The cuticle lining in the hindgut is thinner than in the foregut, as absorption of water and other small molecules occurs here (5, 24, 25).

2.2. Peritrophic matrix

The PM is a tube-like structure that lines the midgut and surrounds the food bolus in most insects (5, 25, 27, 30, 31). The PM is selectively permeable, with pore sizes ranging from 4-10 nm to allow for the discrimination of molecules of differing sizes (27, 32). These small pores allow enzymes to move from the epithelium into the lumen and for digestion products to move in the opposite direction, without compromising the structural integrity of the PM (5, 25, 27, 30, 31).

The PM is formed in two ways, described as Types I or II, though some insect species may use a combination of both (5, 27, 30, 31). Both types of PM are biochemically similar and serve the same functions (27).

Type I PM is secreted along the entire length of the midgut by the columnar epithelial cells (30, 31). It can be produced either in response to the ingestion of a meal, or continuously throughout the insects' life cycle (30, 31). This is the more common form of PM and it is found in Coleoptera, Hymenoptera, and larval Lepidoptera (5, 30, 31). Type II PM is secreted from a specialized structure called the cardia (5, 27, 30, 31). The cardia is formed at the anterior end of the midgut by an invagination of the foregut (5, 27, 30, 31). PM material is secreted from the cardia and is pressed into a thin, unbroken tube (5, 27, 30, 31). This type of PM is common in Dermaptera and Isoptera, as well as in larval Diptera (5, 27, 30, 31).

Both Types I and II PM consist of a network of chitin fibrils (30, 31). Chitin is a major structural component of the PM (30, 33). Chitin is synthesized at the apical ends of the brush border microvilli by the enzyme chitin synthase which catalyzes the addition of GlcNac units to a chitin chain (30). These chitin chains associate with one another to form chitin microfibrils, which in turn associate with other microfibrils to form chitin bundles (30). These associations provide strength and structure to the chitin matrix (30).

The strands of the chitin matrix are cross-linked by various PM proteins to provide additional structure and strength to the matrix (32). While the exact number of proteins associated with the PM is unknown, protein is estimated to account for 20-25% of the total mass of the PM (30, 31). Both Type I and Type II PM share similar protein compositions (30).

There are four classes of proteins associated with the PM, serving either structural or non-structural roles (30, 31, 34). One of these classes, the peritrophins, has been studied in the most detail (30). These proteins contain registers of 6, 8, or 10 cysteine residues in a highly conserved

spacing pattern which constitute the peritrophin A, B, or C domains, respectively (30). Protein folding is aided by the formation of disulfide bonds between the cysteine residues in these proteins (30). These bonds help to produce a three-dimensional pocket called the peritrophin chitin-binding domain (CBD) (30). The CBD is able to interact with chitin and thus PM proteins containing this type of domain are likely to be structural proteins (30). The structure of the CBD is discussed in detail in Section 4.1.2.

The PM serves several physical and physiological functions (30). The first is to compartmentalize the midgut into three distinct regions: an ectoperitrophic space (adjacent to the midgut epithelium), an endoperitrophic space (within the midgut lumen), and an intra-PM compartment (5, 30). This separation allows for the segregation of digestive enzymes and processes, and increases digestion efficiency (5, 30). The PM also helps to retain digestive enzymes within the midgut so that they are not eliminated with the food bolus as it progresses from the midgut to the hindgut (25, 30).

In the absence of a cuticular lining in the midgut, the PM physically separates the contents of the midgut from the epithelium (5, 24, 25, 30, 31). The PM protects the epithelial cells, both from abrasion by rough food particles and from penetration by pathogens or ingested toxins; however, some pathogens are able to circumvent this defensive structure (5, 24, 25, 30, 31).

2.3. Baculoviruses

The family *Baculoviridae* comprises a large group of diverse viruses that exclusively infect arthropod hosts (35, 36). The majority of baculoviruses infect lepidopterans, but they have also been isolated from dipterans and hymenopterans (35, 36). There are no closely related plant or vertebrate-infecting viruses and this specificity makes baculoviruses good candidates for use as biological control agents (37-41).

Baculoviruses have circular, double-stranded DNA genomes ranging in size from 80 to 180 kbp (35, 36, 42). Open reading frame(s) (ORF) are present on both DNA strands and the proportion of ORF is evenly distributed in either orientation (43). There are minimal gaps between adjacent genes, or even small overlaps, between the coding regions (35, 36, 44, 45). Baculoviruses encode 90 to 180 genes, of which 32 core genes are conserved among all species (43). With the exception of the *ie1* gene, baculovirus genes do not contain introns (46).

Until recently, morphology of the occluded virus particles was the basis upon which baculoviruses were classified into two genera: *Nucleopolyhedrovirus* (NPV) and *Granulovirus* (GV) (35, 36). As the genomic sequences of more baculovirus species became available, the phylogenetic relationships between viruses are becoming more clearly defined (47). Currently, there are four described genera of baculoviruses: *Alpha-*, *Beta-*, *Delta-*, and *Gammabaculovirus* (47). Alpha- and Betabaculoviruses exclusively infect lepidopteran hosts, and these groups encompass the former NPV and GV genera, respectively (47). Deltabaculoviruses exclusively infect dipteran hosts and Gammabaculoviruses exclusively infect hymenopteran hosts (47) (Figure 2).

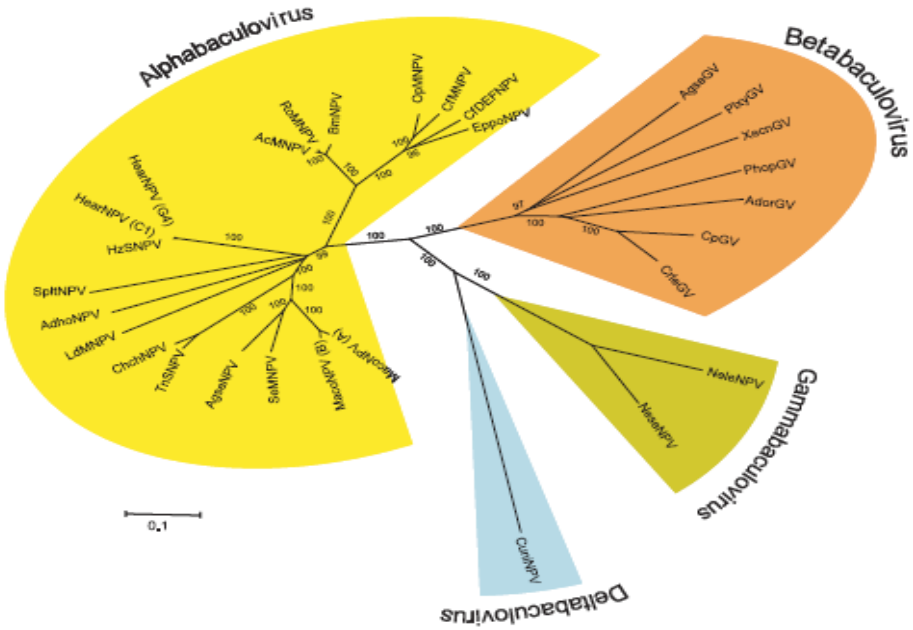

Figure 2. Phylogenetic relationships among the four genera of baculoviruses: *Alpha-*, *Beta-*, *Gamma-*, and *Deltabaculovirus*.
Phylogenetic relationships are based on amino acid alignment of the conserved core genes. The tree was produced using the neighbour-joining method and all branches have bootstrap values greater than 50%. Bootstrap values over 95% are indicated along the branches. Figure reprinted from (47) with permission from Springer Science and Business Media.

The *Alphabaculovirus* genus is divided into two clades, the Group I and Group II NPV, based on their phylogenetic relationships (35, 43, 48, 49). Group I NPV possess 17 conserved genes that are absent from Group II NPV (49). In addition, the Group I NPV use GP64 as the major envelope fusion protein (EFP), whereas Group II NPV use the F protein (35, 36, 49). EFP is required for cell-to-cell transmission (50).

The Alphabaculovirus type-species is *Autographa californica multiple nucleopolyhedrovirus* (AcMNPV) (41). AcMNPV has a 133 kbp circular genome, encoding 156 ORF and was first discovered from the alfalfa looper, *Autographa californica* (35, 51). AcMNPV is the most studied of the baculovirus species and functions have been assigned to a large number of AcMNPV genes. AcMNPV has been identified as a potential biological control agent for greenhouse and crop pests (37, 52). AcMNPV has a relatively broad host range, infecting 43 species in 11 families of Lepidoptera (53).

MacoNPV is an example of a Group II NPV (22). It has a 155 kbp circular genome encoding 169 ORF (22, 23). It was first detected in the bertha armyworm (*M. configurata*), a pest of canola crops (22, 23). MacoNPV has not been studied in as much detail as AcMNPV and there has been less progress made in characterizing the functions of its genes because of a lack of suitable cell line for *in vitro* studies. Because this baculovirus is a natural pathogen of the bertha armyworm, there is an incentive to better characterize this virus so it can be developed for use as a biological control agent.

2.3.1. Baculovirus structure

There are two phenotypes of baculovirus virions (35, 36). The occlusion-derived virus (ODV) is responsible for initiating an infection within the hosts' midgut (35, 36, 54). The budded virus (BV) is released from infected cells and is responsible for propagating a systemic infection within an infected host (35, 36, 54). Both phenotypes carry the same genetic information and share a common nucleocapsid structure (35, 36).

The nucleocapsid protein, P6.9 (NPV/*Alphabaculovirus*) or VP12 (GV/*Betabaculovirus*) forms a complex with the baculovirus DNA genome and it becomes condensed approximately 100-fold into a compact and insoluble form (36, 54, 55). Structural proteins and enzymes form a capsid shell that surrounds the DNA-protein complex (35, 36, 54, 55). The capsid shell, which is flattened at the basal end and has a nipple-like structure at the apical end, has distinct polarity (36, 54) (Figure 3).

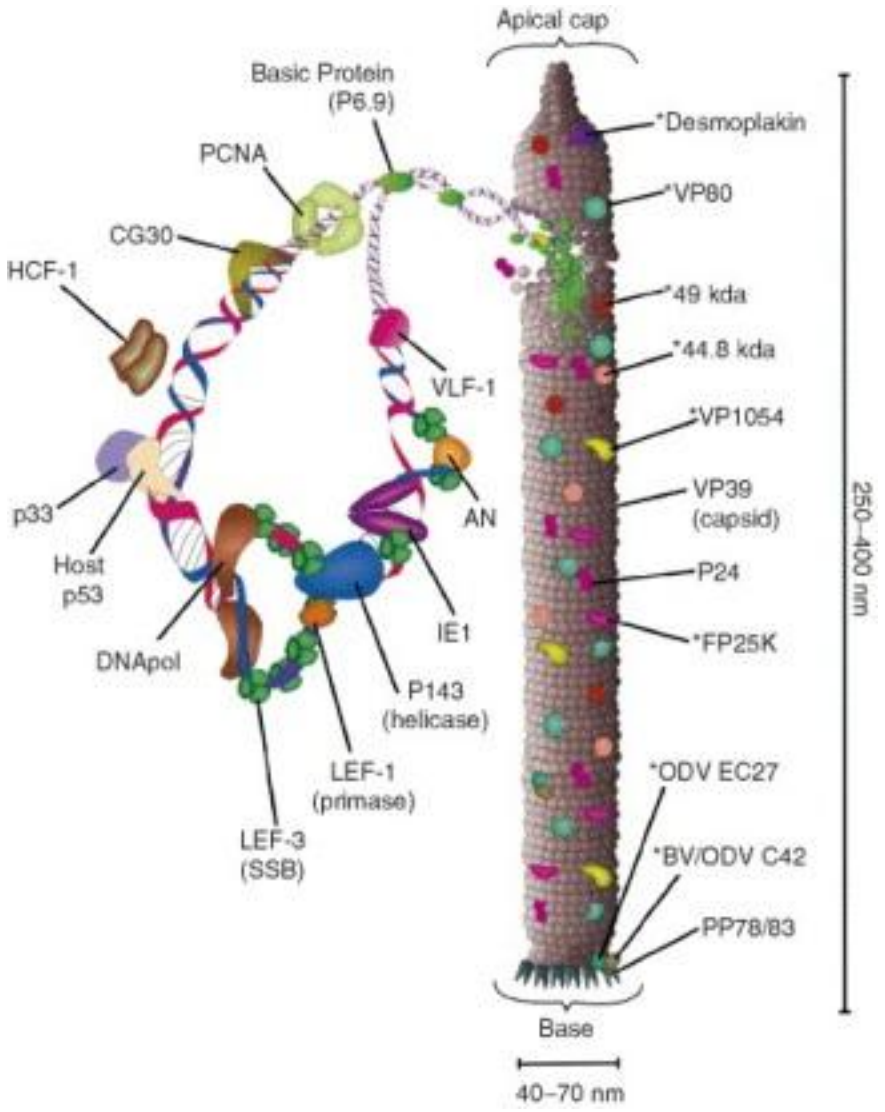

Figure 3. Structure of the baculovirus nucleocapsid.
Viral DNA associates with a basic protein (P6.9) and is condensed. Other nucleocapsid proteins associate with the DNA-protein complex to form a capsid shell. Reprinted from (54) with permission from Elsevier.

2.3.1.1. Occlusion-derived virus

Within the ODV, nucleocapsids are surrounded by an envelope and there may be a single nucleocapsid (SNPV) or multiple nucleocapsids (MNPV) within the same envelope structure (Figure 4) (35, 36, 54). There are a variety of proteins associated with the ODV envelope (54). These proteins may function as host range determinants or as factors which increase infectivity (56). A group of envelope-associated proteins called *per os*/*per oral* infectivity factors (PIF) is discussed in Section 2.3.5.

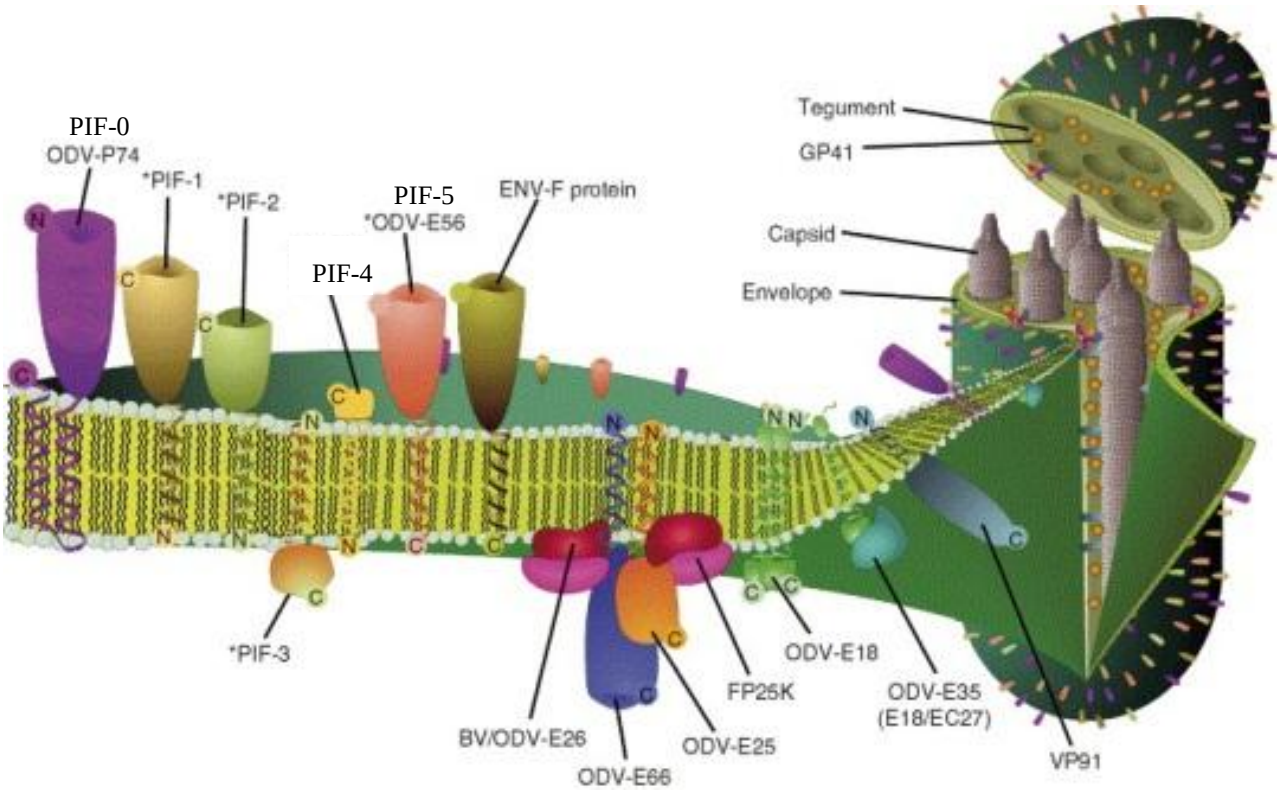

Figure 4. Structure of an ODV with multiple nucleocapsids within the same envelope. The major ODV envelope proteins are indicated. The position of the proteins and the protein complexes indicated are speculative. Reprinted with modifications from (54) with permission from Elsevier.

An occlusion body (OB), or polyhedron, is a proteinaceous structure that surrounds the ODV (35, 36, 54). OB serve to protect ODV from chemical and microbial degradation (35, 36, 54). OB also provide a stable reservoir of virus in the environment, which allows the virus to persist even when insect populations are low or absent (35, 36, 54).

Alphabaculovirus (NPV) OB are 0.15 to 15 µm in diameter and are polyhedral in shape (35, 36, 39, 54). Each OB contains many ODV, which may contain a single or multiple nucleocapsids (35, 36, 54). The proteinaceous matrix of NPV OB is composed primarily of polyhedrin (Polh) (35, 36, 54), which is the most highly conserved of the *Alphabaculovirus* proteins (36).

Betabaculovirus (GV) OB are smaller than the *Alphabaculovirus* OB (150 nm in diameter) and each OB contains only a single ODV (35, 36, 54). GV OB are ovoid in shape and utilize granulin as the major matrix protein (35, 36, 54). The structure of NPV and GV OB is illustrated in Figure 5.

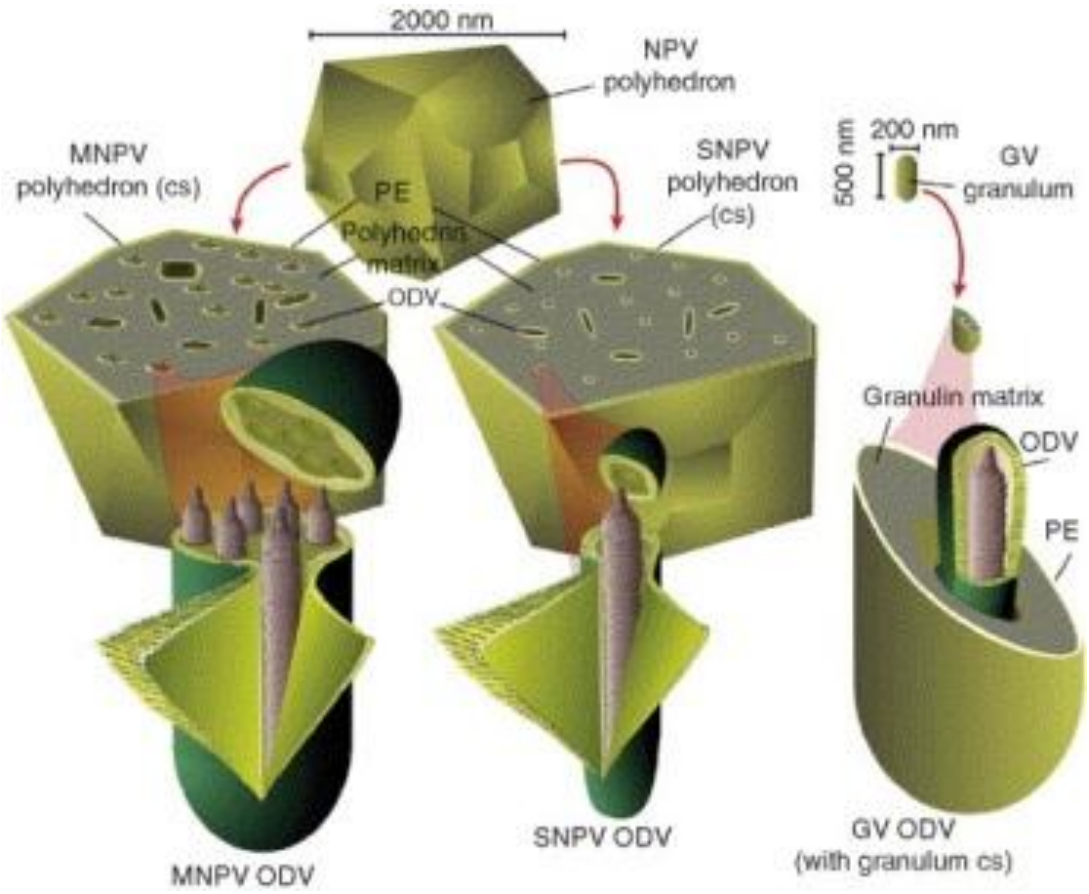

Figure 5. OB morphology of the NPV and GV.
The relative size difference between the NPV and GV is indicated. NPV OB containing ODV with multiple or single nucleocapsids are also indicated. Reprinted from (54) with permission from Elsevier.

OB are surrounded by a porous, multi-layered calyx or envelope (35, 36, 54). In the alkaline midgut of a susceptible host, the porosity of the calyx allows anions to rapidly enter the OB, which causes the OB to dissolve and the ODV to be released (35, 36, 54). The small size of the pores prevents other potentially harmful substances from entering the OB (35, 54).

2.3.1.2. Budded virus

Once an infection has been established, the second virion phenotype, BV, is released from infected cells (35, 36, 54). Unlike the ODV envelope, the BV envelope is asymmetrical (35, 36, 54). BV EFP, GP64 or F protein accumulates at the apical ends of the BV as part of a peplomer structure that protrudes from the BV envelope (35, 36, 54) (Figure 6).

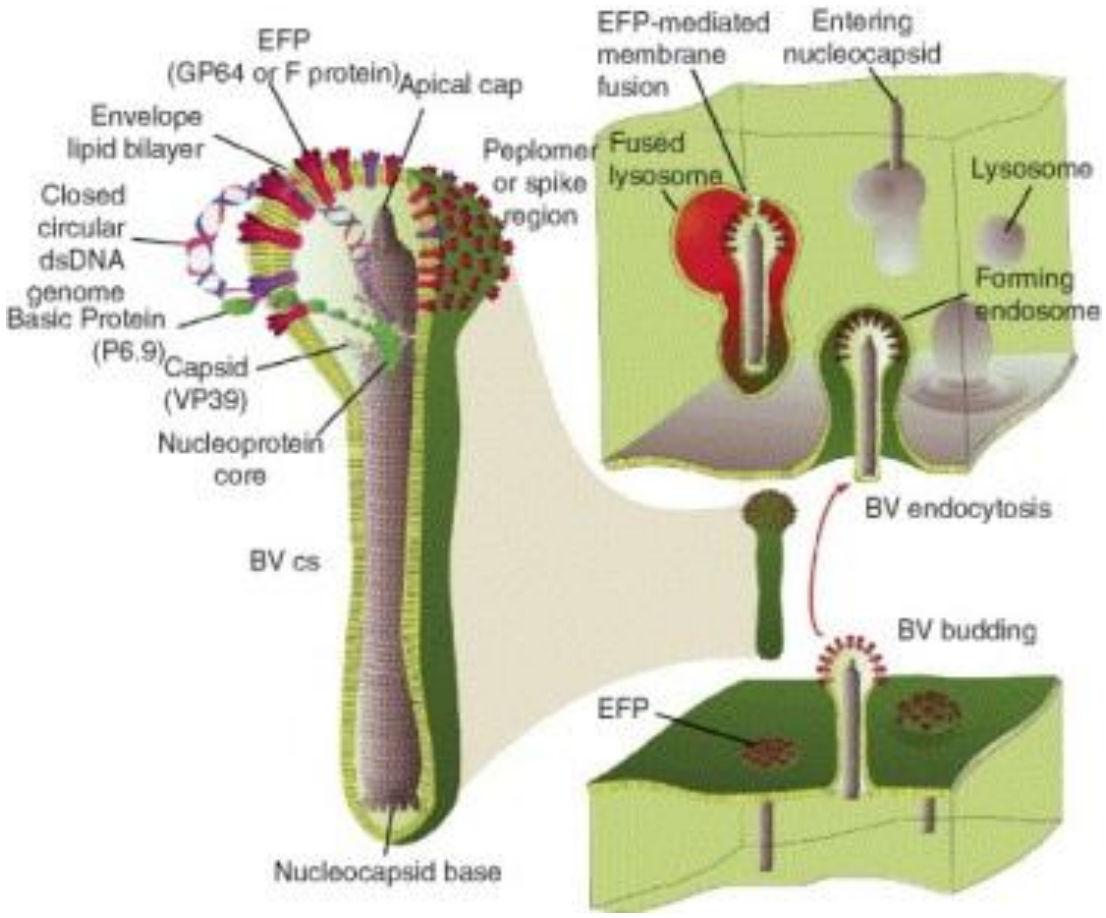

Figure 6. BV structure.
EFP is produced and accumulates in the host cell membrane. Nucleocapsids bud through the cell membrane and accumulate EFP at the apical ends. BV enter other cells via endocytosis. Reprinted from (54) with permission from Elsevier.

2.3.2. Infection cycle

Infection begins in a susceptible host with the ingestion of OB (35, 36, 54). The OB pass unaltered through the foregut and move into the midgut, which is an alkaline environment (35, 36, 54). Here, the OB dissolve and the ODV are released (35, 36, 54). The ODV are able to pass through the PM in a manner that is not well understood (35, 36, 54) (Figure 7).

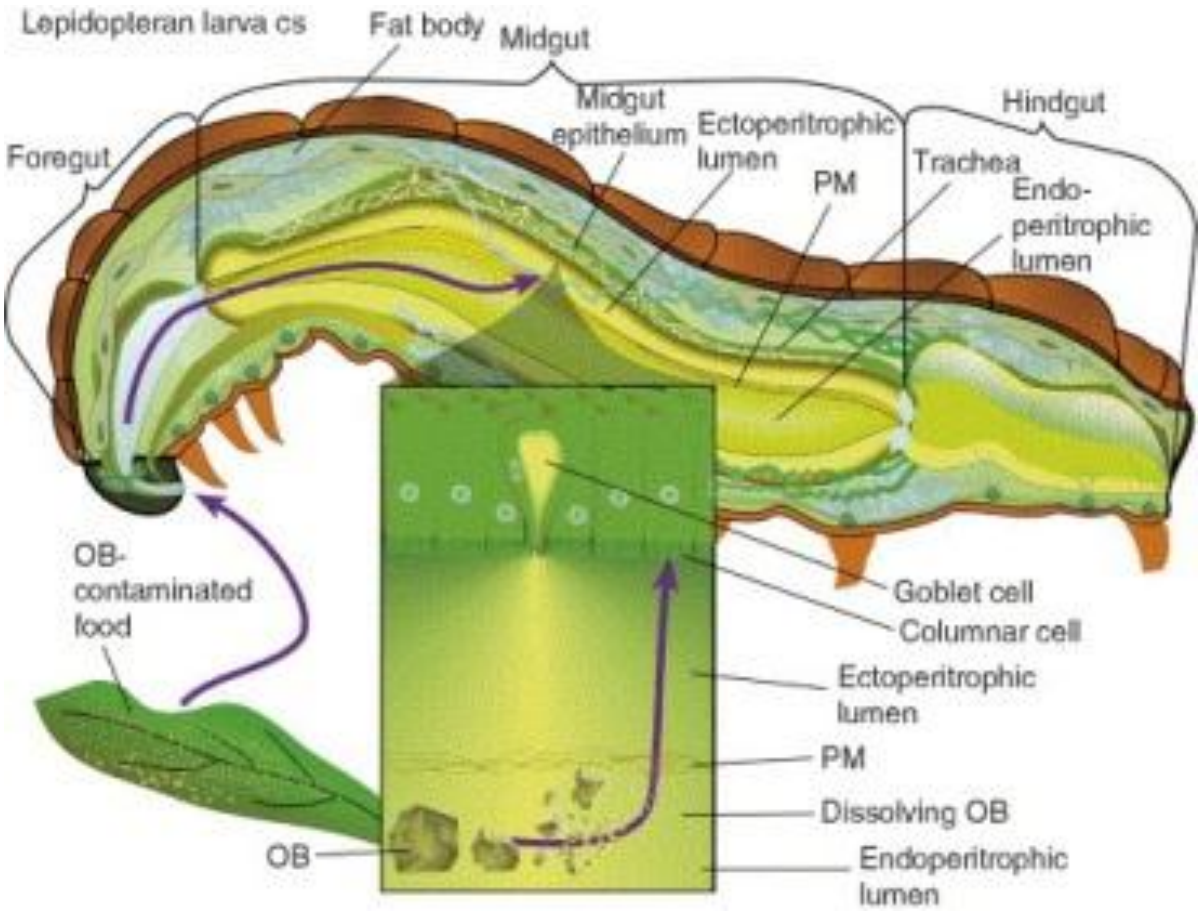

Figure 7. The baculovirus infection cycle.
Reprinted from (54) with permission from Elsevier.

Once through the PM, the envelope of the ODV fuses with the membrane of the columnar epithelial cells at which time the ODV release their nucleocapsid(s) into the midgut cells (35, 36, 54). The nucleocapsid(s) then move(s) towards the nucleus where capsid un-coating, viral DNA replication and gene expression occur (35, 36, 54).

When multiple nucleocapsids infect the same epithelial cell, as is the case with MNPV, some of the nucleocapsids move directly to the basal side of the epithelial cells and bypass the replication phase (35, 36, 54). From here, the nucleocapsids can bud through the plasma membrane as BV (35, 36, 54) (Figure 8).

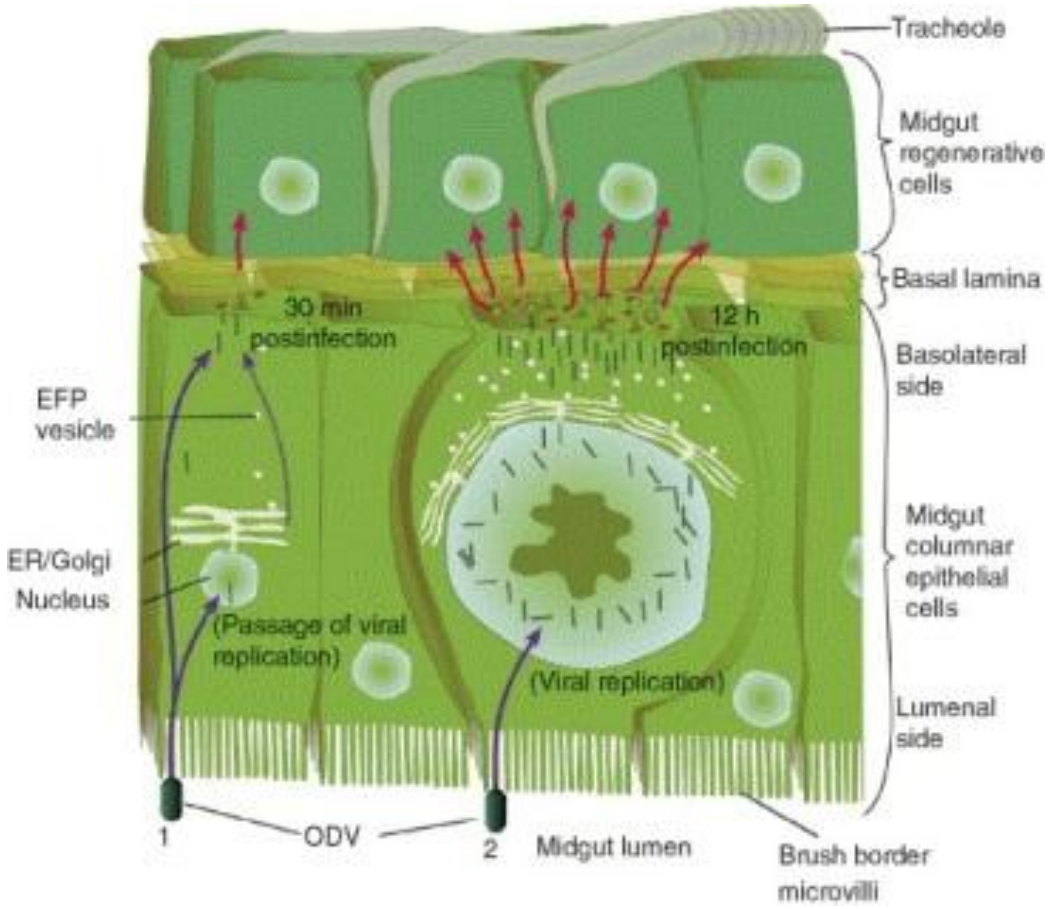

Figure 8. The baculovirus infection cycle within a single epithelial cell.
By bypassing the nucleus, and therefore viral gene expression and replication, some of the virions are able to pass through the epithelial cell and bud directly though the basal lamina. This process takes approximately 30 min, compared to 12 h or longer if the virion undergoes virus replication within the nucleus. This increases the speed at which a systemic infection can occur. Reprinted from (54) with permission from Elsevier.

BV from infected cells enters the insect haemolymph or tracheal system, which facilitates a systemic infection within the host (35, 36, 54). At later times in the infection, BV production slows and nucleocapsids are instead enveloped and packaged into OB within the nucleus (35, 36, 54) (Figure 9).

At very late stages in infection, two viral proteins, chitinase and cathepsin, aid in the breakdown of the insects' tissues and cuticle (35, 36, 54). Prior to death, infected insects may climb to the top of a the plant canopy (37, 57). As the cuticle is broken down, the insect liquefies and releases OB onto the canopy and soil, facilitating horizontal transmission to other susceptible hosts (35-37, 54).

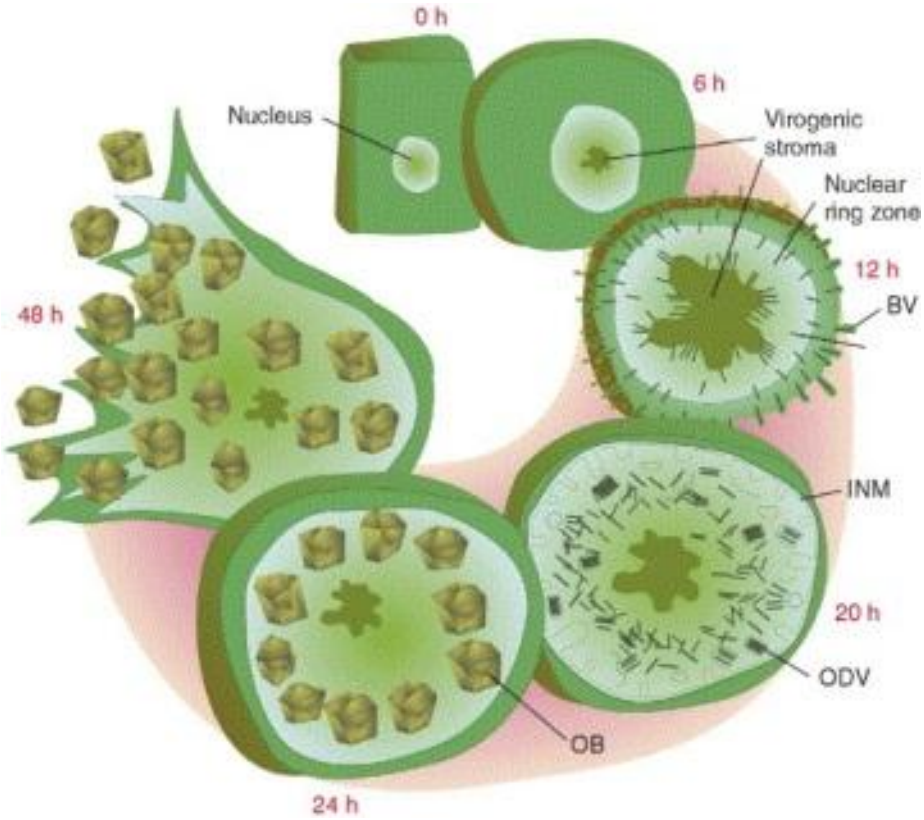

Figure 9. Baculovirus infection cycle through early (0 to 6 hours post-infection [hpi]), late (6 to 24 hpi), and very late (18 to 72 hpi) times.
Following virus entry into a susceptible cell, the cell loses its cuboid structure and begins to round up. Gene expression and viral DNA replication begin at 6 hpi within the virogenic stroma, a *de novo* structure formed in the nucleus, in which nucleocapsids are produced. BV begins to bud from infected cells at 12 hpi. At late times post-infection (20-24 hpi), nucleocapsids become enveloped and are encapsulated within OB. At very late times post-infection (48 hpi and onwards), the infected cells lyse and release the viral OB (35, 36, 54). Reprinted from (54) with permission from Elsevier.

2.3.3. Gene expression

The large genome size of baculoviruses, paired with their complex infection cycle and substantial number of genes demands a coordinated system of gene expression (35, 36, 43, 44). Gene expression is temporally regulated, with genes being transcribed in the early (0-6 hpi), late (6-24 hpi), and very late (18-72 hpi) stages of infection (35, 43, 46). Gene products from earlier stages are required for the expression of genes from later temporal groups (43, 46).

The transcriptional cascade begins with the expression of the early genes, which are

transcribed within the first 6 hpi and prior to the initiation of viral DNA replication (43, 46, 58). There are two subgroups of early genes: the immediate early genes (IE) and the delayed early genes (DE) (43, 46). IE genes are transcribed immediately following infection and do not depend on the presence of other viral proteins for their expression (43, 46). DE genes require the gene products of the IE genes to facilitate their expression (43, 46). Host-cell machinery is required for the expression of both IE and DE genes (46, 58).

Typically, baculovirus genes are transcribed as a single mRNA; however, multiple transcripts sharing a common 3′ end, but different 5′ transcription initiation site, can be produced from a subset of genes (46). All baculovirus transcripts are capped at the 5′ end and are polyadenylated at the 3′ end (46). The length of the 5′ untranslated region (UTR) is typically quite short (< 150 bp), whereas the length of the 3′ UTR varies widely (43).

Early gene promoters consist of a TATA element, an initiator (INR) element, or both (43, 46, 58). Deletion of, or mutations around the TATA element, results in a reduction or abolition of promoter activity and gene expression, suggesting that the TATA element is the main regulatory element for early gene expression (43, 46, 58). The conserved early gene INR motif, ATCA(G/T)T(C/T), contributes to the activity of the promoter complex, but can function independently if a TATA element is not present (46, 58). Early gene INR motifs overlap the transcript initiation site and are typically located within 25 to 31 bp of a TATA element (46, 58).

Late genes are expressed between 6 and 24 hpi and require the onset of viral DNA replication and the prior expression of early viral genes to be expressed (43, 59, 60). Late expression factors (LEF), of which there are 19, can act as transactivators to assist late gene expression (61-63). Four LEF proteins associate to form a viral RNA polymerase (43, 60). Lef-8 and Lef-9 form the catalytic domain of the polymerase, whereas Lef-4 facilitates the addition of a cap to the 5′ end of late and very late expressed mRNA (43, 60). The function of p47, the fourth component of the viral RNA polymerase, is unknown (43, 60). Switching to a virally-encoded RNA polymerase from a host-encoded RNA polymerase may allow the virus to avoid competition with the host cell for resources and may optimize the expression of late and very late genes (59, 60).

The promoter sequence for late genes, as with early genes, is highly conserved among baculovirus species (43, 44, 59, 60). The late gene promoter typically contains a ((A/G/T)TAAG(A/G/T)) motif, which also functions as the transcription initiation site (43, 44, 59, 60). Mutations in the conserved TAAG motif abolish late gene transcription, while mutations

in the nucleotides flanking this motif decrease the amount of transcription, but do not affect the temporal expression pattern of the gene (59, 60).

Very late genes are expressed 18 to 72 hpi (59, 60). The very late gene promoter contains the conserved sequence ATAAG(A/G/T) followed by a "burst" sequence which is highly AT-rich (59, 60). Mutations within the burst region may affect the levels of gene expression, but have no effect on the temporal expression patterns of very late genes (59, 60).

Several baculovirus genes are expressed throughout the infection cycle (43, 59). These genes are preceded by both early and late promoter sites (59). The promoter sites may overlap (e.g., TAT*ATAAG*), but typically the early promoter elements are located upstream from the late or very late promoter element (43, 59).

2.3.4. DNA replication

Baculovirus DNA replication occurs within a structure called the virogenic stroma which is located within the nucleus of infected cells (35, 64). The virogenic stroma is a *de novo* structure formed in response to baculovirus infection (35). Unique sequences in the virus DNA called origins of replication (ORI) help direct the host-cell replication machinery to the virus DNA at the expense of the host cell DNA (35, 65, 66).

Baculoviruses contain two types of ORI: homologous repeat region (*hr*) ORI and non-*hr* ORI (35, 64-66). *Hr* ORI comprise an imperfect palindrome (30 bp) flanked by repeated DNA sequences (approximately 70 bp) (35, 64-66). The sequence of *hr* ORI is highly conserved within a baculovirus species, but can be quite variable among virus species (35, 44, 64-66).

Non-*hr* ORI contain sequence repeats and palindromes (43, 65, 66). This type of ORI is not repeated throughout the genome (43, 65, 66). It is possible that early gene promoters and any DNA sequence that become unwound prior to DNA replication may also function as non-*hr* ORI (35, 65, 66).

Replication proceeds from the ORI using either recombination-dependent replication, rolling-circle replication, or a combination of the two (35, 65). Recombination-dependent replication allows for the concurrent initiation of DNA replication at multiple ORI (35, 65). Following replication of the entire genome, a final recombination event joins the ends of the replicated DNA together to form a covalently-closed circular DNA genome (35, 65). Rolling-circle replication is a unidirectional process which creates multiple copies of a circular genome (67).

This type of replication begins at a single ORI, and produces concataemers of linear, viral genomes which are later processed into multiple circular genomes (67).

2.3.5. Genes required for oral infectivity

A baculovirus infection is initiated by fusion of the ODV envelope with the microvilli brush border membrane of the columnar epithelial cells in the host insects' midgut (35, 36, 54). Nucleocapsids are released into the cytoplasm of the epithelial cells, prior to migrating to the nucleus (54). Within the nucleus, the nucleocapsids un-coat, viral DNA replication and gene expression occur, and progeny virus are produced (35, 36, 54).

As the cells of the midgut are continually sloughed and regenerated throughout the insects' life cycle, they are not the ideal location for a productive infection to occur (54). Non-midgut tissues are better suited to baculovirus replication, as they are not sloughed from the insect (54). To reach these tissues, however, an infection must first be initiated in the midgut cells (54). A group of highly conserved core PIF genes are required for initiating infection in the midgut.

PIF genes are conserved among every species of baculovirus and are members of the 32 core baculovirus genes (35). PIF proteins contain a transmembrane domain, which suggests that they are membrane-bound, and share homology with proteins in other types of insect-infecting viruses, suggesting that they are crucial for infection in invertebrate hosts (35). PIF are required for oral infection, but are not required for systemic infection within a susceptible host (35).

Seven PIF have been identified. P74/PIF-0 (AcMNPV ORF 138) (68) and PIF-1 (56) are specific binding proteins involved in the establishment of primary infection within the midgut. Transcriptional analysis of *P74* and *PIF-1* from *Spodoptera littoralis nucleopolyhedrovirus* (SpliNPV) indicated that both genes are transcribed at very low levels during infection, suggesting that only small amounts of the resultant proteins are required for a productive infection to occur (69). PIF-2 (AcMNPV ORF 22) is associated with the ODV, but it is unclear if this protein localizes to the ODV envelope or nucleocapsid fraction (56, 70, 71). PIF-3 (AcMNPV ORF 115) is not involved in the binding of the ODV envelope to the midgut epithelial cells, yet is still required for initial oral infectivity (56, 72). A hydrophobic region at the N-terminus of PIF-3 may be involved in targeting this protein to the nucleus for incorporation into ODV late in the infection (73). Deletion of this hydrophobic region abolishes the ability of the virus to establish a *per os* infection within the midgut (73). PIF-4 (AcMNPV

ORF 96), unlike the other described PIF, localizes to both the BV and ODV (74). PIF-5 (AcMNPV ODV-E56/AcMNPV ORF 148) is associated with the ODV envelope (75). Deletion viruses lacking *PIF-5* are unable to infect larvae when administered orally (75). However, the *PIF-5* deletion-virus ODV was still observed to bind to the midgut epithelium, suggesting that PIF-5 is not required for this process and likely plays a role prior to, or after, the ODV envelope has fused with the midgut epithelium (75). Finally, PIF-6 (Ac68), like PIF-4, is associated with both the BV and ODV (76).

Functional studies of the *Helicoverpa armigera single nucleocapsid nucleopolyhedrovirus* (HearNPV) PIF indicate that P74/PIF-0, PIF-1, PIF-2 and PIF-3 are required to be present in the same ODV as a complete wild type (wt) virion, or as co-occluded deletion mutants for oral infection to occur (77). Infectivity of the PIF-deletion mutants was not altered by the addition of Calcofluor, a compound that disrupts the structure of the PM, suggesting that the PM is not the target of the HearNPV PIF (77).

Further to the HearNPV study, co-immunoprecipitation studies in AcMNPV determined that P74/PIF-0, PIF-1, PIF-2, PIF-3, PIF-4, PIF-6, Ac83 (P95; AcMNPV ORF 83), Ac5 (AcMNPV ORF 5), and Ac108 (AcMNPV ORF 108), but not PIF-5, form a complex on the surface of the ODV (76, 78, 79). Deletion of *PIF-1*, *PIF-2*, or *PIF-3* completely abolishes the formation of the complex, but these three PIF still form a stable sub-complex when PIF-4 is absent (78, 79). Ac83, which was found to be loosely associated with the PIF complex, contains a CBD, and may play a role in facilitating interaction between the ODV envelope and the chitin fibrils in the PM or the chitin secreting cells of the midgut epithelium (78).

2.3.6. Proteomics of the ODV envelope

Proteomic analyses of the ODV of two Alphabaculoviruses and one Deltabaculovirus identified ODV-associated proteins that may be involved in host range determination, virulence, and oral infectivity (80-82).

Forty-four proteins from the Group I Alphabaculovirus AcMNPV were identified as being ODV-associated (80). Interestingly, P74/PIF-0 was the only PIF determined to be an ODV-associated protein (80). Another surprising discovery was the presence of F protein, the EFP used by Group II Alphabaculoviruses and Betabaculoviruses (35, 36). EFP are required for the attachment and entry of BV into host cells, but were not thought to be required for oral

infectivity (35, 36). It has been suggested that the presence of F protein as part of the ODV envelope in Group I Alphabaculoviruses may enhance oral infectivity by facilitating interaction of the ODV envelope with the membrane of midgut columnar cells (54, 83). A second study analyzed the protein composition of the Group II Alphabaculovirus HearNPV (48, 81, 84). This study identified 23 ODV-associated proteins (81). Twenty-one of these were also identified in the AcMNPV study, indicating that there is a high degree of conservation among ODV-associated proteins between these two virus groups (81).

Further to these studies, Peng et al. (2010) (84) conducted a series of yeast-two-hybrid experiments to determine the protein-protein interactions between the known ODV-associated proteins (84). Several interactions were detected between PIF proteins. PIF-2 interacted with ODV-E66 (AcMNPV ORF 46), 38K (Ac98; AcMNPV ORF 98) and PIF-3, whereas PIF-3 interacted with PIF-5, ODV-E66, 38K, and with itself. Interactions with P74 (PIF-0) and PIF-1 were not detected. These results, as well as the AcMNPV co-immunoprecipitation studies (78, 79), suggest that the proteins involved in oral infectivity and their interactions with one another are quite complex.

2.3.7. Baculovirus 11K genes

In 2001, Dall et al. (85) employed a bioinformatics based approach to identify viral genes which allow certain viruses within specific virus families to infect insect hosts. Two criteria were established to identify these genes. First, the genes must be found in the insect-infecting members of a virus family, but be absent from the vertebrate-infecting members of the same virus family (85). Second, these genes must be found in at least two unrelated taxa of insect viruses (85). To identify these genes, a within-virus-family comparison of virus genomes was undertaken to identify genes which are present in the viruses that infect insect hosts, but are lacking from those viruses that infect vertebrate hosts (85). Using this subset of genes, a between-virus-family search was conducted to identify those genes which are present in more than one taxon of insect-infecting viruses (85). This approach identified six groups of genes which are common among insect-infecting viruses, but are lacking in vertebrate-infecting viruses (85). One of these groups, the 11K genes, is of interest as every baculovirus species characterized to date from the *Alpha-*, *Beta-*, and *Gammabaculovirus* genera, as well as many species of entomopoxvirus contain at least one member of this gene group (85, 86). This high

degree of conservation suggests that these genes may play a key role in allowing a virus to infect an invertebrate host (85-87).

The 11K genes produce putative proteins of between 90 and 110 amino acids in length, with a predicted molecular weight of 11,000 D (85-87). Each 11K gene product has a hydrophobic amino-terminal domain, which is consistent with a membrane transit signal or signal peptide (85-87). Each 11K gene product also contains a highly conserved motif called the peritrophin A CBD (85-87). The peritrophin A CBD comprises a register of six cysteine residues and three aromatic residues in a highly conserved spacing pattern, $C^1X_{13-20}C^2X_{5-6}C^3X_{9-19}C^4X_{10-14}C^5X_{4-14}C^6$, where C is a cysteine and X is any amino acid other than cysteine (85-87). The three conserved aromatic residues are located between C^2 and C^3 (2 residues) and between C^4 and C^5 (1 residue) and extend into the chitin-binding pocket (30, 88). This motif is commonly found in proteins which interact with chitin, including the peritrophin class of PM proteins (30, 85).

There are two subtypes within the 11K gene group: the 145-type and the 150-type (85-87). These names were derived from the 11K gene products produced from ORF 145 and ORF 150, respectively, from AcMNPV (85-87).

The 145-type is a well-defined group, with members found in the Alpha-, Beta-, and Gammabaculoviruses (85-87). The phylogeny of this subgroup closely matches the phylogeny of the associated baculoviruses based on an analysis of a set of other unrelated baculovirus genes (85).

The 150-type forms a less well-defined group than the 145-type (85-87). Some members of *Alpha-* and *Betabaculovirus* contain 150-type 11K genes (85). In some baculovirus species, the 150-type 11K genes are phylogenetically more related to insect sequences than they are to viral sequences, suggesting that these genes may have been acquired via horizontal gene transfer between the virus and its host (85).

Maco164 (MacoNPV ORF 164) has been identified as a homologue to Ac145 based on an analysis of amino acid sequences (22). Maco164 has a conserved peritrophin A domain and is similar in length to Ac145. There have been no studies on the function or temporal expression of this protein.

Maco118 (MacoNPV ORF 118) has been identified as a homologue to Ac150 (22). Maco118 does not have a defined peritrophin A domain, but it is highly cysteine-rich. It also differs

substantially in length from Ac150. Like Maco164, there have been no functional analysis studies done for Maco118.

2.3.8. Previous studies on 11K proteins

There have been two studies aimed at determining the function of Ac145 and Ac150. Specifically, these studies looked at the effect of knocking out either or both of the associated genes on oral infectivity.

Lapointe et al. (87) used a two-pronged approach to study the function of Ac145 and Ac150. First, to determine if Ac145 and Ac150 were able to interact with chitin, they expressed both proteins in a bacterial expression system. Both Ac145 and Ac150 have a highly hydrophobic N-terminus, which is consistent with a membrane transit signal. In developing their expression strategy, the Lapointe group opted to exclude the N-terminal 22 and 30 amino acids from Ac145 and Ac150, respectively, to express the proteins without the membrane transit signal. They produced N-terminal glutathione S-transferase fusions with their truncated proteins and subsequently used glutathione-sepharose beads to purify the expressed proteins from the total cellular proteins. Using these purified, truncated proteins, they were unable to demonstrate chitin-binding under a variety of conditions.

To determine the role that Ac145 and Ac150 play in the infection cycle, Lapointe et al. (87) produced deletion constructs to determine the effect of deleting *Ac145*, *Ac150*, or both together on oral and systemic infection. The deletion constructs were produced using transfer vector plasmids. Briefly, the region of the genome containing the gene of interest (GOI) was cloned into a transfer vector plasmid. The GOI was replaced with a gene encoding green fluorescent protein (*GFP*) in the transfer vector by homologous recombination. This construct was co-transfected with wt AcMNPV in insect cells to produce viral DNA with the GOI replaced with *GFP*. *GFP* was subsequently removed from the deletion virus by creating a second transfer vector plasmid in which *GFP* had been deleted by digesting the plasmid on either side of *GFP* and then re-circularizing the plasmid DNA. This construct was then co-transfected with the *GFP*-tagged deletion virus to produce a deletion virus with no observable tag.

Lapointe et al. (87) found no difference between the wt virus and the single or double deletion viruses when the virus was injected directly into the haemolymph of an insect. By injecting the virus into the haemolymph, the midgut, and therefore the PM, which is a barrier to

pathogenic microorganisms, is bypassed. In oral feeding trials, they found that the *Ac145* deletion mutant was 6-fold less infectious than wt when administered to *Trichoplusia ni* larvae, but as infectious as the wt when administered to *Heliothis virescens* larvae. The *Ac150* deletion mutant was as infectious as wt when administered to either host. Interestingly, the *Ac145* and *Ac150* double deletion virus was 39-fold less infectious than wt in *H. virescens* larvae, but only 6-fold less infectious than wt in *T. ni* larvae. From these results, they speculated that both Ac145 and Ac150 play a role in primary infection, but do so in a host-dependent manner.

Intrigued by the results from the Lapointe et al. study (87), Zhang et al. (86) produced their own set of *Ac150* deletion constructs using transfer vector plasmids. Their constructs were produced in a similar manner to those of Lapointe et al., but they retained an *hsp70*/*LacZ* reporter tag to allow for tracking of their recombinant virus. As with the previous study, there was no difference between the deletion mutants and wt when the virus was injected directly into the haemolymph. In this study, the oral bioassays using the *Ac150* deletion virus indicated that loss of *Ac150* results in a 4.1-fold, 5.6-fold, and 18-fold reduction in infectivity compared to wt in *Spodoptera exigua*, *H. virescens*, and *T. ni* larvae, respectively. Zhang et al. suggested that Ac150 is similar to a PIF as it appears to have an effect on oral infectivity.

These results differ from those of Lapointe et al. (87) who found no change in oral infectivity for *Ac150* deletion viruses in *H. virescens* or *T. ni* larvae compared to the wt. Lapointe et al. were unable to demonstrate chitin-binding activity for either Ac145 or Ac150, even though both proteins are predicted to contain a CBD. As well, Lapointe et al. and Zhang et al. (86) obtained contradictory results as to the function of both Ac145 and Ac150 on oral infectivity. In light of these findings, my study aims to use novel approaches to determine the ability of Ac145 and Ac150 and their homologues in MacoNPV, Maco164 and Maco118, respectively, to bind to chitin and to clarify the role of these proteins in the baculovirus infection cycle.

3. PROJECT OBJECTIVES

As reviewed above, it has been hypothesized that the 11K gene family, common to a variety of virus groups that infect invertebrate hosts, may be pivotal to the host range of these viruses. The overall objective of my project was to determine the function that the 11K genes play in the infection cycle of Alphabaculoviruses; more specifically, if they play a key role in oral infectivity by virtue of their containing a chitin-binding motif.

To achieve this goal, several lines of investigation were developed with the specific goals as follows:

A. To determine if the 11K gene products from MacoNPV and AcMNPV display chitin-binding activity in *in vitro* assays, and if so, to study the mechanisms responsible for binding (Chapter 4).
B. To map the transcriptional regulatory sites and temporal expression patterns for the AcMNPV 11K genes (Chapter 5).
C. To create knockout viruses in which the AcMNPV 11K genes were deleted singularly or together and to monitor the effects of the loss of a gene(s) on the rate of BV production and viral DNA replication (Chapter 6).
D. To determine the role of the 11K gene products in both oral and systemic infection in a susceptible host (Chapter 7).

4. ALPHABACULOVIRUS 11K PROTEINS: CHITIN-BINDING STUDIES

4.1. Introduction

4.1.1. Baculovirus expression system

Baculovirus expression systems were developed to obtain high yields of heterologous protein expressed in insect cells (89, 90). As well, proteins produced in a eukaryotic system are more likely to be folded and modified to be biologically active (89, 90). To increase the speed and efficiency of expressing proteins in a baculovirus system, a bacmid based on the AcMNPV genome was created (89-91).

Bacmids are large circular plasmids (89, 90). The bMON14272 (136 kbp) bacmid (Invitrogen Corporation, Carlsbad, CA) includes the coding sequence for the entire AcMNPV genome, as well as ORI for both bacterial and insect cells (89, 90). The ability for the bacmid to replicate in either bacterial or insect cells classifies it as a shuttle vector. As a shuttle vector, genetic manipulations to the bMON14272 bacmid can be carried out in bacterial cells, which have the advantage of fast generation time, before transferring the bacmid DNA into insect cells for protein expression (89-91).

This system takes advantage of the presence of a non-essential, but highly expressed baculovirus gene, *Polh* (89, 90). Polh is the major OB protein (35, 89, 90). It is required for the production of OB, but not for baculovirus replication, BV production, or cell-to-cell transmission (35, 89, 90). The native *Polh* is under the control of a very strong promoter, which produces high protein yields at late times (> 24 hpi) (35, 89, 90). The native *Polh* ORF in bMON14272 has been replaced with a mini-*att*Tn7 target site by means of homologous recombination (89, 90). The native *Polh* promoter was left intact upstream of the mini-*att*Tn7 site (89, 90).

A recombinant transfer plasmid, pFastBac1 (4.8 kbp, Invitrogen Corporation), carrying a GOI at the multiple cloning site is produced. The multiple cloning site of pFastBac1 is flanked by Tn7L and Tn7R sites (89-91). The transfer plasmid can be transformed into DH10Bac (Invitrogen Corporation) cells, which are *Escherichia coli* cells containing the bMON14272 bacmid and a helper plasmid, pMON7124 (13.2 kbp), which encodes a transposase gene (89-91). The transposase drives a Tn7-mediated transposition event *in trans* between the Tn7L and Tn7R sites of the pFastBac1 transfer vector and the mini-*att*Tn7 target site within the *Polh* locus of bMON14272 (89-91). This transposition event causes an insertion of the GOI from the pFastBac1 vector into bMON14272 at the *Polh* locus in frame with and downstream from the

native *Polh* promoter (89-91). Recombinant bacmid DNA is purified from the bacterial cells and transfected into insect cells in order to express the protein of interest (89-91).

4.1.2. Chitin binding domains

The peritrophin A CBD comprises a register of six cysteine residues and three aromatic residues in a highly conserved spacing pattern, $C^1X_{13-20}C^2X_{5-6}C^3X_{9-19}C^4X_{10-14}C^5X_{4-14}C^6$, where C represents a cysteine residue and X is any amino acid other than cysteine (30). These CBD generally lack secondary structure and protein folding is facilitated by the formation of three disulfide bonds between C^1 and C^3, C^2 and C^6, and C^4 and C^5 (30). The conserved aromatic residues are located between C^2 and C^3 (2 residues) and between C^4 and C^5 (1 residue) (30, 88). The tertiary structure of the protein creates a binding pocket into which the aromatic residues extend (30, 92). Aromatic residues are involved in general saccharide binding (92) and chitin-binding (30, 92) due to the formation of hydrogen bonds between the aromatic residues and the saccharide ligand (30, 92).

4.2. Hypothesis

The 11K gene products from MacoNPV (Maco118 and Maco164) and AcMNPV (Ac145 and Ac150) each contain a peritrophin A CBD (or are highly cysteine-rich). It is predicted that each protein will be able to interact with chitin *in vitro* via this domain. Compounds that disrupt the intramolecular disulfide bonds or the intermolecular hydrogen bonds are predicted to disrupt this binding.

4.3. Materials and methods

4.3.1. Analysis of amino acid sequences, protein motifs, and protein structure

Ac145 and *Ac150* were identified as 11K genes by Dall et al. (85) using a bioinformatics based approach. Maco118 and Maco164 were identified by Li et al. (22) as potential homologues of Ac150 and Ac145, respectively, based on similarities in their predicted amino acid sequences. To confirm this, the amino acid sequences for each of these proteins were obtained from the National Center for Biotechnology Information (NCBI) protein database (NCBI accession numbers: Ac145 NP_054176.1, Ac150 NP_054181.1, Maco118 NP_613201.1, Maco164

NP_613247.1) and alignments were produced using the Vector NTI Advance 11.0 AlignX application (Invitrogen Corporation).

Protein motifs were identified in Ac145, Ac150, Maco118, and Maco164 using the meta search engine MOTIF (GenomeNet, Institute for Chemical Research, Kyoto University, Japan), which simultaneously queries multiple protein databases including PROSITE (Swiss Institute of Bioinformatics), Pfam (Wellcome Trust Sanger Institute, Genome Research Limited), and others.

To determine whether the amino-terminal region of each protein contains a signal peptide or a transmembrane domain, the amino acid sequences were entered into the SignalP 4.0 Server and the TMHMM 2.0 server, respectively (both, Centre for Biological Sequence Analysis, Technical University of Denmark, Lyngby, Denmark).

Three-dimensional protein models were produced for each protein using the homology modelling program, SWISS-MODEL (ExPASy, Swiss Institute of Bioinformatics, Lausanne, Switzerland) (93-95). A fully automated approach was used to model the structure for each protein. The amino acid sequence for each protein was submitted to SWISS-MODEL and a template protein was selected from the SWISS-MODEL template library by the software based on the query protein's primary sequence. The resultant protein structures were visualized using the Vector NTI Advance 11.0 3D Molecule Viewer (Invitrogen Corporation).

4.3.2. Protein expression

Ac145, Ac150, Maco118, and Maco164 were expressed using the Bac-to-Bac® Baculovirus Expression System (Invitrogen Corporation) following the manufacturer's protocol and as described below.

Primer pairs were designed to amplify *Maco118*, *Maco164*, *Ac145,* and *Ac150* (Table 1). The primers were designed such that the entire ORF, excluding the stop codon, was amplified. An *Eco*R1 restriction site was incorporated at the 5′ end of each forward primer and an *Xba*1 restriction site was incorporated at the 5′ end of each reverse primer to allow for directional cloning of the PCR amplicon. The nucleotide sequence corresponding to the human influenza hemagglutinin (HA) epitope tag was also incorporated into each reverse primer between the ORF sequence and the *Xba*1 restriction site. A stop codon was incorporated in the reverse primer immediately following the HA-tag.

PCR amplicons were produced using either MacoNPV-A (90/2) genomic DNA (for amplification of *Maco118* and *Maco164*) or the *Eco*R1 B fragment of AcMNPV E2 genomic DNA (for amplification of *Ac145* and *Ac150*) as a template. Twelve nanograms of template DNA were used in a 25 µL reaction containing 1X Phusion HF buffer containing 1.5 mM $MgCl_2$, 0.4 mM dNTPs, 0.2 µM forward primer, 0.2 µM reverse primer, 3% dimethyl sulfoxide (DMSO), and 0.25 U Phusion High-Fidelity (HF) DNA polymerase (Finnzymes, Thermo Scientific, Vantaa, Finland). The PCR reaction mixture was incubated at 98^{o}C for 30 s, followed by 35 cycles of 98^{o}C for 10 s, 58^{o}C for 30 s, and 72^{o}C for 30 s. A final extension at 72^{o}C for 10 min was followed by incubation at 4^{o}C. Five microlitres of each PCR amplicon were separated in a 1% agarose gel in Tris-acetate-ethylenediaminetetraacetic acid (TAE) buffer, stained with GelRed (Biotium Inc., Hayward, CA) to confirm that the amplicons were the expected size. All agarose gels referenced in this thesis were visualized using the Molecular Imager® Gel Doc™ XR+ System (Bio-Rad Laboratories Inc., Hercules, CA).

The PCR amplicons were cloned into the multiple cloning site of the pFastBac1 (Invitrogen Corporation) plasmid. Briefly, 100 ng of each PCR amplicon and 100 ng of pFastBac1 vector DNA were digested using 1.5 U of *Xba*1 in 1 X React 2 Buffer (Invitrogen Corporation). The reaction mixture was incubated at 37^{o}C for 1 h. The NaCl concentration of the reaction was increased from 50 mM to 100 mM and 1.5 U of *Eco*R1 was added to the mixture. The mixture was incubated at 37^{o}C for an additional 1 h. The digestion products were separated in a 1% agarose gel in TAE buffer stained with GelRed. The digested amplicons and vector DNA were excised from the gel and DNA extracted using the QIAGEN Gel Extraction Kit (QIAGEN, Hilden, Germany) following the manufacturer's protocol. The purified DNA was quantified using a Nanodrop 1000 spectrophotometer (Thermo Fisher Scientific Inc., Ottawa, ON). Digested and gel-purified PCR amplicons were ligated into the pFastBac1 vector by incubating insert DNA and vector DNA in a 3:1 ratio in 1X ligation buffer (Invitrogen Corporation) with 1 U of T4 DNA ligase (Invitrogen Corporation). The ligation reactions mixtures were incubated overnight at 4^{o}C.

Three microlitres of a ligation mixture was transformed into a 25 µL aliquot of *E. coli* DH10B cells (Invitrogen Corporation) by electroporation. The cells were pulsed at 1.5 kV, 25 µF, and 200 Ω using a Gene Pulser II electroporator (Bio-Rad Laboratories Inc.). One millilitre of low salt (5 g NaCl/L) Luria-Bertani (LB) broth was added to the cells immediately following

the pulse. The cells were allowed to recover at 37^{o}C for 1 h. Aliquots of 25 and 250 µL of each transformation were plated onto low salt LB plates supplemented with 100 µg/mL ampicillin (Amp). The plates were incubated overnight at 37^{o}C.

Several colonies were selected from the plates and used to inoculate 3 mL of low salt LB broth supplemented with 100 µg/mL Amp. The cultures were incubated overnight at 37^{o}C with shaking at 225 rpm. Plasmid DNA was extracted from the cells using a standard alkaline lysis miniprep protocol (96) including an isopropanol precipitation of the DNA prior to re-suspension in 50 µL of TE (10 mM Tris-HCl pH 7.5, 1 mM disodium ethylenediaminetetraacetic acid [EDTA] pH 8.0) with 20 µg RNase A. The clones was screened by restriction digest with *Eco*R1 and *Xba*1 as described above prior to Sanger sequencing at the National Research Council, Plant Biotechnology Institute (PBI), Saskatoon Canada, with primers P(Ph) Forward and SV40 poly A Reverse (Table 2).

Table 1. Primer pairs for amplifying *Maco118*, *Maco164*, *Ac145*, and *Ac150* for use in the baculovirus expression system. Restriction sites are underlined with a single line in the sequence. The sequence corresponding to the HA-epitope tag is in bold text and stop codons are underlined with a double line.

Primer Name	Sequence	Amplifies
001 for	CCGGAATTCATGTCAAAACGACTCTAC	*Maco118* + HA tag
007 rev	AGCTCTAGAGCATTA**GGCGTAGTCGGGCACGTCGTAGGGGTA**TTCGGTTAATGCTGCGGCAATCGC	
003 for	CCGGAATTCATGTGGTTGTTATTAGCA	*Maco164* + HA tag
008 rev	AGCTCTAGAGCATTA**GGCGTAGTCGGGCACGTCGTAGGGGTA**TTCTAGTAACAGATTTTTGTAAAG	
2009 for	CCGGAATTCATGAATCAAATTC	*Ac145* + HA tag
2010 rev	AGCTCTAGAGCATTA**GGCGTAGTCGGGCACGTCGTAGGGGTA**TAGTAACAAGTTTCTATA	
2011 for	CCGGAATTCATGTTAAAACCCAACATG	*Ac150* + HA tag
2012 rev	AGCTCTAGAGCATTA**GGCGTAGTCGGGCACGTCGTAGGGGTA**GTTTTGGTTAGCGGTAC	

Table 2. Primer pairs used for sequencing pFastBac1 clones or for amplifying the *Polh* locus of bMON14272 to confirm the presence of the correct PCR amplicon.

Primer Name	Sequence	Amplifies
P(Ph) Forward	AAATGATAACCATCTCGC	pFastBac1 multiple cloning site
SV40 poly A Reverse	GAAATTTGTGATGCTATTGC	
pUC M13 Forward	CCCAGTCACGACGTTGTAAAACG	Polh region of bMON14272 bacmid
pUC M13 Reverse	AGCGGATAACAATTTCACACAGG	

The pFastBac1 plasmids (Amp^R, gentamicin^R [Gen^R]) containing the correct amplicon were transformed into MAX Efficiency DH10Bac chemically competent cells (Invitrogen Corporation). Fifty microlitres of chemically competent MAX Efficiency DH10Bac cells were mixed with 1 ng of a pFastBac1 expression construct in a 15 mL polypropylene tube (Ultident Scientific, St. Laurent, QC). The cells were incubated on ice for 30 min followed by a heat shock at 42^{o}C for 45 s without shaking. The cells were incubated on ice for 2 min and then 900 µL of room temperature (RT) super optimal broth with catabolite repression (SOC) media was added to the cells. The cells were incubated at 37^{o}C for 4 h with shaking at 225 rpm. Aliquots of 10 and 100 µL of the transformed cells were plated onto low salt LB plates supplemented with 50 µg/mL Kan, 7 µg/mL Gen, 10 µg/mL Tet, 50 µg/mL 5-bromo-4-chloro-indolyl-β-D-galactopyranoside (X-gal), and 95.2 µg/mL isopropyl β-D-1-thiogalactopyranoside (IPTG) for blue/white colour selection. Plates were incubated for 48 h at 37^{o}C. Several colonies were selected and used to inoculate 3 mL of low salt LB broth containing 50 µg/mL Kan, 7µg/mL Gen, and 10 µg/mL Tet. The cultures were grown overnight at 37^{o}C with shaking at 225 rpm. Bacmid DNA was extracted from the cells using a standard alkaline lysis miniprep protocol (96). Bacmid DNA was screened using PCR to detect the correct insert as follows: approximately 100 ng of bacmid DNA was used in a 25 µL reaction containing 1X PCR buffer (Invitrogen Corporation), 1.5 mM $MgCl_2$, 0.4 mM dNTPs, 0.2 µM pUC M13 Forward primer, 0.2 µM pUC M13 Reverse primer (Table 2), and 1 U Taq polymerase (Invitrogen Corporation). The PCR reaction mixture was incubated at 95^{o}C for 2 min, followed by 35 cycles of 95^{o}C for 30 s, 55^{o}C for 30 s, and 72^{o}C for 3 min. A final extension of 72^{o}C for 10 min was followed by incubation at 4^{o}C. The PCR products were separated in a 1% agarose gel in TAE buffer, stained with GelRed, to confirm that the correct size amplicon was produced.

The insect cell line Sf9 (from parental strain IPLB-SF21 AE2), derived from pupal ovarian tissue of the fall armyworm (*Spodoptera frugiperda*), was propagated in Grace's Insect Medium (GIM; Gibco, Carlsbad, CA) supplemented with 3,330 mg/L lactalbumin hydrolysate, 3,330 mg/L yeastolate, 600 mg/L L-glutamine, 11 µg/mL Gen , and 10% foetal bovine serum (FBS). Cells were incubated at 27^{o}C and passed twice weekly at a confluent cell suspension to media ratio of 1:5.

Purified recombinant bacmid DNA was transfected into Sf9 cells. Briefly, 1.0 X 10^6 Sf9 cells were dispensed into a 25 cm^2 cell culture flask (Corning Incorporated, Tewksbury MA) in a total

of 5 mL GIM and were allowed to adhere to the flask for 2 h at RT. In a 1.5 mL tube, 5 μL of Cellfectin II Reagent (Invitrogen Corporation) was incubated with 95 μL of GIM (without FBS or Gen) at RT for 30 min. In a separate tube, 1 μg of bacmid DNA was incubated in a total of 100 μL of GIM (without FBS or Gen) at RT for 30 min. The 100 μL of bacmid DNA and GIM were mixed gently with the 100 μL of Cellfectin II and GIM, and this reaction mixture was incubated for 15 min at RT. During the incubation, the GIM was removed from the 25 cm^2 flask and discarded. The cells were washed twice with 1 mL aliquots of GIM (without FBS or Gen) and the wash medium discarded.

Following the 15 min incubation, 800 μL of GIM (without FBS or Gen) were added to the 200 μL of bacmid DNA and Cellfectin II mix. The 1 mL total volume was transferred to the 25 cm^2 flask. The flask was rocked gently at RT for 6 h at which time the viral DNA and Cellfectin II inoculum was removed from the Sf9 cells and replaced with 5 mL of GIM (with FBS and Gen). The transfected cells were incubated for an additional 48 h at 27^oC.

Following the 48 h incubation, the cells were gently scraped from the bottom of the cell culture flask using a rubber cell-scraper (Ultident Scientific). The medium and cells were transferred to a 15 mL Falcon tube (BD Biosciences, Mississauga, ON) and the cells pelleted by centrifugation at 3000 rpm for 2 min in an Allegra X-12 bench top centrifuge (Beckman Coulter, Inc., Mississauga, ON). The supernatant containing the pass 1 BV (P1 BV) was transferred to a new 15 mL Falcon tube. The cell pellet was washed once with 1 mL of phosphate buffered saline ([PBS] 137 mM NaCl, 2.7 mM KCl, 10 mM Na_2HPO_4, 2 mM KH_2PO_4, pH 7.5), pelleted at 3000 rpm for 2 min and then re-suspended in 1 mL of PBS. Both the BV and cell pellet fractions were stored at 4^oC.

To increase viral titre, an infection was set up in Sf9 cells using the P1 BV obtained from the transfection assay. 1.0 X 10^6 Sf9 cells were dispensed into a 25 cm^2 flask in 5 mL total volume of GIM (with FBS and Gen) and the cells were allowed to adhere to the flask for 2 h at RT. The GIM was removed from the flask and discarded. Fifty microlitres of P1 BV were mixed with 950 μL of GIM (with FBS and Gen) in a 1.5 mL tube. The viral inoculum was added to the flask and allowed to bathe the cells by rocking the flask gently at RT for 2 h. The viral inoculum was removed from the flask and replaced with 5 mL of fresh GIM (with FBS and Gen). The infected cells were incubated for 48 h at 27^oC, following which the cells and media containing the pass 2 BV (P2 BV) were collected as described above.

Viral DNA was extracted from the P2 BV by mixing 100 μL of P2 BV with 100 μL of lysis buffer (10 mM Tris-Cl pH8.0, 1 mM EDTA, 0.5% sodium dodecyl sulfate [SDS], 80 μg/mL Proteinase K) and incubating overnight at 50^{o}C. Viral DNA was extracted one time using 200 μL of phenol:chloroform:isoamyl alcohol (25:24:1). The sample was mixed gently and centrifuged at 14,000 rpm for 8 min in a bench top microcentrifuge. The upper aqueous layer was transferred to a new 1.5 mL tube. This sample was mixed once with 200 μL of chloroform:isoamyl alcohol (24:1) and then centrifuged at 14,000 rpm for 8 min in a bench top microcentrifuge. The upper aqueous layer containing the DNA was transferred to a new 1.5 mL tube. The DNA solution was diluted 1:10 using sterile distilled water and 2 μL was used in a PCR reaction as described above using the pUC M13 Forward and Reverse primers. The PCR products were separated in a 1% agarose gel in TAE buffer, stained with GelRed, to confirm the presence of viral DNA containing the correct insert.

A second infection was set up as described above in a 25 cm^2 cell culture flask by infecting 1.0 X 10^6 Sf9 cells with 50 μL of the P2 BV to produce pass 3 (P3) BV with a higher virus titre. The infected cells were incubated at 27^{o}C for 48 h and collected as described above.

The P3 BV supernatant and cell pellet fractions were screened for expressed protein production. One hundred microlitres of P3 BV and half of the P3 cell pellet were transferred to new 1.5 mL tubes. Mock-infected Sf9 cells were used as a negative control to ensure that there was no cross-reactivity between cellular or media proteins and the detection antibody. Protein sample buffer (1 M Tris pH 6.8, 10% w/v SDS, 2.5 mg/mL bromophenol blue, 50% v/v glycerol, 1% v/v β-mercaptoethanol [β-ME]) was added to each sample and the samples boiled for 10 min. The samples were immediately cooled on ice for 10 min and then centrifuged at 14,000 rpm for 5 min to pellet any insoluble protein. Thirty microlitres of each sample were analyzed by SDS-polyacrylamide gel electrophoresis (PAGE). The protein samples were separated in a 12% polyacrylamide gel with a 5% polyacrylamide stacking gel at 110 V for 90 min in a Mini-PROTEAN® Tetra-Cell electrophoresis apparatus (Bio-Rad Laboratories Inc.).

The separated proteins were transferred from the polyacrylamide gel to a nitrocellulose membrane (General Electric Company, Mississauga, ON) at 100 V for 60 min in a Mini Trans-Blot® electrophoretic transfer cell (Bio-Rad Laboratories Inc.). The nitrocellulose membrane was blocked overnight at 4^{o}C in 5% skim milk in PBS with 0.05% Tween-20 (PBS-T). The membrane was washed twice, 5 min per wash, with PBS-T. The membrane was then incubated

for 1 h at RT with gentle rocking with a 1:1000 dilution of HA.11 Clone 16B12 purified mouse monoclonal antibody (Covance Inc., Montreal, QC) prepared in 5% skim milk in PBS-T. The membrane was washed three times, 5 min per wash, with PBS-T and then incubated for 1 h at RT with gentle rocking with a 1:50,000 dilution of a goat anti-mouse IgG-horseradish peroxidase (HRP) conjugated antibody (Bio-Rad Laboratories Inc.) prepared in 5% skim milk in PBS-T. The membrane was washed three times with PBS-T and then developed with the Millipore Immobilon Western Chemiluminescent HRP substrate (EMD Millipore Corporation, Billerica, MA). The membrane was covered in plastic wrap and enclosed in a Spectroline Monotec lightproof autoradiography cassette with a Kodak X-Omatic intensifying screen (Krackeler Scientific Inc., Albany, NY). Kodak BioMax MR film (Kodak, Rochester, NY) was placed on top of the membrane for a variety of exposure times. The films were developed in a dark room using a Kodak M35A X-OMAT processor (Kodak).

Each of the expressed proteins was purified from the total infected-cell protein preparations using an anti-HA-tag purification kit (MBL International Corporation, Woburn, MA). Infected Sf9 cells from a 75 cm^2 flask (approximately 1.0 X 10^7 cells) were washed twice with 5 mL aliquots of PBS. The cells were pelleted by centrifugation at 3000 rpm for 2 min in a bench top centrifuge and the supernatant discarded. The cell pellet was re-suspended in 1 mL of lysis buffer (25 mM Tris-HCl pH 7.5, 100 mM NaCl, 5 mM EDTA, 1% Triton X-100) and the cells lysed by sonication using a Misonix S-4000 sonicator (QSonica, Newtown, CT) with an amplitude of 50 and pulse time of 15 s. The lysate was incubated on ice for 15 min and then centrifuged at 14,000 rpm for 5 min in a bench top microcentrifuge to pellet any cellular debris. Five hundred microlitres of lysate were incubated with 20 µL of anti-HA-tag bead slurry in a spin column (MBL International Corporation). The cell lysate and beads were incubated for 1 h at 4^oC with end-over-end rotation. The spin column was inserted into a 1.5 mL collection tube and centrifuged at 14,000 rpm for 10 s in a bench top microcentrifuge. The flow through containing unbound protein was saved for future analysis. The beads were washed three successive times with 200 µL aliquots of wash buffer (supplied with the purification kit) and each wash fraction was saved for future analysis. The spin column was transferred to a new 1.5 mL tube and 20 µL of HA elution peptide (2 mg/mL, supplied with the purification kit) was added directly to the beads in the column. The column was incubated at 4^oC for 5 min and then centrifuged at 14,000 rpm for 10 s to collect the eluate. A second elution was completed using another 20 µL fraction

of HA elution peptide. The beads were incubated for 1 min at 4^{o}C and then centrifuged at 14,000 rpm for 10 s. The two elution fractions were pooled and stored at -80^{o}C for future analysis.

4.3.3. Chitin-binding assays

A chitin-binding assay was performed to determine if the expressed proteins interacted with the chitin beads. In this experiment, infected Sf9 cells from a 75 cm^2 flask (approximately 1.0 X 10^7 cells) were re-suspended in 1 mL of lysis buffer and sonicated as described in Section 4.3.2. The total cellular lysate was incubated on ice for 15 min and cellular debris pelleted by centrifugation at 3000 rpm for 5 min in a bench top centrifuge.

One millilitre of chitin magnetic-bead slurry (New England Biolabs Inc., Ipswich, MA) was transferred to a 1.5 mL tube. The beads were isolated using a DynaMag^{TM}-2 magnetic rack (Life Technologies Corporation, Carlsbad, CA) and the supernatant discarded. The beads were washed three times with 1 mL aliquots of column binding buffer (500 mM NaCl, 0.02 M Tris-HCl pH 8.0, 0.001 M EDTA, 0.05% Triton X-100) and the supernatant from each wash discarded. One millilitre of cell lysate was added to the washed chitin beads and incubated overnight at 4^{o}C with end-over-end rotation. The chitin beads were isolated using the DynaMag^{TM}-2 rack and the supernatant fraction, containing unbound protein, was transferred to a new 1.5 mL tube. The beads were washed 10 successive times with 1 mL aliquots of PBS. The supernatant from the 1st and 10th wash steps were kept for future analysis. To elute any bound protein, the beads were boiled in protein sample buffer for 10 min. The samples were separated in a polyacrylamide gel, transferred to a nitrocellulose membrane, and probed using the monoclonal anti-HA antibody as described in Section 4.3.2.

To determine the mechanism(s) involved in binding, various chemicals were assessed for their ability to release the chitin-bound protein. Infected Sf9 cells from a 75 cm^2 flask were lysed by sonication, protein purified using the anti-HA tag purification kit, and incubated with 1 mL of washed chitin bead slurry overnight at 4^{o}C as described above. The flow through was collected and the beads washed 10 times with PBS. One millilitre of PBS was added to the beads and the beads were divided into four equal fractions. The beads were isolated using the DynaMag^{TM}-2 rack and the PBS discarded. Each fraction was weighed to ensure that approximately the same amount of beads were in each of the four fractions. Various chemicals were added to each fraction in an attempt to liberate any bound protein. These included 500 mM NaCl, 2% SDS, 5%

β-ME, 1% Calcofluor White M2R (Sigma-Aldrich Co., Oakville, ON) or the following combinations: 2% SDS + 5% β-ME, 2% SDS + 1% Calcofluor, or 2% SDS + 5% β-ME + 1% Calcofluor. The samples were incubated for 1 h at RT with end-over-end rotation. Following the 1 h incubation, the beads were pelleted and the supernatant removed. Fifty microlitre aliquots of the supernatant samples were transferred to new 1.5 mL tubes and protein sample buffer added. The bead fractions were washed once with 1 mL of PBS and then 100 µL of protein sample buffer and 100 µL of sterile water were added to each bead fraction. The supernatant aliquots and bead fractions were boiled for 10 min prior to separating in a polyacrylamide gel and detection by western blot as described in Section 4.3.2.

The chitin-binding assays were validated using bovine serum albumin (BSA) (Invitrogen Corporation) as a negative binding control, and wheat-germ agglutinin (WGA) (Sigma-Aldrich Co.), as a positive binding control. A chitin-binding assay was performed by incubating 1 mg of BSA or 1 mg of WGA with 1 mL of pre-washed chitin bead slurry overnight at 4^{o}C. The supernatant was removed from the beads as described above and the beads washed 10 times with 1 mL aliquots of PBS. Protein sample buffer was added to the chitin beads and to aliquots of the supernatant and wash fractions and the samples were boiled for 10 min. The samples were separated in a polyacrylamide gel as described in Section 4.3.2, and visualized by staining with Coomassie Brilliant Blue or silver stain (Silver Xpress Kit, Invitrogen Corporation). A second binding assay was performed with WGA to determine the mechanism(s) involved in binding. This experiment was carried out using 2% SDS, 5% β-ME, 0.2% Calcofluor, or combinations of these to elute bound protein from the chitin beads. This experiment was performed as described above for Maco118, Maco164, Ac145, and Ac150.

Chitin-binding assays were performed using one other HA-tagged protein to ensure that any binding that was detected was not due to an interaction between the HA-tag and the chitin beads. The protein used was MsOSP-HA, an oviposition-stimulating protein from the migratory grasshopper *Melanoplus sanguinipes* (97), which was expressed in the Bac-to-Bac® baculovirus expression system. MsOSP is a 242 amino acid protein that is not predicted to contain a CBD and is not cysteine rich (4 cysteine residues). Non-purified protein was incubated overnight with the chitin beads and bound-protein was released by boiling in protein sample buffer. A second set of chitin-binding assays was performed for MsOSP using 2% SDS, 5% β-ME, 0.2%

Calcofluor, or combinations of these to elute bound protein from the chitin beads. This experiment was performed as described above.

4.4. Results

4.4.1. Analysis of amino acid sequences, protein motifs, and protein structure

AcMNPV ORF 145 was predicted to encode a 77 amino acid protein with a hydrophobic N-terminus consistent with a membrane transit signal (85-87). The only protein motif predicted by the meta search engine MOTIF was a chitin-binding Type 2/peritrophin A domain between amino acids 11 and 69 as identified in the PROSITE profiles (prf) and protein families (Pfam) databases with e-values of 0.17 and 0.0012, respectively. Ac145 was not predicted to possess either a signal peptide (D score = 0.126, cut-off score = 0.450) according to the Signal P server or a transmembrane domain (expected number of amino acids in a transmembrane helix (TMH) = 0) according to the TMHMM server.

AcMNPV ORF 150 was predicted to encode a 99 amino acid protein with a hydrophobic N-terminus (85-87). Ac150 was also predicted to contain a chitin-binding Type 2/peritrophin A domain between amino acids 38 and 96, as identified in prf, Pfam HMMs local models (Pfam Fs), and Pfam HMMs global models (Pfam Is), with e-values of 4.5×10^{-6}, 7.6×10^{-13}, and 1.9×10^{-10}, respectively. Ac150 was predicted to contain a RGD integrin-binding motif at amino acids 29-31 as predicted by PROSITE patterns frequent match producers (freq pat). RGD domains are predicted to play a role in both cell attachment and in integrin-mediated signalling. Ac150 was not predicted to contain a signal peptide (D score = 0.411, cut-off score = 0.500), but it was predicted to have 1 TMH with amino acids 7 to 25 predicted to span a membrane (expected number of amino acids in a TMH = 19).

MacoNPV ORF 164, the homologue of AcMNPV ORF 145, was predicted to encode a 92 amino acid protein with a chitin-binding Type 2/peritrophin A domain between amino acids 29 and 84. This was confirmed by prf, Pfam Fs, and Pfam Is, with e-values of 0.0026, 4.5×10^{-7}, and 3.5×10^{-5} respectively. Maco164 was predicted to contain a signal peptide (D score = 0.811, cut-off score = 0.450) with a predicted cleavage site between amino acids 16 and 17. Maco164 was not predicted to contain a TMH (expected number of amino acids in a TMH = 0).

MacoNPV ORF 118 is substantially longer than its homologue, AcMNPV ORF 150, and encodes a putative protein of 249 amino acids. This protein was predicted to have a partial

chitin-binding Type 2/peritrophin A domain between amino acids 39 and 76 as determined by prf and Pfam Fs, with e-values of 16 and 3.2 X 10^{-5}, respectively. Maco118 was not predicted to contain a signal peptide (D score = 0.360, cut-off score = 0.500), but it was predicted to contain a transmembrane domain between amino acids 5 and 27 (expected number of amino acids in TMH = 20).

An alignment of the homologous proteins Ac145/Maco164 and Ac150/Maco118 indicating the location of the predicted chitin-binding/peritrophin A domains and other relevant motifs is provided in Figure 10.

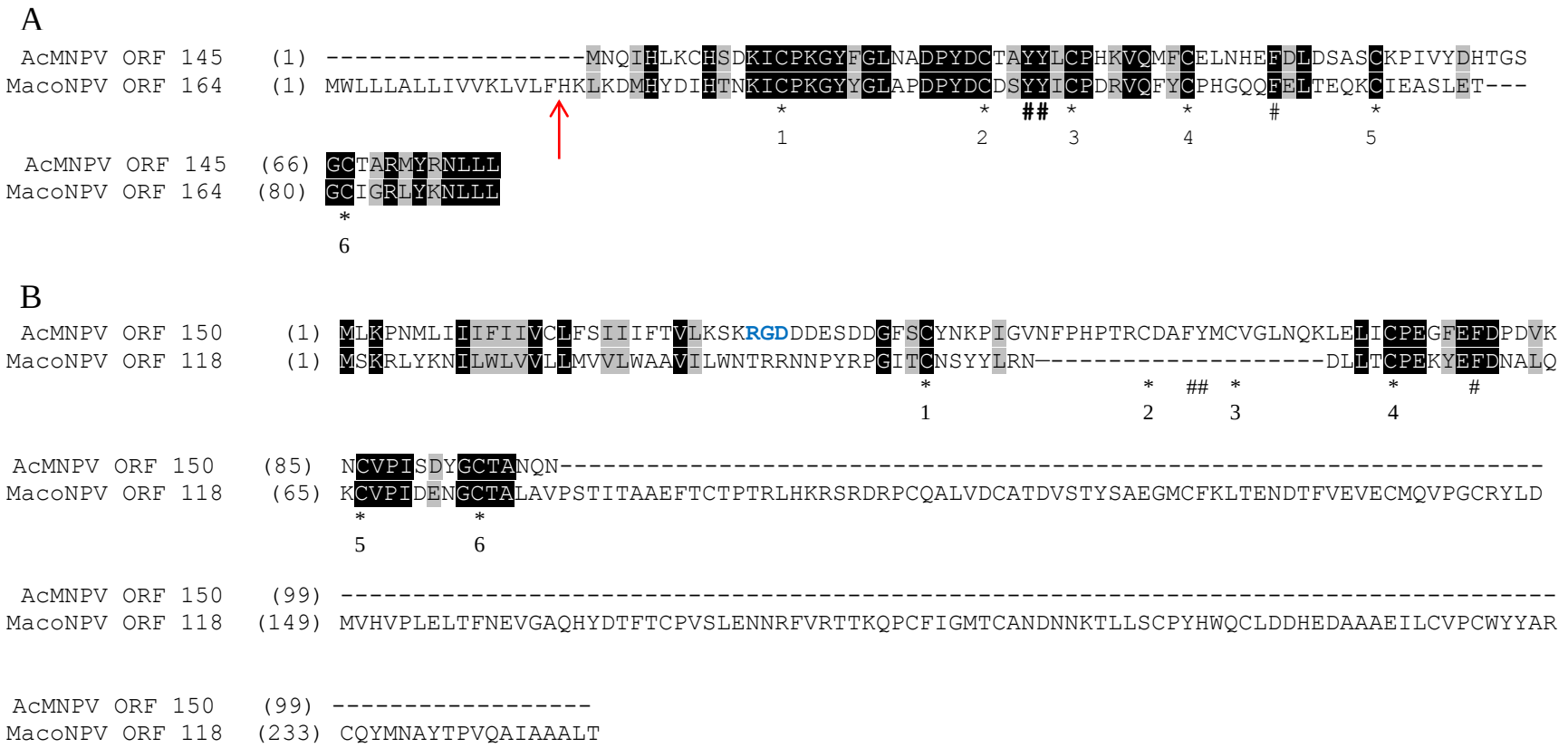

Figure 10. Amino acid alignment of homologous 11K proteins.
Panel A: Ac145 and Maco164 alignment. Panel B: Ac150 and Maco118 alignment. Conserved cysteine residues are indicated by an asterisk and are labelled 1 through 6 to indicate the 6 cysteine residues present in the CBD. The conserved aromatic residues, phenylalanine (F) and tyrosine (Y) are indicated by #. Non-similar amino acids are represented with black text on a white background. Similar amino acids are represented by black text on a grey background, and identical amino acids are represented by white text on a black background. The predicted cleavage site for the Maco164 signal peptide is indicated by a red arrow. The RGD motif in Ac150 is indicated in blue bold text.

The online homology modeling software SWISS MODEL was used to predict the tertiary structures of Ac145, Ac150, Maco118, and Maco164. The SWISS MODEL program identified the antimicrobial peptide Tachycitin (protein database identifier 1dqcA) from the horseshoe crab, *Limulus polyphemus*, as the best fit template for Maco164 (e-value = 4.1 X 10^{-11}), Ac145 (e-value = 1.5 X 10^{-6}) and Ac150 (e-value = 9.4 X 10^{-14}). A suitable template protein was not found for Maco118. Structural models for Ac145, Ac150, Maco164, and Tachycitin are provided in Figure 11.

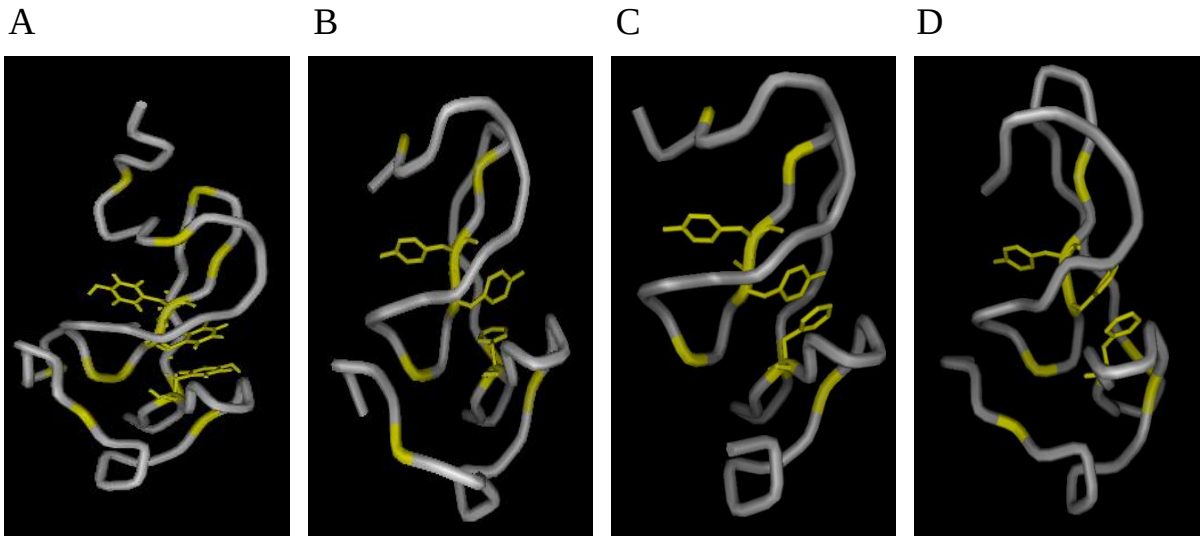

Figure 11. Protein structure model of the Tachycitin (A) protein from the horseshoe crab, *Limulus polyphemus*, compared to Maco164 (B), Ac145 (C), and Ac150 (D).
The 6 cysteine residues (10 in Tachycitin) are highlighted on the protein backbone in yellow. The three key aromatic residues involved in chitin binding are indicated by the yellow stick figures extending into the chitin-binding pocket.

4.4.2. Chitin-binding assays

Preliminary chitin-binding assays were performed for each of the four expressed proteins. The results from these experiments showed that each of the four proteins interacts with chitin (Figure 12).

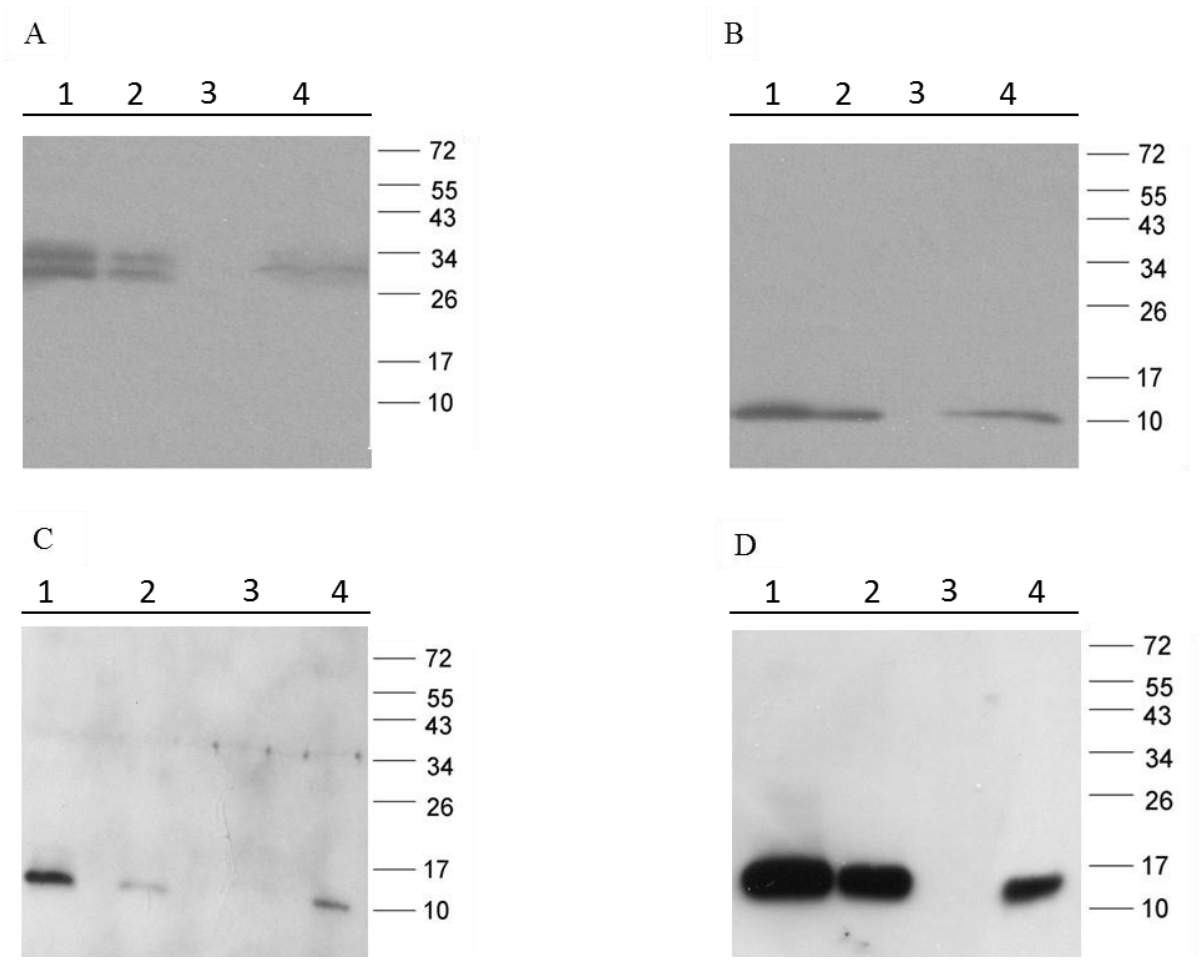

Figure 12. Preliminary chitin-binding assays for Maco118 (A), Maco164 (B), Ac145 (C), and Ac150 (D).
Lane 1 is the flow through fraction, lane 2 is the first wash, lane 3 is the tenth wash, and lane 4 is the released protein. A size marker (kDa) is provided for reference on the right hand side of each panel. The western blots were probed with a 1:1000 dilution of a purified HA.11 Clone 16B12 mouse monoclonal antibody followed by a 1:50,000 dilution of a goat anti-mouse IgG- HRP conjugated antibody. Expected protein sizes are 29.8 (A), 12.2 (B), 10.3 (C), and 12.6 (D) kDa, respectively.

A second set of chitin-binding assays was performed using HA-tag purified proteins in an attempt to determine the mechanism(s) involved in binding. Treatment with 2% SDS was able to release some, but not all of the bound protein from the chitin beads. Treatment with 0.5 M NaCl, 5% β-ME, and 0.2% or 1% Calcofluor did not cause a release of any of the bound protein from the chitin beads (Figure 13). Following treatment with various compounds, protein was bound to each bead fraction, including that which was treated with 2% SDS. This indicates that there is likely more than one mechanism involved in binding these proteins to the chitin beads.

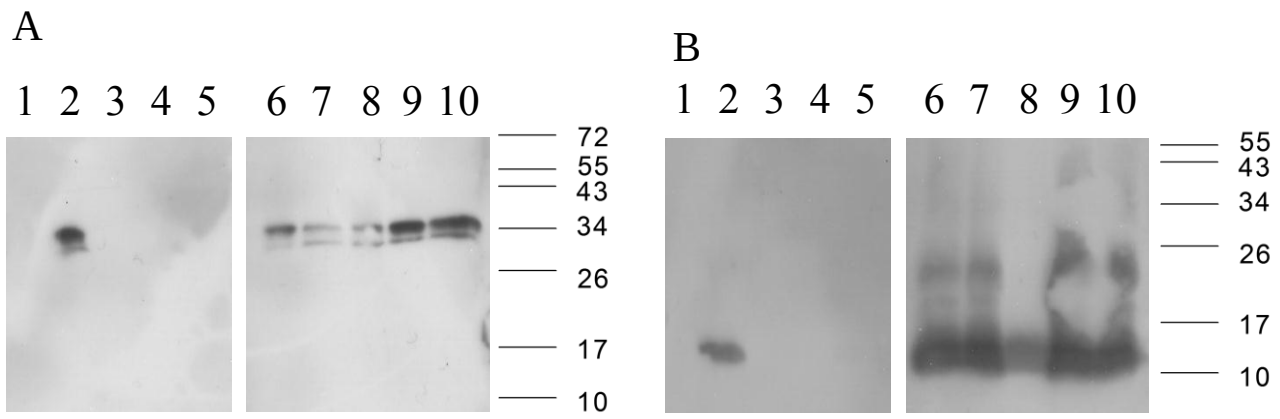

Figure 13. Chitin-binding assay to determine mechanisms involved in binding.
Chitin beads were incubated with HA-tag purified proteins overnight. The chitin beads were split into equal fractions and a different chemical was added to each fraction. Lanes 1 through 5 are the eluates from treatment with 0.5 M NaCl (1), 2% SDS (2), 5% β-ME (3), 0.2% Calcofluor (4), and 1% Calcofluor (5). Lanes 6 through 10 are the eluates from boiling the chitin beads in protein sample buffer after treatment with the various compounds. These samples are in the same order as lanes 1 to 5. The western blots were probed with a 1:1000 dilution of a purified HA.11 Clone 16B12 mouse monoclonal antibody, followed by a 1:50,000 dilution of a goat anti-mouse IgG- HRP conjugated antibody. The results for Maco118 are shown in panel A and Maco164 in

Exon 0

panel B. A size marker (kDa) is provided for reference on the right hand side of each panel. Expected protein sizes are 29.8 kDa and 12.2 kDa for Maco118 and Maco164, respectively. The elution pattern for Ac150 was the same as for the Maco118 and Maco164. The level of expression obtained for Ac145 did not allow for this type of follow-up binding experiment.

A third set of chitin-binding assays using combinations of 2% SDS, 5% β-ME, and 1% Calcofluor were performed. Protein was released following each treatment, which is consistent with the results from the second chitin-binding assay that showed that treatment with 2% SDS caused a release of some but not all of the bound protein. The addition of 5% β-ME or 1% Calcofluor to 2% SDS, or all three compounds together, does not appear to increase the amount of protein released from the chitin beads. The bead fractions were washed one time with PBS and then boiled in protein sample buffer to release any proteins that were still bound to the beads. Protein was released from each bead fraction, suggesting that another mechanism, which is still to be determined, is also involved in binding. The results from this experiment are presented in Figure 14.

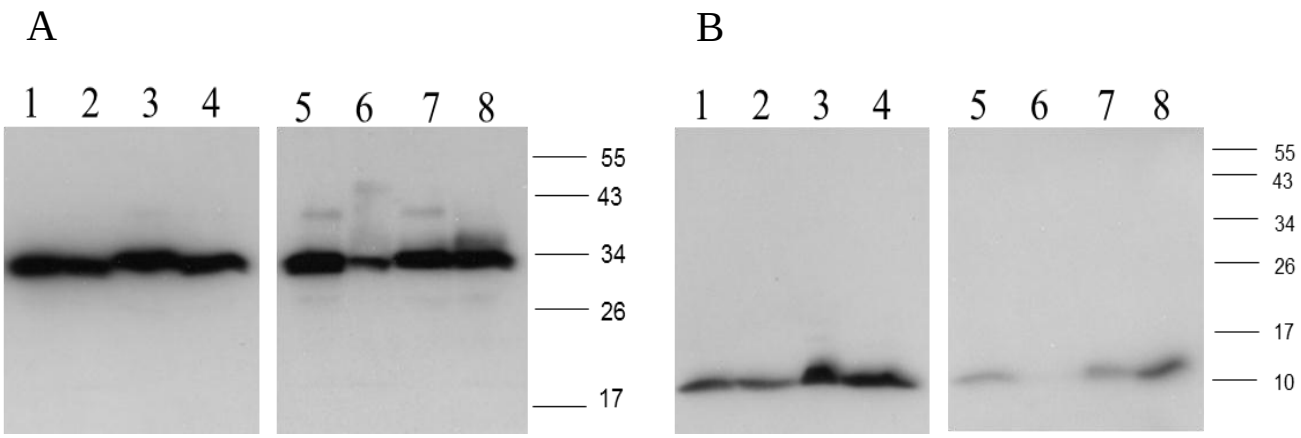

Figure 14. Second chitin-binding assay to determine mechanisms involved in binding. Chitin beads were incubated with HA-tag purified proteins overnight. The chitin beads were split into equal fractions and a different compound was added to each fraction. Lanes 1 through 4 are the eluates from treatment with 2% SDS (1), 2% SDS + 5% β-ME (2), 2% SDS + 1% Calcofluor (3), and 2% SDS + 5% β-ME + 1% Calcofluor (4). Lanes 5 through 8 are the eluates from boiling the chitin beads in protein sample buffer after treatment with the various compounds. These samples are in the same order as lanes 1 to 4. The western blots were probed with a 1:1000 dilution of a purified HA.11 Clone 16B12 mouse monoclonal antibody, followed by a 1:50,000 dilution of a goat anti-mouse IgG- HRP conjugated antibody. A size marker (kDa) is provided for reference on the right hand side of each panel. Expected protein sizes are 29.8 kDa for Maco118 (A) and 12.2 kDa for Maco164 (B). The elution pattern for Ac150 was the same as for the Maco118 and Maco164. The level of expression obtained for Ac145 did not allow for this type of follow-up binding experiment.

The specificity of the chitin-binding assay was examined using BSA and WGA. BSA does not contain a CBD and is not expected to bind to chitin. WGA contains a CBD and is known to bind specifically to chitin (98, 99). BSA or WGA were incubated with chitin beads overnight and bound protein was released from the beads by boiling in protein sample buffer. As expected, BSA did not bind to the chitin beads. The majority of BSA was present in the flow through fraction as unbound protein. Some BSA was recovered following the 1st wash of the chitin beads. No BSA was recovered in the 10th wash fraction, or in the eluent from boiling the chitin beads in protein sample buffer. The results for the BSA binding experiment are provided in Figure 15.

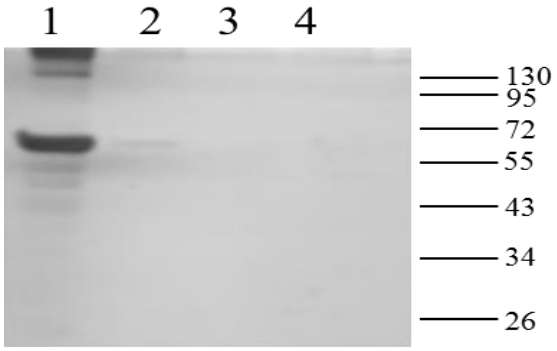

Figure 15. BSA chitin-binding assay.
Lane 1 is the flow through, collected following the overnight incubation of BSA with chitin beads. Lane 2 is the first wash, lane 3 is the tenth wash, and lane 4 is the eluate after boiling the beads with protein sample buffer. A size marker (kDa) is provided for reference on the right hand side of the panel. Expected protein size for BSA is 66.4 kDa. This gel was stained with the Invitrogen Silver Xpress Kit.

As predicted, WGA bound to the chitin beads. As with the 11K proteins, some of the bound WGA was released from the chitin beads following treatment with 2% SDS and the combinations of compounds containing SDS. Each bead fraction retained some of the bound protein after treatment, suggesting that another mechanism is involved in the interaction. These results are consistent with the results from Maco118, Maco164, and Ac150. The results from this experiment are shown in Figure 16.

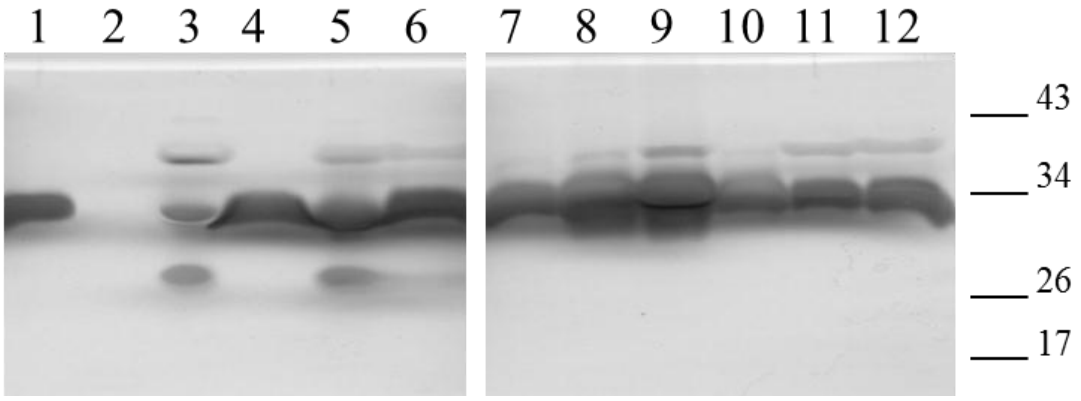

Figure 16. WGA chitin-binding assay.
Lanes 1 through 6 show the WGA fractions eluted from chitin beads using 2% SDS (1), 5% β-ME (2), 0.2% Calcofluor (3), 2% SDS + 5% β-ME (4), 2% SDS + 0.2% Calcofluor (5), and 2% SDS + 5% β-ME + 0.2% Calcofluor (6). Lanes 7 through 12 are the eluates from boiling the chitin beads in protein sample buffer after treatment with the various compounds. These samples are in the same order as lanes 1 to 6. A size marker (kDa) is provided for reference on the right hand side of each panel. Expected protein size for WGA is 36 kDa. This gel was stained with the Invitrogen Silver Xpress Kit.

Chitin binding experiments using HA-tag purified MsOSP were performed to eliminate the possibility that the HA tag was involved in an interaction with the chitin beads. The results from this experiment indicated that MsOSP protein interacts with chitin. Treatment with 0.5 M NaCl does not appear to have an effect on binding. Treatment with 2% SDS caused a release of all bound protein from the chitin beads, whereas treatment with 1% Calcofluor causes some, but not all of the protein to be released from the chitin beads (Figure 17 A). Treatment with combinations of 2% SDS with 5% β-ME or 1% Calcofluor or all three together, also caused a release of all bound protein (Figure 17 B).

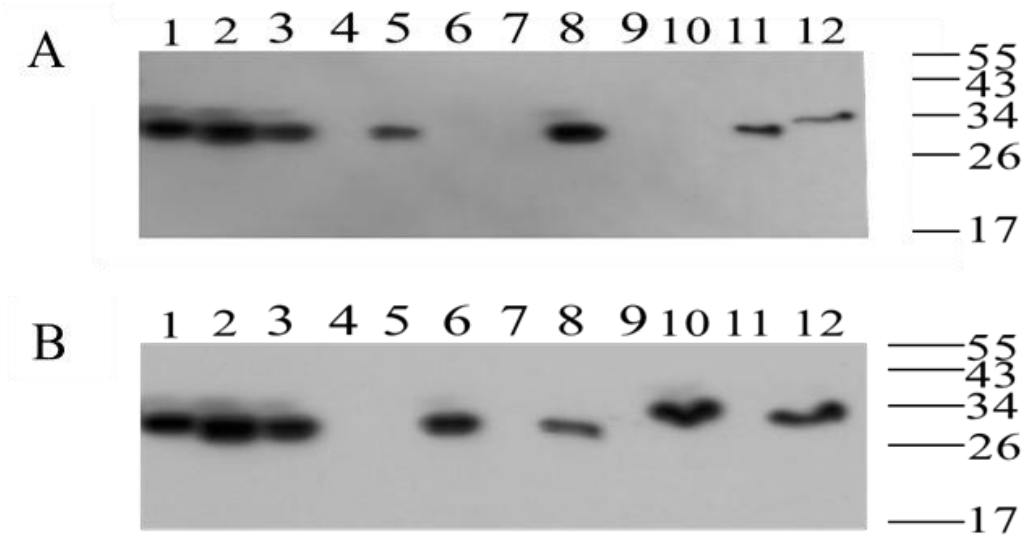

Figure 17. Chitin-binding experiments using HA-tag purified MsOSP-HA protein.
Panel A: First chitin-binding experiment. Lane 1: Neat HA-tag purified MsOSP, lane 2: Flow through, lane 3: wash 1, lane 4: wash 10, lane 5: chitin beads following treatment with 0.5 M NaCl, lane 6: supernatant from treatment with 0.5 M NaCl, lane 7: chitin beads following treatment with 2% SDS, lane 8: supernatant from treatment with 2% SDS, lane 9: chitin beads following treatment with 5% β-ME, lane 10: supernatant from treatment with 5% β-ME, lane 11: chitin beads following treatment with 1% Calcofluor, lane 12: supernatant from treatment with 1% Calcofluor. Panel B: Second chitin-binding experiment. Lane 1: Neat HA-tag purified MsOSP, lane 2: Flow through, lane 3: wash 1, lane 4: wash 10, lane 5: chitin beads following treatment with 2% SDS, lane 6: supernatant from treatment with 2% SDS, lane 7: chitin beads following treatment with 2% SDS + 5% β-ME, lane 8: supernatant for treatment with 2% SDS + 5% β-ME, lane 9: chitin beads following treatment with 2% SDS + 1% Calcofluor, lane 10: supernatant for treatment with 2% SDS + 1% Calcofluor, lane 11: chitin beads following treatment with 2% SDS + 5% β-ME + 1% Calcofluor, lane 12: supernatant for treatment with 2% SDS + 5% β-ME + 1% Calcofluor. A size marker (kDa) is provided for reference on the right hand side of the panel. Expected protein size for MsOSP-HA is 28.3 kDa.

4.5. Discussion

Ac145 and Ac150 are predicted to encode small proteins of approximately 11 kDa in size, with a hydrophobic N-terminus, corresponding to a membrane transit signal, and a 6 cysteine motif called a peritrophin A CBD (85-87). As expected, both proteins contain a CBD according to the prf and Pfam databases. Neither Ac145 nor Ac150 was predicted to have a signal peptide using the Signal P server. This is not in contradiction with the presence of a predicted membrane transit signal, as signal peptides and membrane transit signals serve different purposes. A membrane transit signal targets a pro-protein to a cellular organelle, whereas a signal peptide targets a pro-protein to the endoplasmic reticulum to be processed before being transported out of the cell via a secretory pathway (100, 101). The lack of a signal peptide, and therefore lack of secretion from the infected cell, is consistent with the findings of Lapointe et al. (87) who detected Ac145 and Ac150 within the nucleus of infected cells.

Zhang et al. (86) noted that Ac150 contains an RGD motif between the membrane transit signal and the CBD. This was confirmed *in silico* using the PROSITE freq pat database. RGD is an integrin-binding domain, which is predicted to play a role both in integrin-mediated signalling pathways as well as in cell attachment (102). The RGD motif has been shown to play a role in many cellular functions, including regulating gene expression, endocytosis, cell survival, and apoptosis (102, and references therein), though the exact role that the RGD motif plays in baculovirus infections remains to be determined (86, 102).

Ac145 and Ac150 have been shown to be incorporated into BV as well as OB (87). Localization specifically to the nucleocapsid or envelope fraction of the BV or ODV has yet to be demonstrated for these proteins. Ac145, which lacks a transmembrane domain and is therefore not predicted to be membrane-bound, is predominantly found within the BV, but is also incorporated to a lesser degree into the OB (87). Ac150, which does contain a transmembrane domain and is therefore predicted to be membrane-bound, is found in similar abundance in both BV and OB (87).

The presence of both Ac145 and Ac150 in the OB supports the hypothesis that these proteins may be required for initial oral infection of a host insect's midgut. The differences in abundance of Ac145 and Ac150 within the OB may be indicative of different roles for each protein within the infection cycle, specifically during initial infection. For example, the presence of an RGD motif within Ac150 may enhance attachment of the ODV envelope to the midgut epithelial cells,

or may facilitate the uptake of viral DNA and gene expression within the nucleus. The significance of Ac145 and Ac150 localizing to the BV is not clear, but will be studied in more detail, along with the functions of both proteins in Chapters 6 and 7 of this thesis.

The MacoNPV homologues to Ac145 and Ac150, Maco164 and Maco118, respectively, are predicted to contain a complete (Maco164) or partial (Maco118) CBD. Maco164 is comparable in size to Ac145, and these two proteins align well at the amino acid level. Maco164 was predicted to contain a signal peptide consisting of the first 16 N-terminal amino acids. This suggests that unlike Ac145, which is retained within the nucleus, Maco164 is likely secreted from the cell. Localization studies for Maco164 were not undertaken, and it is not clear what function Maco164 would have if secreted from the cell during the course of infection.

Maco118 is substantially larger than its AcMNPV homologue, Ac150. Maco118 contains a partial CBD at the amino terminus, and it aligns well with Ac150 at the amino acid level in this region. Maco118 does not contain an RGD integrin-binding domain, but like Ac150, it is predicted to contain a transmembrane domain at the amino terminus. To date, localization studies have not been undertaken for Maco118. The functions of Maco164 and Maco118 will be studied in greater detail in Chapters 6 and 7 of this thesis.

Ac145, Ac150, and Maco164 are predicted to have structures similar to that of the antimicrobial peptide Tachycitin from the horseshoe crab, *Limulus polyphemus*. Tachycitin is a known chitin-binding protein (103). It contains ten cysteine residues that form five disulphide bonds which promote the correct folding of the protein (103). Two aromatic residues, present as a "sandwich" platform, extend into a binding pocket (34, 103). These residues allow for an interaction to occur with the pyranose ring of chitin (104). A third aromatic residues protrudes into a secondary groove, but to date, there is no direct evidence that this residue is involved in the interaction with chitin (34).

As Ac145, Ac150, and Maco164 are expected to be chitin-binding proteins, the similarity in predicted structure between these proteins and Tachycitin supports this hypothesis. As Maco118 contains only a partial CBD and no other major motifs, it was not surprising that a suitable template structure was not found using the SWISS MODEL software. Lack of a suitable template does not indicate that Maco118 does not fold in a comparable way to the other 11K proteins, simply that there was no template protein with a similar primary sequence available on

which to base the predicted folding of Maco118. Further studies are required to determine the structure of Maco118.

Ac145, Ac150, Maco164, and Maco118 were expressed in the Bac-to-Bac baculovirus expression system. Each protein was tagged with an HA-epitope tag at the carboxy terminus to allow tracking via western blot analysis. Protein expression levels were qualitatively the highest between 72 and 96 hpi for all proteins.

Migration of the expressed proteins was close to what would be expected based on their molecular weights (Ac145 10.3 kDa, Ac150 12.6 kDa, Maco118 29.8 kDa, and Maco164 12.2 kDa). With the exception of Maco118, which migrates as a protein doublet at 28 and 34 kDa, all other proteins run as a single discrete band. The Maco118 protein doublet could indicate post-translational modification(s) or catalytic cleavage of the protein into alternate forms. *In silico* analysis of possible post-translational modification sites on Maco118 using the prediction software NetNGlyc 1.0 and NetOGlyc 3.1 (Centre for Biological Sequence Analysis, Technical University of Denmark), indicated a possible N-linked glycosylation site at amino acid 129, and possible O-linked glycosylation sites at amino acids 91, 93, and 249. Post-translational glycosylation or other modifications could explain the Maco118 protein doublet. Interestingly, Lapointe et al. (87) found that Ac150, the homologue of Maco118, migrated as a protein doublet when extracted from BV, but migrated as a single band of intermediate size when extracted from OB. As all protein expression experiments in this study used cell lysates and not BV, further work is required to determine if differential processing occurs in the BV and OB forms of Ac150 and Maco118.

Expressed proteins were purified from the total cellular milieu using an anti-HA tag purification kit. This kit greatly reduces, but does not eliminate, non-HA tagged proteins. To maintain the structure of the expressed proteins, the proteins were eluted from the anti-HA tag beads using purified HA peptide. This resulted in protein samples containing a considerable amount of free peptide. This prevented the accurate quantification of the expressed proteins using standard protein quantification assays. For all chitin-binding experiments, a set volume of infected cells was used in an attempt to standardize the amount of protein added to the chitin beads. It is recognized, however, that each protein may be expressed with varying efficiency and that different amounts of proteins were likely applied to the beads. As purified protein could

always be detected in the first wash fraction after binding, it was assumed that sufficient protein was used to saturate the chitin beads.

The majority of chitin-binding assays described in the literature demonstrate chitin-binding in one of two ways. Both methods involve incubating an expressed or purified protein with chitin (beads, powder, or reconstituted chitosan) then either boiling the protein-chitin mixtures in protein sample buffer to release the bound protein (see(103, 105, 106)for representative examples), or using a spectrophotometric or a colourmetric assay to determine the amount of free protein before and after incubation with chitin (see(107-109)for representative examples). Although this can be informative in that it provides information on the ability of a protein to interact with chitin, it does not provide any details about the mechanism(s) involved in, or the specificity of, the interaction. The approach used in this study was to determine if the proteins of interest were in fact able to bind to chitin, and if so, to investigate the mechanism(s) involved in binding.

Preliminary chitin-binding experiments using the expressed Ac145, Ac150, Maco118, and Maco164 indicated that all four proteins bound to chitin. Low levels of expression of Ac145 were observed in comparison to Ac150, Maco118, and Maco164. Several attempts were made to optimize the level of expression of Ac145 to produce sufficient amounts of protein for further binding studies. Unfortunately, sufficient quantities of Ac145 could not be produced, and further binding studies were carried out using Ac150, Maco118, and Maco164 only.

We predicted that the addition of compounds that disrupt the intramolecular disulfide bonds or intermolecular hydrogen bonds would likely interrupt binding, as disulfide bonds play a major role in the proper folding of the CBD (30, 88) and hydrogen bonds are involved in binding proteins containing a CBD to chitin (30, 92). It was expected that by treating the protein-bound beads with a disulfide bond reducing agent, such as β-ME, the protein would unfold and be released from the chitin beads. Treatment with up to 5% β-ME did not release of any of the proteins from the chitin beads. Likewise, neither treatment with NaCl (to disrupt potential ionic bonds), nor Calcofluor, a known chitin-binding compound (110), was able to release bound protein. This suggests that ionic bonds are not involved in this type of chitin-binding, and that Calcofluor may bind using a different mechanism than the 11K proteins or that the 11K proteins bind very tightly to the chitin beads so that Calcofluor could not compete for binding space.

The only compound that was able to release a portion of the bound protein was 2% SDS. No additional protein was stripped from the chitin beads when combinations of SDS with β-ME or Calcofluor or all three together were used. The ability of SDS to release some of the bound protein suggests that non-covalent interactions are a key factor in mediating binding. This finding supports the hypothesis that intermolecular hydrogen bonds or hydrophobic interactions exist between proteins containing a CBD and chitin. In addition, even though Maco118 does not contain a classic CBD, it is highly cysteine rich. As cysteine is a hydrophobic amino acid, it follows that this protein may interact with chitin via hydrophobic interactions. Combinations of SDS, β-ME, and Calcofluor could not release all of the bound protein, as demonstrated by protein remaining on the beads following elution with the various compounds. When the beads were boiled in sample buffer, more protein was released. This indicates that there is another mechanism involved in binding that has yet to be determined.

Positive and negative controls were run to validate the chitin binding assays. BSA was used as a negative control for binding. This protein was not expected to bind to chitin, and binding experiments confirmed this hypothesis. WGA, a known chitin-binding plant lectin (98, 99), was used as a positive control for binding. As expected, chitin-binding was demonstrated for WGA. Like Ac150, Maco118, and Maco164, some of the bound WGA was released from the chitin beads following treatment with 2% SDS. Release of bound WGA was not enhanced by the addition of Calcofluor or β-ME, which suggests that the mechanism of binding of WGA may be similar to that of Ac150, Maco118, and Maco164.

Chitin-binding assays were carried out using the HA-tagged MsOSP protein from the grasshopper *Melanoplus sanguinipes* to eliminate the possibility that the HA tag was involved in binding. MsOSP is predicted to be 242 amino acids in length (97). *In silico* analysis indicates that this protein is not cysteine-rich, but does contain a number of hydrophobic amino acids (40% of amino acids are hydrophobic). As MsOSP lacks a classic CBD, it was not expected to interact with chitin. An initial binding study using non-purified MsOSP indicated that there was an interaction between this protein and the chitin beads. Subsequent chitin-binding experiments indicated that treatment with 2% SDS released all bound protein into the supernatant fraction. Treatment with 5% β-ME caused MsOSP to precipitate out of solution and therefore no protein could be detected in either the supernatant or the bead fractions. Treatment with 1% Calcofluor caused some, but not all, of the bound protein to release. As treatment with 2% SDS released all

bound protein from the chitin beads, it does not appear that the addition of 5% β-ME and/or 1% Calcofluor to 2% SDS had an effect on protein binding. These results suggest that the interaction between MsOSP and chitin is mediated by non-covalent interactions. It also suggests that MsOSP binds to chitin via a similar mechanism to Calcofluor, but uses a different mechanism than the baculovirus 11K proteins. Based on these results, it does not appear that the HA tag is involved in the interaction between the expressed proteins and chitin.

Lapointe et al. (87) looked at the ability of Ac145 and Ac150 to bind to chitin *in vitro*. They used various conditions including high pH (up to 10.5) to mimic the larval midgut environment and attempted to show binding in the presence of midgut juice. All of their attempts to demonstrate chitin binding failed. There could be several reasons why they were unable to demonstrate chitin binding. First, they expressed Ac145 and Ac150 in a bacterial expression system, pGEX-KG. This could be problematic as these proteins presumably rely on disulfide bonds between the cysteine residues for proper tertiary structure. This type of folding can sometimes be difficult to induce in bacterial expression systems resulting in mis-folded proteins (111-114). In addition, Lapointe et al. omitted the N-terminal 22 or 30 amino acid in Ac145 and Ac150, respectively, in the expressed proteins. In Ac150, this region contains the predicted transmembrane domain and RDG integrin binding motif. It is not clear how the loss of either of these motifs would affect chitin-binding, but as they constitute approximately one third of the full-length protein, it is reasonable to suggest that deletion of this region would adversely affect folding of Ac150. In addition, it appears that for Ac145 removal of the N-terminal 22 amino acid results in deletion of the first cysteine residue of the CBD. Thus, only five of the six-cysteine residues involved in forming the CBD were expressed. It is therefore not surprising that they were unable to demonstrate chitin binding for this protein.

4.6. Conclusions and future research

The 11K gene products from AcMNPV, Ac145 and Ac150, and from MacoNPV, Maco118 and Maco164, bind to chitin. For Ac150, Maco118, and Maco164, the binding is mediated by hydrophobic interactions, but there is likely a secondary (and possibly other) binding mechanism involved in the interaction of the protein to chitin. The mechanism(s) involved in binding these proteins with chitin is similar to that of WGA, a plant lectin that is known to bind specifically with chitin. Further binding studies using other carbohydrate compounds, such as cellulose or

chitosan, should be conducted to ensure that the binding of Ac145, Ac150, Maco118, and Maco164 with chitin is specific. Optimization of expression of Ac145 should also be conducted to determine if this protein interacts with chitin via similar mechanisms to Ac150, Maco118, and Maco164.

In vivo or *in situ* binding studies could be conducted to determine the localization of these proteins during infection. Binding studies using tagged (fluorescent or otherwise) proteins could be conducted to see if the proteins bind to the chitin fibrils of the PM, the midgut epithelium, or to other insect tissues during the initial stages of infection.

Site directed mutagenesis could also be used to individually mutate each of the 6 cysteine residues or the 3 conserved aromatic residues in the predicted CBD and subsequently determine the effect on chitin binding. While this may not prove to be especially important in the case of these particular proteins and their role in infection, it may also be useful in developing a better chitin-binding assay to understand how proteins containing a CBD function. In particular, it would be interesting to determine if the aromatic residue predicted to extend into the secondary groove of the protein is involved in the interaction with chitin. There has been no direct evidence of an interaction between this residue and chitin or any other carbohydrate in the literature.

What remains to be determined for the 11K proteins is the role that they play in the baculovirus infection cycle. These questions will be addressed in Chapters 5-7 of this thesis.

5. TRANSCRIPTIONAL ANALYSIS OF AcMNPV ORF 145, 149, and 150

5.1. Introduction

5.1.1. AcMNPV

AcMNPV is the type species for the *Alphabaculovirus* genus. It is a large (133.9 kbp) double stranded DNA virus containing 151 ORF (51, 115). A significant amount of research has been conducted to determine the functions of the AcMNPV genes, with definitive functions being assigned for at least 60 of the ORF (115).

The two 11K genes from AcMNPV, ORF 145 and ORF 150, have been studied previously (see Section 2.3.8 for a review). Homologues of AcMNPV ORF 145 have been identified in all Alpha-, Beta-, and Gammabaculoviruses (115). Homologues of ORF 150 have been identified in a few *Alpha*- and *Betabaculovirus* species (115). While neither Ac145 nor Ac150 appears to effect cell-to-cell transmission in *in vitro* or *in vivo* studies (86, 87), their role in oral infectivity remains unclear. The degree of conservation of these genes among baculovirus species suggests that they likely play an important role in the baculovirus infection cycle.

Lapointe et al. (87) demonstrated that Ac145 and Ac150 are expressed from 24 hpi onwards, suggesting that ORF 145 and ORF 150 are late or very late genes. The locations of the transcription initiation and termination sites for these genes have not yet been mapped. The temporal transcription patterns and transcription regulatory regions of ORF 145 and ORF 150 will be investigated in this chapter. An *in silico* analysis will be conducted to predict the location of their transcriptional regulatory motifs. The location of these motifs will be confirmed by the use of 5′ and 3′ Rapid Amplification of cDNA Ends (RACE). The temporal transcription patterns of these genes will be determined using northern blot analysis. An additional AcMNPV gene, ORF 149 will also be studied, as this ORF overlaps with ORF 150. AcMNPV ORF 149 is not highly conserved among baculovirus species and no functional analysis has been conducted for this gene (115). A detailed description of this gene region is provided in Section 6.3.1.

5.2. Hypothesis

AcMNPV ORF 145 and ORF 150 are predicted to be late or very late genes, with transcripts detectable by 24 hpi. Transcription initiation for both genes is predicted to begin at a late gene [(A/G/T)TAAG(A/G/T)] or a very late gene promoter (ATAAG).

5.3. Materials and methods

5.3.1. Mapping the transcriptional regulatory sites for AcMNPV ORF 145, 149, and 150 using 5′ and 3′ RACE

The insect cell line TnHi5 (from parental strain BTI-TN-5B1-4 which was derived from embryonic tissue of the cabbage looper, *T. ni*), was propagated in GIM. Cells were incubated at 27^{o}C and passed weekly at a confluent cell suspension to medium ratio of 1:10.

Two 25 cm^{2} cell culture flasks (Corning Incorporated) were inoculated with 1.0 X 10^{6} TnHi5 cells per flask in 5 mL of GIM. The cells were allowed to adhere to the flask for 2 h at RT at which time the GIM was removed and discarded. P2 BV from AcMNPV strain E2 was added to each flask at a multiplicity of infection (MOI) of 5. The virus was allowed to bathe the cells by rocking the flask gently at RT for 2 h. The viral inoculum was removed from the flask, the cells washed once with 2 mL of GIM, and 5 mL of fresh GIM added to each flask. The flasks were incubated at 27^{o}C. Infected cells and BV were collected from one flask at 4 hpi and from a second flask at 24 hpi as described in Section 4.3.2., with the exception that the infected cell pellets were re-suspended in 350 µL of RLT buffer (QIAGEN) and frozen at -80^{o}C. The BV fractions were stored at 4^{o}C.

The infected cells were lysed by passing them several times through a 26-gauge sterile needle attached to a sterile, RNase-free syringe. Total RNA was extracted from the cell lysate using the QIAGEN RNeasy kit (QIAGEN) which included an on-column DNase 1 digestion to remove any contaminating genomic DNA. The RNA was quantified using a Nanodrop 1000 spectrophotometer and RNA quality confirmed by separating 2 µL of each sample in a 1.2% agarose gel in 10 mM sodium phosphate buffer and staining with GelRed.

The locations of the transcriptional start sites for *Ac145*, *Ac149*, and *Ac150* were mapped by 5′ RACE using the Invitrogen GeneRacer^{TM} kit (Invitrogen Corporation). Briefly, 3 µg of total RNA was dephosphorylated to select against non-full length mRNA by incubating with 1 X calf intestinal alkaline phosphatase (CIP) buffer, 40 U of RNaseOUT^{TM}, and 10 U CIP in a 10 µL total volume at 50^{o}C for 1 h. The 5′ cap structure was removed from the full length mRNA by incubating the dephosphorylated RNA with 1 X tobacco acid pyrophosphatase (TAP) buffer, 40 U of RNaseOUT^{TM}, and 0.5 U TAP at 37^{o}C for 1 h. The GeneRacer^{TM} RNA-oligo, which contains a priming site for the GeneRacer^{TM} 5′ Primer and GeneRacer^{TM} 5′ Nested Primer (Table 3), was ligated to the 5′ end of the de-capped RNA and the RNA reverse transcribed to cDNA

using gene-specific primers (GSP) and SuperScript III reverse transcriptase (Table 3) as described in the GeneRacer™ manual. RNA was removed by incubation with 2 U of RNase H at 37°C for 20 min.

The 5′ cDNA ends were amplified by PCR using a nested GSP (GSP 2) and the GeneRacer™ 5′ Primer (Table 3) as follows: in a 50 µL total reaction volume, 0.6 µM GeneRacer™ 5′ Primer was mixed with 0.3 µM GSP 2, 1 µL of the reverse transcribed cDNA, 1 X HF PCR buffer (Invitrogen Corporation), 10 mM of each dNTP, 2 mM $MgSO_4$, and 2.5 U of HF Platinum® *Taq* DNA polymerase (Invitrogen Corporation). A modified touchdown PCR method was used to amplify the cDNA ends. The reaction mixture was incubated at 95°C for 2 min followed by 5 cycles of 95°C for 30 s and then 72°C for 1 min. This was followed by 5 cycles of 95°C for 30 s and then 70°C for 1 min, followed by 25 cycles of 95°C for 30 s, 65°C for 30 s, and 68°C for 1 min. A final elongation step was carried out at 68°C for 10 min before holding the reaction at 4°C. Five microlitres of each PCR product were separated in a 1% agarose gel in TAE buffer with GelRed to ensure that a single product had been produced.

Nested PCR was performed to eliminate any non-specific PCR amplicons. The PCR reaction mixtures and the thermo cycling profile were the same as described above, except that 0.6 µM GeneRacer™ 5′ Nested Primer and 0.3 µM GSP 3 were used to prime the amplification. The nested PCR products were separated in a 1% agarose gel in TAE buffer with GelRed. The PCR bands were excised from the gel and the DNA was extracted using the QIAGEN Gel Extraction kit.

The gel-purified PCR products were cloned into the pGEM®-T-Easy vector (Promega Corporation, Madison, WI) by mixing the pGEM®-T-Easy vector DNA and gel-purified PCR product in a 1:3 ratio with 1 X Rapid Ligation Buffer with 3 U of T4 DNA ligase in a 10 µL total volume at 4°C overnight. Three microlitres of a ligation mixture were used to transform a 25 µL aliquot of electrocompetent *E.coli* DH10B cells as described in Section 4.3.2. Plasmid DNA was extracted from the *E.coli* cells following a standard alkaline lysis protocol. Five microlitres of plasmid DNA were digested with 1.5 U of *Eco*R1 in a 10 µL reaction with 1 X React 3 Buffer (Invitrogen Corporation) at 37°C for 2 h. The digested DNA samples were separated in a 1% agarose gel in TAE buffer and visualized with GelRed to identify clones with an appropriately sized insert. Several clones were selected and sequenced at PBI with primers SP6 and T7 (Table 3).

Table 3. Primers used to amplify the 5′ cDNA ends of *Ac145*, *Ac149*, and *Ac150*.

Primer Name	Sequence
GeneRacer™ RNA Oligo	CGACUGGAGCACGAGGACACUGACAUGGACUGAAGGAGUAGAAA
GeneRacer™ 5′ Primer	CGACTGGAGCACGAGGACACTGA
GeneRacer™ 5′ Nested Primer	GGACACTGACATGGACTGAAGGAGTA
AcORF 145 5′ RACE GSP 1	CATAGTAACAAGTTTC
AcORF 149 5′ RACE GSP 1	TGCAAAACTGCCGTCGTC
AcORF 150 5′ RACE GSP 1	GGTTAGCGGTACATCCATA
AcORF 145 5′ RACE GSP 2	ACCCGCTGCCCGTGTGA
AcORF 149 5′ RACE GSP 2	GGCAGCGGCGTCATGTTGGTAA
AcORF 150 5′ RACE GSP 2	ATCAAATTCAAATCCTTCAG
AcORF 145 5′ RACE GSP 3	GGCGGAGTCCAAGTCAAA
AcORF 149 5′ RACE GSP 3	TGGGCGAGAAGGCGCATTTGT
AcORF 150 5′ RACE GSP 3	TTGATTTAAACCGACACA
SP6 Universal Primer	ATTTAGGTGACACTATAG
T7 Universal Primer	TAATACGACTCACTATAGGG

The location of the downstream polyadenylation sites for *Ac145*, *Ac149*, and *Ac150* were determined by 3′ RACE using the GeneRacer™ kit (Invitrogen Corporation). One microgram of total RNA was used for each reaction. The RNA was reverse transcribed as described in the 5′ RACE section above, except that the GeneRacer™ Oligo dT primer (Table 4) was used for each reaction instead of a GSP. The initial and nested amplifications of the 3′ cDNA ends were carried out as described above. The initial amplification was carried out using 0.6 µM of the GeneRacer™ 3′ Primer and 0.3 µM of the 3′ RACE GSP 1 primer (Table 4), and the nested amplification was carried out using 0.6 µM of the GeneRacer™ 3′ Nested Primer and 0.3 µM of the 3′ RACE GSP2 primer. The 3′ cDNA products were gel-purified and cloned into pGEM®-T-Easy as described above, and several clones were sequenced with the SP6 and T7 primers.

Table 4. Primers used to amplify the 3′ cDNA ends of *Ac145*, *Ac149*, and *Ac150*.

Primer Name	Sequence
GeneRacer™ Oligo dT	GCTGTCAACGATACGCTACGTAACGGCATGACAGTG$(T)_{24}$
GeneRacer™ 3′ Primer	GCTGTCAACGATACGCTACGTAACG
GeneRacer™ 3′ Nested Primer	CGCTACGTAACGGCATGACAGTG
AcORF 145 3′ RACE GSP 1	AAAGGGTATTTTGGCCTCAAC
AcORF 149 3′ RACE GSP 1	ATGATATCTCTCCATTGTATGATCGC
AcORF 150 3′ RACE GSP 1	TTTGAAATCTAAAAGAGGTGACG
AcORF 145 3′ RACE GSP 2	TCTGTGTCCGCATAAAGTGC
AcORF 149 3′ RACE GSP 2	ATGCGCTCCACGGCGCGCGTTGATACGG
AcORF 150 3′ RACE GSP 2	TGGAGTAAATTTTCCGCATCC

5.3.2. Northern blot analysis

Six 75 cm^2 flasks were inoculated with 3.0 X 10^6 TnHi5 cells in GIM and the cells allowed to attach to the flasks overnight at RT. The GIM was removed and P2 BV from AcMNPV strain E2 added to each flask at an MOI of 5. The virus was allowed to bathe the cells by rocking the flask gently at RT for 2 h. The viral inoculum was removed and the cells washed once with 5 mL of GIM. The wash buffer was removed and 20 mL of fresh GIM added to each flask. This was recorded as time 0. The flasks were incubated at 27^{o}C and infected cells and BV collected from a single flask at 3, 6, 12, 18, 24, and 48 hpi as described in Section 4.3.2., with the exception that the infected cell pellets were re-suspended in 350 µL of RLT buffer and stored at -80^{o}C. The BV fractions were stored at 4^{o}C. Total RNA was extracted from the cell pellets using the QIAGEN RNeasy Kit as described above. Purified RNA samples were stored at -80^{o}C.

Six micrograms of total RNA from each time point were mixed with RNA sample buffer (30% v/v glycerol, 1.2% w/v SDS, 18.5 mM $NaPO_4$ dibasic, 21.5 mM $NaPO_4$ monobasic, 0.25% w/v bromophenol blue, 0.25% w/v xylene cyanol) and diethylpyrocarbonate (DEPC)-treated water in a final volume of 20 µL. The RNA samples were denatured by incubating at 70^{o}C for 10 min and then immediately chilled on ice. The RNA samples, along with 3 µg of a RNA marker (Invitrogen Corporation), were separated in a 1.2% agarose gel prepared in TAE buffer at 80 V for 2 h and stained with EnviroSafe dye (Helixx Technologies, Scarborough, ON). The RNA was transferred to a Nylon Hybond-N+ membrane (GE Healthcare) by capillary blotting following a standard northern blot protocol (96).

Strand-specific, ^{32}P-labelled RNA probes were produced to detect the *Ac145*, *Ac149*, and *Ac150* transcripts, as well as the *VP39* (major nucleocapsid protein) and *GP64* (EFP) transcripts.

Primers were designed to amplify small (approximately 200 bp) fragments from the 3′ end of each ORF (Table 5).

In a 50 µL reaction volume, 30 ng of AcMNPV E2 genomic DNA was mixed with 1 X HF PCR buffer (Invitrogen Corporation), 10 mM of each dNTP, 2 mM $MgSO_4$, 0.3 µM of each primer, and 2.5 U of HF Platinum® *Taq* DNA polymerase (Invitrogen Corporation). The PCR reaction mixture was incubated at 95°C for 2 min, followed by 35 cycles of 95°C for 30 s, 55°C for 30 s, and 72°C for 30 s. A final elongation step was carried out at 72°C for 10 min before holding the reaction at 4°C. The PCR products were separated in a 1% agarose gel in TAE buffer and stained with GelRed. The PCR amplicons were excised from the gel and DNA was extracted using the QIAGEN gel extraction kit. The PCR products were quantified using a Nanodrop 1000 spectrophotometer.

Table 5. Primer pairs used to amplify regions at the 3′ end of AcMNPV ORF 89 (*vp39*), 128 (*gp64*), 145, 149, or 150 for use as a single-stranded, ^{32}P-labelled probes for northern blot analysis.
Gene-specific sequences are in black, the T7 RNA polymerase promoter region is in blue bold, and additional nucleotides to aid in binding of the T7 RNA polymerase to the promoter site are in red bold. The sequences for primers 2022, 2023, 2024, and 2025 were kindly provided by Dr. David Theilmann, Agriculture and Agri-Food Canada (AAFC), Summerland BC, Canada.

Primer Name	Sequence	Amplifies
1991	AGGGTATTTTGGCCTCAACG	AcMNPV ORF 145
2019	**AGTATTATGCTGAGTGATATCCC**ATACATGCGAGCCGTACACC	
1994	TTGCTTCATACGTCGAGATACC	AcMNPV ORF 149
2020	**TCATAATACGACTCACTATAGGG**TGCCGTCGTCAATACAACAC	
1995	GAATCAGACGACGGGTTCAG	AcMNPV ORF 150
2021	**AGTATTATGCTGAGTGATATCCC**TTTTGGTTAGCGGTACATCC	
2022	**TCATAATACGACTCACTATAGGG**TGCGCTTGGAATTAAAATTCGCT	AcMNPV ORF 89 (VP39)
2023	GCGTATCATGACGATGGATG	
2024	**CATAATACGACTCACTATAGGG**TCAGCTCCTCTTGAATATGCA	AcMNPV ORF 128 (GP64)
2025	AGCTGCGTGTCTGCTCATTA	

T7 RNA polymerase was used to produce single-stranded RNA products from the double-stranded PCR products. T7 RNA polymerase recognizes the T7 RNA polymerase promoter region, which was engineered into each reverse primer and uses this region as the initiation site for synthesizing RNA from the DNA template in a strand-specific manner. Five hundred nanograms of purified PCR product were incubated at 95°C for 10 min to separate the two strands. The DNA was cooled on ice for 5 min and then the denatured DNA mixed with 50 U

RNaseOUT^{TM}, 500 µM ATP, CTP and GTP, 10 µM UTP, 1 X RNA polymerase reaction buffer (New England Biolabs Inc.), 50 U T7 RNA polymerase, and 50 µCi of ^{32}P labelled UTP (PerkinElmer Inc., Waltham, MA) in a final volume of 50 µL. The reaction mixture was incubated at 37^{o}C for 80 min. Two units of high quality, amplification grade DNase1 (Invitrogen Corporation) was added to the reaction mixture and then incubated at 37^{o}C for 15 min.

The nylon Hybond-N+ membrane was placed in a hybridization bottle and pre-hybridized with 20 mL of hybridization buffer (7% SDS, 0.25 M $NaPO_4$ dibasic, 0.25 M $NaPO_4$ monobasic, and 1% BSA) for 21 h at 65^{o}C. The probe was added to the hybridization solution and incubated with the membrane for 21 h at 65^{o}C. The membrane was washed twice, 15 min per wash, with 2 X saline-sodium citrate buffer (SSC) with 0.1% SDS at 65^{o}C, and then once with 0.2 X SSC with 0.1% SDS at 65^{o}C for 50 min. The membrane was wrapped in plastic wrap and placed inside a Spectroline Monotec lightproof autoradiography cassette. Kodak BioMax MR film was placed on top of the membrane for a variety of exposure times and films developed in a dark room using a Kodak M35A X-OMAT processor.

5.4. Results

5.4.1. Mapping transcriptional regulatory elements

Three potential transcription initiation sites were identified for *Ac145* using 5′ RACE. The bolded nucleotide represents the end of the 5′ or 3′ RACE product. These sites are indicated as initiation site (a), (b), and (c), respectively, on Figure 18. Initiation site (a) is a **G**AAT motif, which overlaps with the G of the predicted *Ac145* start codon (underlined). Initiation site (b) is a **C**TAA motif that is located 15 nt downstream from the *Ac145* predicted start codon, and initiation site (c) is an **A**AAA motif located 33 nt downstream from the *Ac145* predicted start codon. Two transcription termination sites were identified for *Ac145* using 3′ RACE. Termination site (a) is a CAGTT**G** motif, and termination site (b) is a CGCGC**G** motif, which are located 12 nt and 84 nt downstream from the predicted *Ac145* stop codon, respectively. A string of adenine residues was present following each of the termination sites.

Three transcription initiation sites were identified for *Ac149* using 5′ RACE. Initiation site (a) is an **A**TCA motif, site (b) is a **C**ATA site, and initiation site (c) is a second **A**TCA site, located 79 nt, 63 nt, and 61 nt downstream from the predicted *Ac149* start codon, respectively. A single termination site was identified using 3′ RACE. The transcript terminates at a TGCTT**T** motif,

located 19 nt downstream of the predicted *Ac149* stop codon. All transcripts that terminated at this location had a string of adenine residues appended following the TGCTT**T** motif.

Two transcript initiation sites were identified for *Ac150* using 5′ RACE. Transcript initiation site (a) is a **G**GCG motif located 411 nt upstream from the predicted *Ac150* start codon. Initiation site (b) is an **A**ATT motif located 57 nt downstream from the predicted *Ac150* start codon. A single termination site was identified by 3′ RACE at a CTAAC**C** motif located 5 nt upstream from the predicted *Ac150* stop codon. A string of adenine residues followed the CTAAC**C** motif.

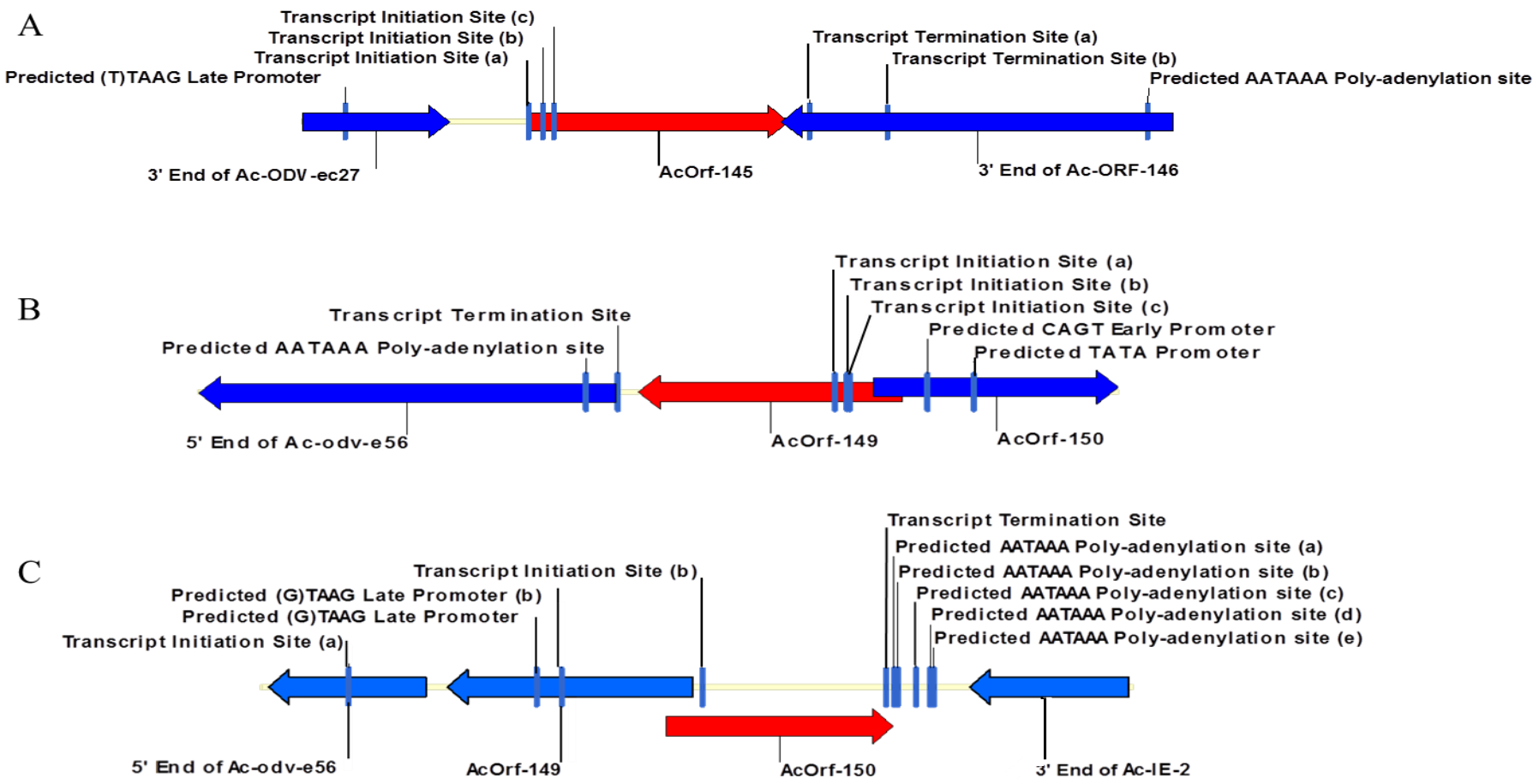

Figure 18. Location of transcription initiation and termination sites for *Ac145*, *Ac149*, and *Ac150* as determined by 5′ and 3′ RACE. The location of the predicted promoter motifs, which overlap the site of transcription initiation in most baculovirus genes, and the location of predicted polyadenylation signals are also indicated. The regulatory elements for *Ac145* are indicated in Panel A, *Ac149* in Panel B, and *Ac150* in Panel C. If multiple initiation or termination sites were indicated by the RACE data, these were designated as site (a), (b), (c), etc.

5.4.2. Northern blot analysis

Transcript sizes and temporal transcription patterns were determined for *Ac145*, *Ac149*, *Ac150*, *Ac128* (*gp64*), and *Ac89* (*vp39*) using northern blot analysis (Figure 19). Temporal expression patterns and transcript sizes for *Ac128* (1.59 kbp early and 1.66 kbp late transcript) (116, 117) and *Ac89* (2.2 kbp transcript) (118) have been previously determined, and these genes were included in the northern blot assay as control samples for early gene transcription (*Ac128*) and late gene transcription (*Ac128* and *Ac89*). The RNA samples used for the northern blot analysis were denatured by heat-treatment prior to electrophoresis on an agarose gel. As the transcript sizes obtained for *Ac128* and *Ac89* were not the same sizes as reported in the literature, estimates of transcript size are provided as millimetres migrated from the origin as opposed to absolute size, as we could not ensure that the RNA remained denatured during electrophoresis in agarose gels that did not contain standard denaturing agents.

Ac145 was transcribed from 18 hpi onwards. There appears to be one or more transcripts produced, with the predominant band migrating at 58 mm from the origin. Four different sized transcripts were produced for *Ac149*, migrating at 50 mm, 58 mm, 60 mm, and 67 mm from the origin. The 58 mm transcript was detected from 3 hpi to 6 hpi, while the 50 mm, 60 mm, and 67 mm transcripts were detected from 18 hpi to 48 hpi. Five transcripts were detected for *Ac150*, migrating at 45 mm, 54 mm, 56 mm, 59 mm, and 64 mm. The 64 mm transcript was detectable from 18 through 48 hpi, with the other transcripts detectable from 24 through 48 hpi. Two transcripts were produced for *Ac128*, one that migrated at 58 mm from 3 to 12 hpi, and a second that migrated at 55 mm from 18 through 48 hpi. Finally, *Ac89* produced a single transcript migrating 39 mm from the origin, which was present from 12 through 48 hpi.

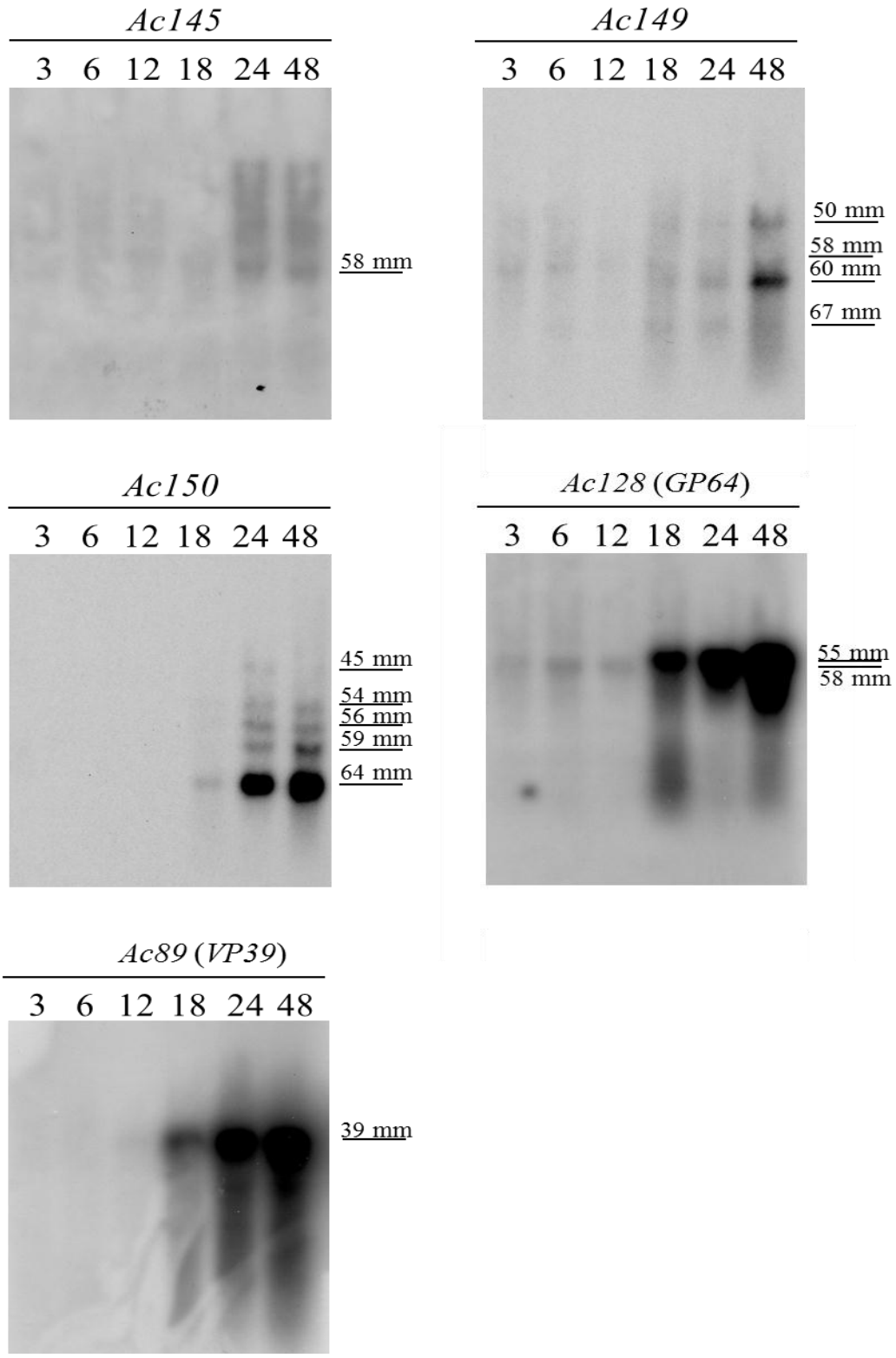

Figure 19. Northern blot analysis to determine the temporal transcription patterns and approximate transcript sizes of AcMNPV ORF 145, 149, 150, 128, and 89.
The numbers across the top of the gel (3, 6, 12, etc.) indicate hours post-infection. The distance migrated from the origin are provided in mm at the right hand side of each image.

5.5. Discussion

In silico analysis was conducted prior to completing the 5′ and 3′ RACE studies in order to predict the location of potential transcription initiation and termination sites. The sequence 200 nt upstream of the predicted start codon was scanned for the conserved early (CAGT), late (TAAG), or very late (ATAAG) promoters. Baculovirus promoter motifs typically overlap with the site of transcription initiation (43, 44, 46, 59, 60). The search was limited to 200 nt upstream of the start codon as the 5′ UTR for baculovirus genes tend to be less than 150 nt (43). If a CAGT early gene promoter was identified, a second search was conducted to locate an upstream TATA motif. A search was conducted in the 500 nt downstream of the predicted stop codon for each ORF to locate a polyadenylation signal (AATAAA). The 3′ UTR regions for baculovirus genes can be varied in length and 500 nt was selected as a starting point for locating the polyadenylation signal.

A putative late gene promoter, (T)TAAG, was located 156 nt upstream of the predicted start codon for *Ac145*. There was no CAGT early gene motif within 200 nt of the predicted start codon. This agrees with the findings of Lapointe et al. (87) who found that *Ac145* was expressed at late times post-infection. A putative polyadenylation signal was located 322 nt downstream of the predicted stop codon for *Ac145*. Using this information, the *Ac145* transcript was predicted to be 723 nt and be expressed at late times post-infection.

A CAGT early gene promoter motif was located 31 nt upstream of the *Ac149* predicted start codon. A further search revealed a TATA motif 88 nt upstream from the *Ac149* start codon. No late or very late gene promoter elements were identified within 200 nt of the *Ac149* start codon suggesting that it is an early gene. A polyadenylation signal was located 58 nt downstream from the predicted stop codon. Based on the location of the TATA motif and polyadenylation signal, the predicted transcript size for *Ac149* is 423 nt and is expected to be expressed at early times post-infection.

Two possible late gene promoters were identified upstream of the predicted *Ac150* start codon. One (G)TAAG motif was located 167 nt upstream of the start codon and another at 134 nt upstream. An early gene promoter was not identified within 200 nt of the start codon, suggesting that *Ac150* is a late gene. This agrees with the work of Lapointe et al. (87) who determined that *Ac150* is expressed at late times post infection. Several possible polyadenylation signals were located downstream from the predicted stop codon. These were located 1 nt, 6 nt, 30 nt, and 49

nt downstream from the predicted stop codon. It is possible that multiple transcripts are produced for *Ac150*, with predicted sizes ranging between 445 nt and 531 nt.

The 5′ RACE data indicated that *Ac145* is transcribed at late times (24 hpi) as expected. A 5′ RACE product was not detected at the 4 hpi time point. Several possible transcript initiation sites were identified. Site (a) was at a GAAT motif, which overlaps the G of the ATG predicted start codon. Site (b) was at CTAA site located 15 nt downstream of the predicted start codon, and site (c) was at an AAAA motif 33 nt downstream from the predicted start codon. These results were unexpected, as none of these motifs are classic baculovirus late gene promoter motifs. Although the 5′ RACE was completed using the Invitrogen GeneRacer^{TM} kit, which selects for full-length transcripts by excluding transcripts that lack a 5′ cap, it is possible that 5′ RACE product was prematurely truncated for *Ac145*. The 200 nt upstream of the *Ac145* start codon are highly AT rich (82%) and this could be problematic in terms of producing a full-length transcript through this region.

The 3′ RACE data for *Ac145* also did not agree with the predictions for location of the polyadenylation signal. The *Ac145* transcript was found to terminate in two locations: one at a CAGTTG site located 12 nt downstream of the predicted stop codon, or at a CGCGCG site located 84 nt downstream of the predicted stop codon. A polyA sequence was appended to each 3′ RACE product at these sites, suggesting that these may be true transcript termination sites. Using the experimentally located transcription initiation and termination sites, transcripts ranging in size from 211 nt to 316 nt are expected to be produced for *Ac145*. These sizes do not agree with the predicted transcript size of 723 nt. As the *Ac145* RACE results indicated that transcripts did not initiate or terminate at conserved transcriptional regulatory sites, it is possible that the RACE results were truncated.

Strand-specific northern blot experiments were used in an attempt to confirm the temporal expression patterns and transcript sizes of *Ac145*, *Ac149*, and *Ac150*. The northern blot results for *Ac145* indicate that it is transcribed from 18 hpi through 48 hpi, which agrees with the RACE data that suggests that it is a late gene. As well, Lapointe et al. (87) determined that *Ac145* is expressed at late times post infection. The predominant transcript migrated 58 mm from the origin. It is possible that other longer transcripts are also produced, but these bands were not easily distinguishable from one another on the northern blot. As *Ac145* lies within the intron region of the IE-0 gene, and as *Ac145* and IE-0 are in the same transcriptional orientation, it is

possible that the strand-specific probe designed for the northern blot analysis also anneals with the IE-0 transcript, which may explain some of higher molecular weight transcripts.

The RACE data for *Ac149* suggests that this gene is expressed both at early (4 hpi) and late (24 hpi) times. This agrees with the prediction that *Ac149* is an early gene, based on the presence of an early gene promoter complex consisting of a TATA motif and CAGT motif located 88 nt and 31 nt upstream of the ORF 149 start codon, respectively. The nearest late gene promoter motif (TAAG) is located 365 nt upstream of the predicted *Ac149* start codon. This motif was not identified in the initial search for promoter motifs as it is outside of the 200 nt window upstream from the start codon. Based on the 5′ RACE results obtained, it is impossible to say if transcription of *Ac149* at late times post-infection initiates at this point.

The 5′ RACE data for *Ac149* indicated that transcription initiates at one of three sites: an ATCA site, a CATA site, or a second ATCA site, located 79 nt, 63 nt, or 61 nt downstream from the predicted start codon, respectively. ATCA is part of the conserved baculovirus early gene INR motif (46), ATCA(G/T)T(C/T). Although the CAGT portion of the INR motif is most commonly used as the site of transcription initiation for baculovirus early genes, it is possible that the transcription of *Ac149* initiates at the ATCA motif. An ATCA motif is also part of the conserved gene promoter motif for many insect genes (119, 120). As baculovirus early gene transcription relies on host cell machinery, transcription initiation at a motif common to insect genes could facilitate this process.

The *Ac149* 3′ RACE data indicates that transcription terminates at a TGCTTT site, which is 19 nt downstream from the predicted stop codon and 33 nt upstream from the predicted polyadenylation signal. Sequence data from the 3′ RACE clones indicates that a string of adenines follows the TGCTTT site, suggesting that this is likely a true termination site of the *Ac149* transcript.

Northern blot analysis of *Ac149* indicates that four distinct transcripts were produced. A transcript that migrated 58 mm from the origin is present from 3 to 6 hpi, and three transcripts migrating at 50 mm, 60 mm, and 67 mm were present from 18 to 48 hpi, which is consistent with the RACE data that suggests that *Ac149* is expressed at both early and late times in infection. These results are significant because no studies have been completed for *Ac149* or its homologues in other baculovirus species to determine its temporal transcriptional patterns or the location of the transcription initiation and termination sites.

The RACE data for *Ac150* suggests that this gene is expressed at late times (24 hpi) in infection, which supports the findings of Lapointe et al. (87). RACE products were not detected for *Ac150* at the 4 hpi time point. Experimentally, the 5′ RACE data suggests that transcription of *Ac150* initiates at one of two locations: a GGCG motif located 411 nt upstream from the predicted start codon, or at an AATT motif located 57 nt downstream from the predicted start codon. Neither of these sites is a conserved baculovirus late gene promoter. If transcription actually initiated at the AATT motif it would result in a truncated protein with the nearest methionine residue producing a protein of 40 amino acids, which is not consistent with the expression results produced in Chapter 4 of this thesis or with the expression experiments of Lapointe et al. (87). It is likely that the transcripts initiated at this point were truncated during the 5′ RACE process. The nearest late gene promoter motif to the GGCG transcript initiation site is located 353 nt upstream. If this site were used, it would produce a 773 nt 5′ UTR for *Ac150*, which is significantly longer than the typical 150 nt baculovirus 5′ UTR.

Ac150 transcription terminates at a CTAACC site, which is 5 nt upstream of the predicted stop codon. A poly-A tail was appended to the transcript following the CTAACC motif, suggesting that this is the true transcript termination site. Transcriptional analysis by northern blot indicates that five distinct transcripts are produced for *Ac150*. These migrate at 45, 54, 56, 59, and 64 mm from the origin. The transcript that migrated to 64 mm is detectable from 18 hpi through to 48 hpi, while all others are present from 24 hpi through 48 hpi. This agrees with the 5′ RACE data and the findings of Lapointe et al. (87) which indicate that *Ac150* is a late gene.

5.6. Conclusions and future research

Ac145 and *Ac150* are late genes as confirmed by 5′ and 3′ RACE and northern blot. This agrees with the findings of Lapointe et al. (87) who determined that *Ac145* and *Ac150* are expressed at late times post infection. *Ac149* is transcribed at both early and late times post infection. This is the first report of the temporal transcription patterns for this gene. As non-denaturing agarose gels were used in the northern blot assay, future research should be conducted to determine the actual size of the *Ac145*, *Ac149*, and *Ac150* transcripts. Several attempts were made using two different methods to determine the location of the transcription initiation sites for *Ac145*, *Ac149*, and *Ac150*. As the 5′ RACE data for these genes did not terminate at conserved baculovirus promoter motifs, follow up studies should be conducted to

determine if these RACE results were prematurely truncated, or if these genes employ non-traditional promoter motifs.

6. CREATION AND CHARACTERIZATION OF KNOCKOUT AND REPAIR VIRUSES

6.1. Introduction

Determining the function of a specific gene can be quite difficult (121). The development of gene knockout constructs, in which a specific gene(s) is functionally deleted from the organisms genome, allows for the observation of changes in phenotype obtained from the loss of the individual gene(s) (121). Observable changes in phenotype can be compared to that of the wt, and inferences can be made about the function of the deleted-gene based on this comparison (121). A bacmid system, based on AcMNPV, has been developed and employed extensively in gene function studies (89-91). This system allows for the precise deletion of a specific gene(s), and provides an opportunity to study the function of individual AcMNPV genes.

6.1.1 Baculovirus knockout and repair constructs using bacmid technology

The bMON14272 bacmid (Invitrogen Corporation), which was introduced in Section 4.1.1, contains the entire AcMNPV genome and ORI for both bacterial and insect cells. It also has a modified *Polh* locus in which the native *Polh* ORF has been replaced with a mini-*att* Tn7 target site. Although designed for use as a protein expression vector, this bacmid has been used successfully as an efficient system for producing gene-knockout constructs in an AcMNPV backbone.

An AcMNPV GOI is replaced with an antibiotic selection marker via homologous recombination. Recombinant clones are selected using medium containing this selection marker. In order for the recombinant bacmid to produce OB within infected cells, the native *Polh* gene must be re-inserted into the bacmid backbone. This is done using the transfer vector, pFAcT-GFP (7.7 kbp) (122), which contains the native AcMNPV *Polh* gene, a *GFP* gene, and a second antibiotic resistance gene, all of which are flanked by Tn7L and Tn7R sites. When this vector is introduced into *E.coli* cells containing the recombinant bacmid and a helper plasmid, pMON7124 (13.2 kbp, Invitrogen Corporation) that carries a transposase gene, a Tn7-mediated transposition event occurs, in which the *Polh*, *GFP*, and antibiotic resistance gene are transferred from the pFAcT-GFP vector to the recombinant bacmid at the mini-*att* Tn7 target site. These recombinant knockout bacmids can be selected using the appropriate antibiotics and screened by PCR to confirm that the GOI has been deleted.

Repair constructs in which the native GOI has been re-inserted into the bacmid backbone are created using a similar technique. The pFAcT-GFP vector is modified so that in addition to the *Polh*, *GFP*, and antibiotic selection marker, it also contains the coding sequence for the GOI. This repair-pFAcT-GFP vector can be transformed into *E.coli* cells containing the recombinant knockout construct as described above to produce bacmids in which the GOI is replaced with an antibiotic selection marker, and has the native *Polh*, a *GFP* gene, a second antibiotic selection marker, and the GOI inserted at the mini-*att* Tn7 target site.

Producing a repair construct in addition to each knockout construct is important to ensure that any change in the phenotype of the virus is due to the loss of the GOI and not due to any of the genetic manipulations to the bacmid backbone. The repair construct is expected to rescue the wt phenotype. If it does not, then the phenotype observed for the knockout construct may be due to an unintentional mutation elsewhere in the genome and cannot be attributed to the loss of the GOI. If the wt phenotype is rescued with the repair virus, then one has more confidence that any change in phenotype between the knockout and the wt or repair is due to the loss of the GOI and not due to altering another gene within the genome.

Knockout constructs will be produced for AcMNPV ORF 145, ORF 150, or both together using the bMON14272 bacmid system. A range of repair constructs will be produced in which the GOI will be repaired with the native AcMNPV gene or with the MacoNPV homologue.

6.2. Hypothesis

The AcMNPV 11K genes, *Ac145* and *Ac150*, are predicted to be involved in oral infectivity; therefore, deletion of ORF 145, ORF 150, or both together from the viral genome is not predicted to alter the level of, or timing of transcription of other genes within the AcMNPV genome. Deletion of the 11K genes is not predicted to have an effect on the rate of budded virus production or viral DNA replication.

6.3. Materials and methods

6.3.1. Primer design for gene knockout and repair bacmid constructs

Special attention was required when designing the primers to produce the knockout and repair constructs as the intragenic regions in the AcMNPV baculovirus, and consequently the bMON14272 bacmid, are quite short, and in some cases adjacent ORF or transcripts overlap.

When disruption of a promoter, stop codon, or polyadenylation signal could not be avoided due to overlap with a GOI, these elements were engineered into the knockout primers to ensure that the expression of non-target genes was not altered.

The AcMNPV ORF 145 gene resides within the intron of the IE0/IE1 gene – the only known spliced baculovirus gene (Figure 20). Care was taken to ensure that transcription of IE0 and IE1 were not affected by knocking out ORF 145.

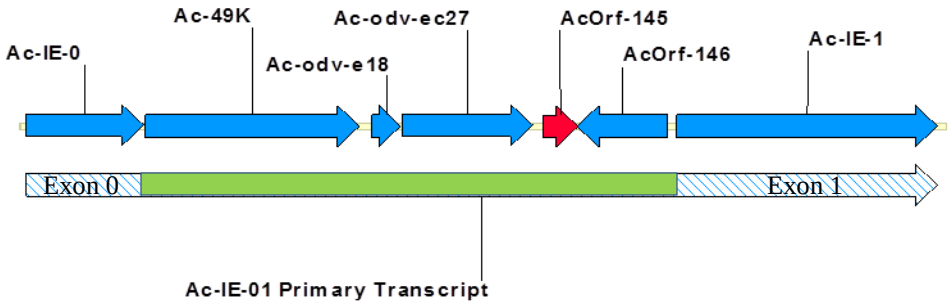

Figure 20. The AcMNPV IE0/IE-1 gene region.
AcMNPV ORF 145 is indicated by the red arrow. The IE-0/IE-1 primary transcript extends from exon 0 (IE-0/ORF 141) to exon 1 (IE-1/ORF 147). The intronic region of this transcript, indicated on the figure by a green bar, is spliced out to produce a mature IE-0 transcript (exon 0 and exon 1). The IE-1 mature transcript consists of exon 1 only. As IE-0 and IE-1 share a common 3′ end (exon 1), they are indistinguishable from one another in this region (123).

The transcriptional regulatory elements for the genes flanking ORF 145, ODV-EC27 and ORF 146, have been mapped (124, 125). There is a 6 bp overlap between the 3′ end of ORF 145 and the 3′ end of ORF 146. The polyadenylation signal for ORF 146 (AATAAA) has been mapped to a location 299 bp downstream of the ORF 146 stop codon. This long 3′ UTR encompasses the entire ORF 145 (Figure 21). The polyadenylation signal (AATAAA) and the stop codon (TAA) for ODV-EC27 are immediately adjacent to one another (AATAAA**TAA)** and do not overlap with ORF 145.

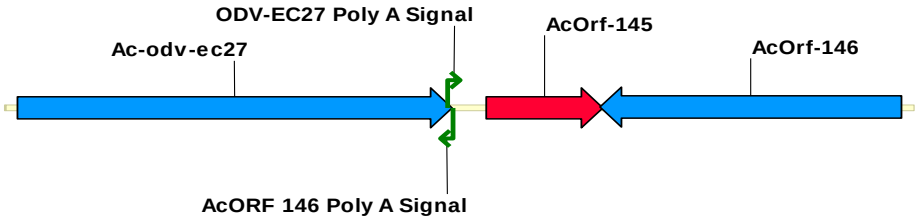

Figure 21. Location of the AcMNPV ODV-EC-27 and AcMNPV ORF 146 polyadenylation signals.

To create the ORF 145 knockout cassette, the primer pair 1953 and 1954 (Table 6) were used. The forward primer, 1953, contains 50 nt at its 5′ end that are homologous to the extreme 3′ end of ODV-EC27 (ORF 144). As there is no overlap between this ORF and ORF 145, the native ODV-EC27 polyadenylation signal and stop codon remain intact within this primer. The 20 nt at the 3′ end of primer 1953 provide a priming region for the amplification of the chloramphenicol acetyl-transferase (CAT) gene.

The reverse primer, 1954, includes 44 nt at the 5′ end that are homologous to the extreme 3′ end of ORF 146 including the ORF 146 native stop codon. As the native polyadenylation signal for ORF 146 is located in the knockout region between ORF 146 and ODV-EC27, a polyadenylation signal was engineered into primer 1954 immediately following the stop codon for ORF 146. The 18 nt at the 3′ end of primer 1953 provide a priming region for the amplification of the CAT gene.

There is a 35 bp overlap at the 5′ ends of ORF 149 and ORF 150 (Figure 22). At the time of production of these knockout constructs, the temporal expression of ORF 149 was not known, nor was the location of the transcriptional regulatory elements for this gene. As it was unknown if ORF 149 was an early or late gene, transcriptional regulatory elements could not be engineered into the knockout primer without the risk of altering the temporal expression of this gene. To circumvent this problem, a double knockout construct was created in which both ORF 149 and ORF 150 were deleted. The function of ORF 149 was subsequently restored through the use of specially designed repair constructs.

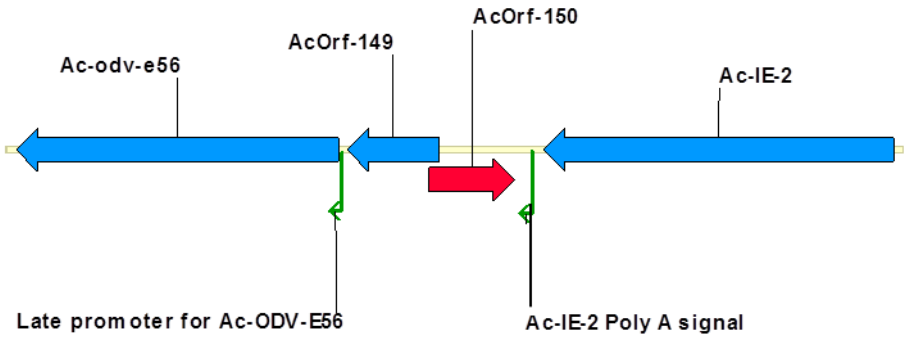

Figure 22. The AcMNPV ORF 149 and 150 gene region including the location of the AcMNPV ODV-E56 promoter and IE-2 polyadenylation signal.

The promoter region for ODV-E56 (ORF 148) had been mapped previously (126), as had the polyadenylation signal of IE-2 (ORF 151) (127) (Figure 22). Primers 1955 and 1956 (Table 6) were designed to knockout both ORF 149 and ORF 150. Primer 1955 contains 43 nt at the 5′

end, which are homologous to the region surrounding the ODV-E56 start codon and include the native ODV-E56 late promoter. The 3′ terminal 20 nt of primer 1955 provide a priming site for amplification of the Zeocin (Zeo) resistance gene. Primer 1956 has 40 nt at the 5′ end, which are homologous to the extreme 3′ end of IE-2 (ORF 151). A polyadenylation signal was engineered into 1956 and it overlaps with the native IE-2 stop codon (TAA). The remaining 24 nt at the 3′ end of this primer allow for amplification of the Zeo resistance gene.

PCR primers were designed to produce repair cassettes containing the native *Ac145* (primers 1960 and 1961) or the MacoNPV homologue, *Maco164* (primers 1985 and 1986). The forward primer for both cassettes comprise an *Xho*1 restriction site, followed by a late promoter (TAAG) motif and the 5′ UTR leader sequence from MacoNPV ORF 89 (*enhancin*). This leader sequence is quite short (14 bp) and has been used successfully in these types of repair constructs to replace native UTR regions, which can be up to 150 bp long. The reverse primer for both cassettes incorporates the sequence for the HA-epitope tag, an engineered stop codon and polyadenylation signal, as well as an *Xba*1 restriction site. A third set of primers (2001 and 2002) was produced to amplify *Ac145* as described above, but these primers contain *Not*1 and *Sst*1 restriction sites instead of *Xba*1 and *Xho*1.

A double repair construct to rescue function of both ORF 149 and ORF 150 was produced using primers 1958 and 1959. Primer 1958 contains sequence corresponding to the 3′ end of ORF 149, followed by the sequence for a c-MYC-epitope tag (derived from the myc family of transcription factors), an engineered stop codon and polyadenylation signal, and an *Xho*1 restriction site. Primer 1959 contains sequence corresponding to the 3′ end of ORF 150, followed by the sequence for an HA-epitope tag, an engineered stop codon and polyadenylation signal, and an *Xba*1 restriction site.

Primers for a second repair cassette were produced to amplify the MacoNPV homologue for *Ac150*, *Maco118*. Primer 1983 contains a *Not*1 restriction site followed by a late promoter motif, the leader sequence from *enhancin*, and sequence corresponding to the 5′ end of *Maco118*. Primer 1984 contains an *Sst*1 restriction site, an engineered polyadenylation signal and stop codon, the sequence corresponding to the HA-epitope tag, and sequence corresponding to the 3′ end of *Maco118*. Primers for a third repair cassette, which would restore the function of ORF 149, but not ORF 150, were also designed. Primers 1989 and 1990, which are reverse complements of one another, contain three engineered stop codons in the coding region of ORF

150. The coding region of ORF 149 was unaltered. All primer pairs used to create the repair constructs are listed in Table 7.

Table 6. Primer pairs used to produce the gene knockout constructs.
The regions of sequence that are underlined with a single line are homologous to the gene flanking the GOI. The region of the primer in bold black text is homologous to an antibiotic resistance cassette (chloramphenicol [Chl] or Zeo). Sequences in bold blue text are native transcriptional regulatory sequences. Sequences in bold black text and double underlined are native stop codons. The sequences in bold red text were engineered into the primer to maintain proper expression of non-target genes. The sequence AATAAA is a standard baculovirus polyadenylation signal.

Primer Name	Sequence	Amplifies
1953	ACTCAAATTCTGTAACATCAGGGTTTAATATATATAATTTT**AATAAA**<u>**TAA**</u>**GTGTAGGCTGGAGCTGCTTC**	ORF 145 knockout cassette (Chl. resistance)
1954	AAATCGATAATAGTGTTGTGCAACTGGAAACCCGCTCTTCA<u>**TAG**</u>**AATAAA****ATATGAATATCCTCCTTA**	
1955	TCACAGTAAAGGTTTTGCAAAACTGCCGTCGTCAATACAACAC**GGATCTCTGCAGCACGTGTT**	ORF 149 and 150 knockout cassette (Zeo. resistance)
1956	GATTTAGTTTCTAAGTTACAAACTGTTATGTCTAGACGTT<u>**AA**</u>**TAAA****AGACATGATAAGATACATTGATGA**	

Table 7. Primer pairs for creating the repair constructs.
Restriction sites are in black, bold and underlined text. The late promoter sequence (TAAG) along with the 5′ UTR leader sequence from MacoNPV ORF 89 (*enhancin*) are in black, bold text. The sequence corresponding to the HA-epitope tag is in green bold text. Stop codons are in red bold text. Polyadenylation signals are underlined with a double line. The sequence corresponding to the c-MYC-epitope tag is in purple bold text.

Primer Names	Sequences	Amplifies
1960 1961	CCG**CTCGAG**CCG**TTAAGCCATTATTATCATT**ATGAATCAAATTCATCTAAA GCG**TCTAGA**TTTATT**TTAGGCGTAGTCGGGCACGTCGTAGGGGTA**TAGTAACAAGTTTCTATACATG	AcMNPV ORF 145 repair cassette
1985 1986	CCG**CTCGAG**CCG**TTAAGCCATTATTATCATT**ATGTGGTTGTTATTAGCACT GCG**TCTAGA**TTTATT**TTAGGCGTAGTCGGGCACGTCGTAGGGGTA**TAGTAACAGATTTTTGTAAAG	MacoNPV ORF 164 repair cassette
1958 1959	GCG**CTCGAG**TTTATT**TCAAAGATCTTCTTCAGAAATAAGTTTTTGTTC**CAGTAAAGGTTTTGCAA GCG**TCTAGA**TTTATT**TTAGGCGTAGTCGGGCACGTCGTAGGGGTA**GTTTTGGTTAGCGGTAC	AcMNPV ORF 149 and 150 repair cassette
1958 1989 1959 1990	GCG**CTCGAG**TTTATT**TCAAAGATCTTCTTCAGAAATAAGTTTTTGTTC**CAGTAAAGGTTTTGCAA CGTCTGATTCGTCATCGTCACC**TCATTA**AGA**TTA**CAAAACAGTAAAAATAATTATTGA GCG**TCTAGA**TTTATT**TTAGGCGTAGTCGGGCACGTCGTAGGGGTA**GTTTTGGTTAGCGGTAC TCAATAATTATTTTTACTGTTTTG**TAA**TCT**TAATGA**GGTGACGATGACGAATCAGACGACGGGTTCAG	AcMNPV ORF 149 repair cassette
1983 1984	GAAT**GCGGCCGC**CCG**TTAAGCCATTATTATCATT**ATGTCAAAACGACTCTACAAA GCG**GAGCTC**TTTATT**TTAGGCGTAGTCGGGCACGTCGTAGGGGTA**GGTTAATGCTGCGGCAATCG	MacoNPV ORF 118 repair cassette
2001 2002	GAAT**GCGGCCGC**CCG**TTAAGCCATTATTATCATT**ATGAATCAAATTCATCTAAA GCG**GAGCTC**TTTATT**TTAGGCGTAGTCGGGCACGTCGTAGGGGTA**TAGTAACAAGTTTCTATACATG	AcMNPV ORF 145 repair cassette (for use in the triple knockout)
DT 882 DT 891	CGCACCACAAAGATGT TATTAGTTTGTGCGT	Sequencing pFAcT-GFP constructs

6.3.2. Production of knockout and repair bacmid constructs

The preparation of the knockout bacmids is based the protocol developed by Datsenko and Wanner (128). An overview of the process is provided in Figure 23. The complete process is described below.

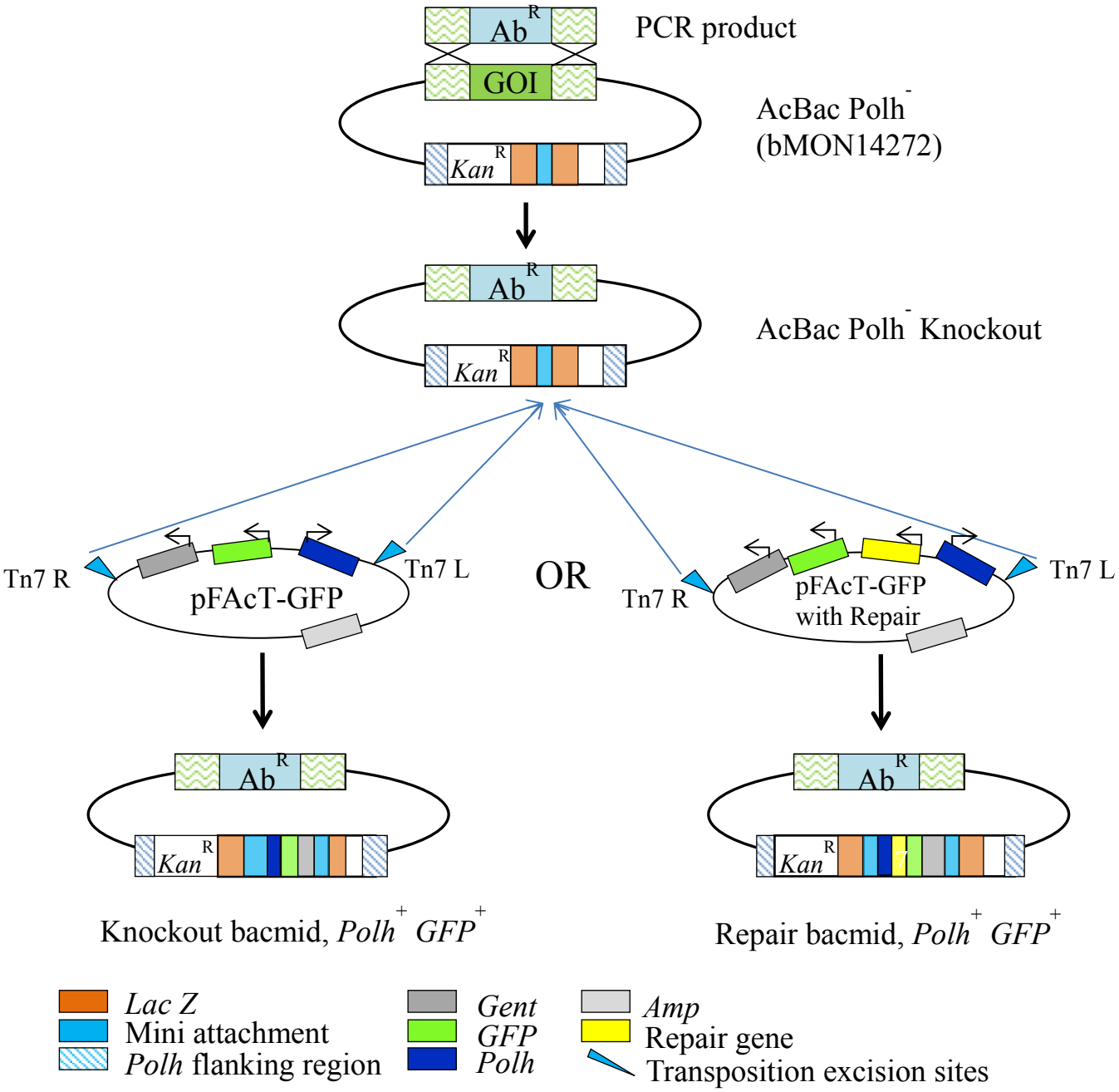

Figure 23. Procedure for creating knockout and repair bacmids.
Adapted from the Bacmid Knockout Protocol used in the Theilmann lab, AAFC, Summerland BC, Canada.

The preparation of electrocompetent *E.coli* cells using no salt media is based on Sharma and Schimke (129). *E.coli* K-12 strain BW25113 harboring the pKD46 (Amp^R) recombination plasmid and the bMON14272 bacmid (Kan^R) were grown on low salt LB plates supplemented with 100 µg/mL Amp and 50 µg/mL Kan overnight at 30°C. A single colony was selected and used to inoculate 5 mL of yeast extract and nutrient broth (YENB – 0.75% yeast extract, 0.8% nutrient broth) medium supplemented with 100 µg/mL Amp, 50 µg/mL Kan, and 1 mM of L-arabinose. The cultures were incubated overnight at 30°C with shaking at 225 rpm. The 5 mL culture was used to inoculate 500 mL of YENB supplemented with 100 µg/mL Amp, 50 µg/mL Kan, and 1 mM of L-arabinose. The culture was incubated at 30°C for 4 h with shaking at 225 rpm and the cells were pelleted at 3000 rpm for 10 min at 4°C in a Sorvall RC5C Plus centrifuge (Thermo Fisher Scientific). The cells were re-suspended in 100 mL of cold sterile distilled water and then re-pelleted by centrifugation. This wash process was repeated a second time. The wash process was carried out a third time with the cells being re-suspended in 20 mL of cold 10% glycerol. The cells were pelleted a final time and then re-suspended in 2 mL of cold 10% glycerol. The cells were divided into 40 µL aliquots and stored at -80°C.

Recombination cassettes were produced by PCR. Primers 1953 and 1954 were used to amplify the CAT gene from the plasmid pKD3 (Appendix A). Primers 1955 and 1956 were used to amplify the Zeo resistance gene from the plasmid p2ZOp-2F (Appendix B). In a 25 µL reaction, 1 X Phusion HF buffer containing 1.5 mM $MgCl_2$ (New England Biolabs Inc.) was mixed with 0.5 µM of forward primer, 0.5 µM of reverse primer, 0.4 mM dNTP mix, 0.25 U Phusion HF DNA polymerase, and 0.5 ng of template DNA. The PCR reactions were incubated at 98°C for 30 s, followed by 30 cycles of 98°C for 10 s, 65°C for 30 s, and 72°C for 15 s, followed by a final extension at 72°C for 10 min before holding at 20°C. The PCR products were separated in a 0.7% agarose gel in TAE buffer at 50 V for approximately 1 h and visualized by staining with ethidium bromide. The PCR products were excised from the gel and the DNA extracted using the E.Z.N.A. ® Gel Extraction Kit (VWR International, Radnor, PA) following the manufacturer's protocol. The DNA was quantified using a BioPhotometer 6131 spectrophotometer (Eppendorf, Mississauga, ON).

One hundred nanograms of a recombination cassette were transformed into electrocompetent BW25113 cells containing the bMON14272 bacmid and the pKD46 plasmid. The cells were pulsed at 1.5 kV, 25 µF, and 200 Ω. One millilitre of low salt LB broth was added to the cells

immediately following the pulse. The cells were allowed to recover overnight at 37^{o}C with shaking at 225 rpm. Two hundred microlitres of the transformation mixture were plated onto low salt LB plates supplemented with 50 µg/mL Kan and either 17 µg/mL Chl (for cells transformed with the 1953-1954 cassette) or 30 µg/mL Zeo (for cells transformed with the 1955-1956 cassette). The plates were incubated at 37^{o}C overnight. Colonies were replica plated onto low salt LB plates supplemented with 50 µg/mL Kan and either 17 µg/mL Chl or 30 µg/mL Zeo, as well as onto low salt LB plates supplemented with 100 µg/mL Amp. This step was done to select for clones that had lost the pKD46 plasmid (Amp^{R}) during outgrowth at 37^{o}C.

Several colonies were selected from each transformation to inoculate 5 mL of low salt LB supplemented with appropriate selection antibiotics. The cultures were incubated overnight at 37^{o}C. Bacmid DNA was extracted from the *E.coli* cells using a standard alkaline lysis miniprep procedure (96) with an isopropanol precipitation of the bacmid DNA. Following the re-suspension, the bacmid DNA was incubated at 65^{o}C for 10 min to denature any nucleases. The DNA was allowed to cool to RT and was then stored at -80^{o}C.

Triple knockout constructs in which AcMNPV ORF 145, ORF 149, and ORF150 were all deleted were created using a similar approach, except that the 1955-1956 recombination cassette was transformed into electrocompetent *E.coli* BW25113 cells containing the pKD46 recombination plasmid and the bMON14272$^{Ac145\ \text{null}}$ bacmid.

PCR was used to produce each repair cassette using the following primer combinations: 1960/1961, 1985/1986, 2001/2002, 1958/1959, and 1983/1984. In a 50 µL reaction, 1 X Phusion HF buffer containing 1.5 mM $MgCl_2$, was mixed with 0.4 mM dNTPs, 0.2 µM forward primer, 0.2 µM reverse primer, 0.25 U Phusion HF DNA polymerase, and 50 ng of vAcBac 887 DNA. The PCR reaction mixture was incubated at 98^{o}C for 30 s, followed by 30 cycles of 98^{o}C for 10 s, 55^{o}C for 30 s, and 72^{o}C for 10 s. A final extension of 72^{o}C for 10 min was followed by incubation at 4^{o}C.

The ends of the repair PCR cassettes were digested using either 3 U of *Xba*1 and 3 U of *Xho*1 or 3 U of *Sst*1 and 3 U of *Not*1, depending on the restriction sites present in the primers. All digests were carried out in 60 µL reaction volume at 37^{o}C for 2 h. The digested cassettes were separated in a 1% agarose gel in TAE buffer at 100 V for 40 min. The cassettes were excised from the gel and the DNA extracted using the QIAGEN Gel Extraction Kit.

Two PCR cassettes were produced using primer pairs 1958-1989 and 1959-1990. Primers 1989 and 1990 are reverse complements of one another. They were engineered to introduce three stop codons into the coding sequence of ORF 150 while leaving the coding sequence of ORF 149 intact. In a 50 µL reaction, 1 X Phusion HF buffer containing 1.5 mM $MgCl_2$ was mixed with 0.4 mM dNTPs, 0.2 µM forward primer, 0.2 µM reverse primer, 0.25 U Phusion HF DNA polymerase, and 50 ng of vAcBac 887 DNA. The PCR reaction mixture was incubated at 98^{o}C for 30 s, followed by 30 cycles of 98^{o}C for 10 s, 55^{o}C for 30 s, and 72^{o}C for 10 s. A final extension of 72^{o}C for 10 min was followed by incubation at 4^{o}C. The PCR products were separated in a 1% agarose gel in TAE buffer at 100 V for 40 min. The PCR cassettes were excised from the gel and DNA extracted using the QIAGEN Gel Extraction Kit. The gel purified PCR products were used as templates for a second PCR reaction. Seventy-five nanograms of each PCR product were mixed with 1 X Phusion HF buffer containing 1.5 mM $MgCl_2$, 0.4 mM dNTPs, and 0.25 U Phusion HF DNA polymerase in a 50 µL reaction. The samples were incubated at 98^{o}C for 30 s, followed by 5 cycles of 98^{o}C for 10 s, 55^{o}C for 30 s, and 72^{o}C for 20 s. A final elongation step was conducted at 72^{o}C for 5 min before cooling the samples to 20^{o}C for 1 min. This short reaction lacking primers allowed the ends of the overlapping PCR products to anneal to one another and produce a full-length PCR cassette. Primers 1958 and 1959 (0.1 µM each) were then added to the PCR reaction mixture and it was incubated at 98^{o}C for 30 s, followed by 25 cycles of 98^{o}C for 10 s, 55^{o}C for 30 s, and 72^{o}C for 20 s, followed by a final elongation at 72^{o}C for 10 min. The PCR products were separated in a 1% agarose gel in TAE at 100 V for 40 min. The PCR amplicon (1958-1959^{Mut}) was excised from the gel and the DNA extracted using the QIAGEN Gel Extraction Kit. The PCR amplicon was digested with *Xba*1 and *Xho*1 as described above.

The plasmid pFAcT-GFP (7.7 kbp), which contains genes to confer resistance to Amp and Gen, the native AcMNPV *Polh* gene, and a *GFP* gene was used to create the repair constructs. The *Gen*^{R}, *Polh*, and *GFP* genes are flanked by Tn7L and Tn7R sites. The sequences between these two sites are transferred into the mini-*att*Tn7 site in the *Polh* locus of the bMON14272 bacmid via Tn7 mediated transposition. There are *Xba*1 and *Xho*1 restriction sites located between *Polh* and *GFP* that allows for insertion of a repair gene in this region.

Five hundred nanograms of pFAcT-GFP plasmid were digested with *Xho*1 and *Xba*1 as described above. One unit of CIP was added directly to the restriction digest and incubated at

37°C for 5 min to dephosphorylate the ends of the plasmid DNA. EDTA was added to the mixture to a final concentration of 10 mM and the mixture incubated at 65°C for 15 min to inactivate the CIP. The CIP-treated DNA was separated in a 1% agarose gel in TAE buffer at 100 V for 40 min. The plasmid DNA was excised from the gel and the DNA extracted using the QIAGEN Gel Extraction Kit.

The digested 1960/1961, 1985/1986, 1958/1959, and 1958/1959^{Mut} repair cassettes were ligated in separate reactions into the pFAcT-GFP plasmid in a 3:1 ratio in 1 X T4 DNA ligase buffer with 1 U of T4 DNA ligase in a 10 µL reaction. The reaction mixtures were incubated overnight at 4°C. Five microlitres of each ligation was used to transform 25 µL aliquots of *E.coli* DH10B cells as described in above. Aliquots of 25 and 250 µL of each transformation were plated onto low salt LB supplemented with 100 µg/mL Amp, 50 µg/mL X-gal, and 95.2 µg/mL IPTG. The plates were incubated overnight at 37°C. Single, isolated colonies were selected from the transformation plates and used to inoculate 3 mL of low salt LB supplemented with 100 µg/mL Amp. The cultures were incubated overnight at 37°C with shaking at 225 rpm. Plasmid DNA was extracted from the *E.coli* cells following a standard alkaline lysis miniprep procedure. The plasmid DNA was digested with *Xba*1 and *Xho*1 as described above to select for clones that contained inserts of the correct size. These clones were sequenced at PBI using primers DT 882 and DT 891 (Table 7).

Three additional repair constructs were produced: 1983/1984 + 1958/1959^{Mut} pFAcT-GFP, 2001/2002 + 1958/1959 pFAcT-GFP, and 2001/2002 + 1958/1959^{Mut} pFAcT-GFP. The 1958/1959 pFAcT-GFP and 1958/1959^{Mut} pFAcT-GFP plasmids and 1983/1984 and 2001/2002 PCR cassettes were digested with *Not1* and *Sst*1 as described above. The PCR products were ligated to the digested plasmid DNA as described above. These constructs were transformed into DH10B cells and screened by restriction digest and sequencing as described above.

Electrocompetent *E.coli* DH10B cells containing the pMON7124 plasmid were prepared as described by Sharma and Schimke (129) using YENB media supplemented with 10 µg/mL Tet. Five hundred nanograms of a knockout bacmid were transformed into the competent cells by electroporation using the method described above. Aliquots of 25 and 250 µL of the transformation mixture were plated onto low salt LB plates supplemented with 50 µg/mL Kan, 10 µg/mL Tet, 50 µg/mL X-gal, and 95.2 µg/mL IPTG. The plates were incubated for 48 h at 37°C. Several colonies were re-streaked onto low salt LB plates supplemented with 50 µg/mL

Kan, 10 µg/mL Tet, 50 µg/mL X-gal, 95.2 µg/mL IPTG, and either 17 µg/mL Chl, 30 µg/mL Zeo, or 17 µg/mL Chl and 30 µg/mL Zeo. These plates were incubated at 37^{o}C for 48 h. A single colony was used to inoculate 5 mL of YENB supplemented with appropriate selection antibiotics. The cultures were incubated at 37^{o}C overnight with shaking at 225 rpm. Two millilitres of overnight culture were used to inoculate 50 mL of YENB supplemented as described above. This culture was incubated for 6 h at 37^{o}C with shaking at 225 rpm. The cells were made competent following the protocol of Sharma and Schimke (129) to produce competent *E.coli* cells containing the knockout bacmid and the pMON7124 helper plasmid.

To create a knockout construct with the native *Polh* repaired and tagged with GFP, the native pFAcT-GFP plasmid (without a repair cassette) was transformed into the competent *E.coli* cells harbouring the pMON7124 plasmid and a knockout bacmid following the method described above. The cells were allowed to recover overnight at 37^{o}C with shaking at 225 rpm. Aliquots of 1, 10, and 100 µL of each transformation mixture were plated onto low salt LB plates supplemented with 50 µg/mL Kan, 10 µg/mL Tet, 7 µg/mL Gen, 50 µg/mL X-gal, 95.2 µg/mL IPTG, and either 17 µg/mL Chl, or 30 µg/mL Zeo, or 17 µg/mL Chl and 30 µg/mL Zeo. The plates were incubated at 37^{o}C for 48 h. Several colonies were selected and re-streaked onto low salt LB plates supplemented as described above, but lacking Tet. The Tet is not included in this medium to promote the loss of the pMON7124 plasmid.

Overnight cultures were established for several putative positive clones in 3 mL low salt LB supplemented as described above. The cultures were grown overnight at 37^{o}C with shaking at 225 rpm. The bacmid DNA was extracted from the *E.coli* cells following a standard alkaline lysis miniprep protocol.

A repair construct in which the native *Polh* was repaired, the native GOI re-inserted back into the genome, and the GFP tag incorporated, was generated by transforming competent *E.coli* cells harbouring the pMON7124 plasmid and a knockout bacmid with the repair construct following the method described above. A full list of knockout and repair constructs and the primer pairs used to produce them is provided in Tables 8 and 9.

A wt bacmid construct, vAcBac 887, which contains the full suite of AcMNPV genes, the native *Polh* gene, and *GFP* was kindly provided by Dr. David Theilmann (AAFC Summerland, BC, Canada).

Each knockout and repair bacmid was screened by PCR to confirm that the gene(s) of interest had been knocked out and that a repair construct had been inserted at the *Polh* locus. In a 25 µL reaction, 1 X PCR buffer (Invitrogen Corporation) was mixed with 1.5 mM $MgCl_2$, 0.2 mM dNTP mix, 0.2 µM forward primer, 0.2 µM reverse primer, 2.5 U Taq Polymerase (Invitrogen Corporation), and 100 ng of bacmid DNA. The reaction mixture was incubated at 95^{o}C for 2 min, followed by 35 cycles of 95^{o}C for 30 s, 62^{o}C for 30 s, and 72^{o}C for 1.5 min. A final elongation step was carried out at 72^{o}C for 10 min. The PCR products were separated in a 1% agarose gel in TAE buffer at 100 V for 40 min. A list of PCR primers, the regions they amplify, and the expected product sizes are provided in Table 10. A map showing the location of each primer is provided in Figure 24.

Table 8. Primer pairs used to create the knockout and repair constructs.

Name of Construct	Primers Used to Create Construct	Antibiotic Resistance
vAc^{145null}	1953-1954 KO	Kan, Chl, Gen
vAc$^{145null\text{-}AC145\text{-}HA}$	1953-1954 KO, 1960-1961 REP	Kan, Chl, Gen
vAc$^{145null\text{-}MC164\text{-}HA}$	1953-1954 KO, 1985-1986 REP	Kan, Chl, Gen
vAc$^{149/150null}$	1955-1956 KO	Kan, Zeo, Gen
vAc$^{149/150null\text{-}AC149\text{-}MYC}$	1955-1956 KO, 1958-1989/1959-1990 REP	Kan, Zeo, Gen
vAc$^{149/150null\text{-}MC118\text{-}HA+AC149\text{-}MYC}$	1955-1956 KO, 1983-1984/1958-1989/1959-1990 REP	Kan, Zeo, Gen
vAc$^{149/150null\text{-}AC149\text{-}MYC+AC150\text{-}HA}$	1955-1956 KO, 1958-1959 REP	Kan, Zeo, Gen
vAc$^{145/149/150null}$	1953-1954/1955-1956 KO	Kan, Chl, Zeo, Gen
vAc$^{145/149/150null\text{-}AC149\text{-}MYC}$	1953-1954/1955-1956 KO, 1958-1989/1959-1990 REP	Kan, Chl, Zeo, Gen
vAc$^{145/149/150null\text{-}AC145\text{-}HA+AC149\text{-}MYC}$	1953-1954/1955-1956 KO, 2001-2002/1958-1989/1959-1990 REP	Kan, Chl, Zeo, Gen
vAc$^{145/149/150null\text{-}AC149\text{-}MYC+AC150\text{-}HA}$	1953-1954/1955-1956 KO, 1958-1959 REP	Kan, Chl, Zeo, Gen
vAc$^{145/149/150null\text{-}AC145\text{-}HA+AC149\text{-}MYC+AC150\text{-}HA}$	1953-1954/1955-1956 KO, 2001-2002/1958-1959 REP	Kan, Chl, Zeo, Gen
vAcBac 887	None	Kan

Table 9. List of deleted and repaired genes in the knockout and repair constructs.

Name of Construct	AcMNPV Deleted Gene(s)	Gene(s) Repaired
$vAc^{145null}$	ORF 145	Polh, GFP
$vAc^{145null\text{-}AC145\text{-}HA}$	ORF 145	AcMNPV ORF 145, Polh, GFP
$vAc^{145null\text{-}MC164\text{-}HA}$	ORF 145	MacoNPV ORF 164, Polh, GFP
$vAc^{149/150null}$	ORF 149 and 150	Polh, GFP
$vAc^{149/150null\text{-}AC149\text{-}MYC}$	ORF 149 and 150	AcMNPV ORF 149, Polh, GFP
$vAc^{149/150null\text{-}MC118\text{-}HA+AC149\text{-}MYC}$	ORF 149 and 150	MacoNPV ORF 118 and AcMNPV ORF 149, Polh, GFP
$vAc^{149/150null\text{-}AC149\text{-}MYC+AC150\text{-}HA}$	ORF 149 and 150	AcMNPV ORF 149 and 150, Polh, GFP
$vAc^{145/149/150null}$	ORF 145, 149, and 150	Polh, GFP
$vAc^{145/149/150null\text{-}AC149\text{-}MYC}$	ORF 145, 149, and 150	AcMNPV ORF 149, Polh, GFP
$vAc^{145/149/150null\text{-}AC145\text{-}HA+AC149\text{-}MYC}$	ORF 145, 149, and 150	AcMNPV ORF 145 and 149, Polh, GFP
$vAc^{145/149/150null\text{-}AC149\text{-}MYC+AC150\text{-}HA}$	ORF 145, 149, and 150	AcMNPV ORF 149 and 150, Polh, GFP
$vAc^{145/149/150null\text{-}AC145\text{-}HA+AC149\text{-}MYC+AC150\text{-}HA}$	ORF 145, 149, and 150	AcMNPV ORF 145, 149, and 150, Polh, GFP
vAcBac 887	None	Polh, GFP

Table 10. PCR primer pairs and resultant products used to confirm the knockout and repair constructs.

Primer Name	Sequence	Region Amplified	Amplicon Size		
			WT	1953-1954 KO	1955-1956 KO
1962	ACCGTCGAACATGCCTAT	5′ end of ORF 145 KO	No product	439 bp	No product
766	CAAGGCGACAAGGTGCTGATGC				
1976	GGCATGCTAGCGCACACGGA	3′ end of ORF 145 KO	No product	439 bp	No product
1725	TACGCCCGGTAGTGATCT				
1962	ACCGTCGAACATGCCTAT	Internal to ORF 145	394 bp	No product	394 bp
1963	AATACGCCGTGCAATCAT				
1982	ATTGACTGCGCGAAGATT	5′ end of ORF 150 KO	No product	No product	216 bp
520	CCGGAACGGCACTGGTCAACTT				
1978	AGCTGCGAGCCAAGACCAGC	3′ end of ORF 150 KO	No product	No product	611 bp
1919	GTCCACGAACTTCCGGGACGC				
1964	GGATGTACCGCTAACCAA	Internal to ORF 150	328 bp	328 bp	No product
1965	CTGTCGCCGAATTAGATT				
pUC M13 rev	AGCGGATAACAATTTCACACAGG	5′ end of repair insert	593 bp	593 bp	593 bp
1987	AGCCATACCACATTTGTAGAGG				
pUC M13 for	CCCAGTCACGACGTTGTAAAACG	3′ end of repair insert	687 bp	687 bp	687 bp
1988	AGGTTTGAGCAGCCGCGTAGTGAG				

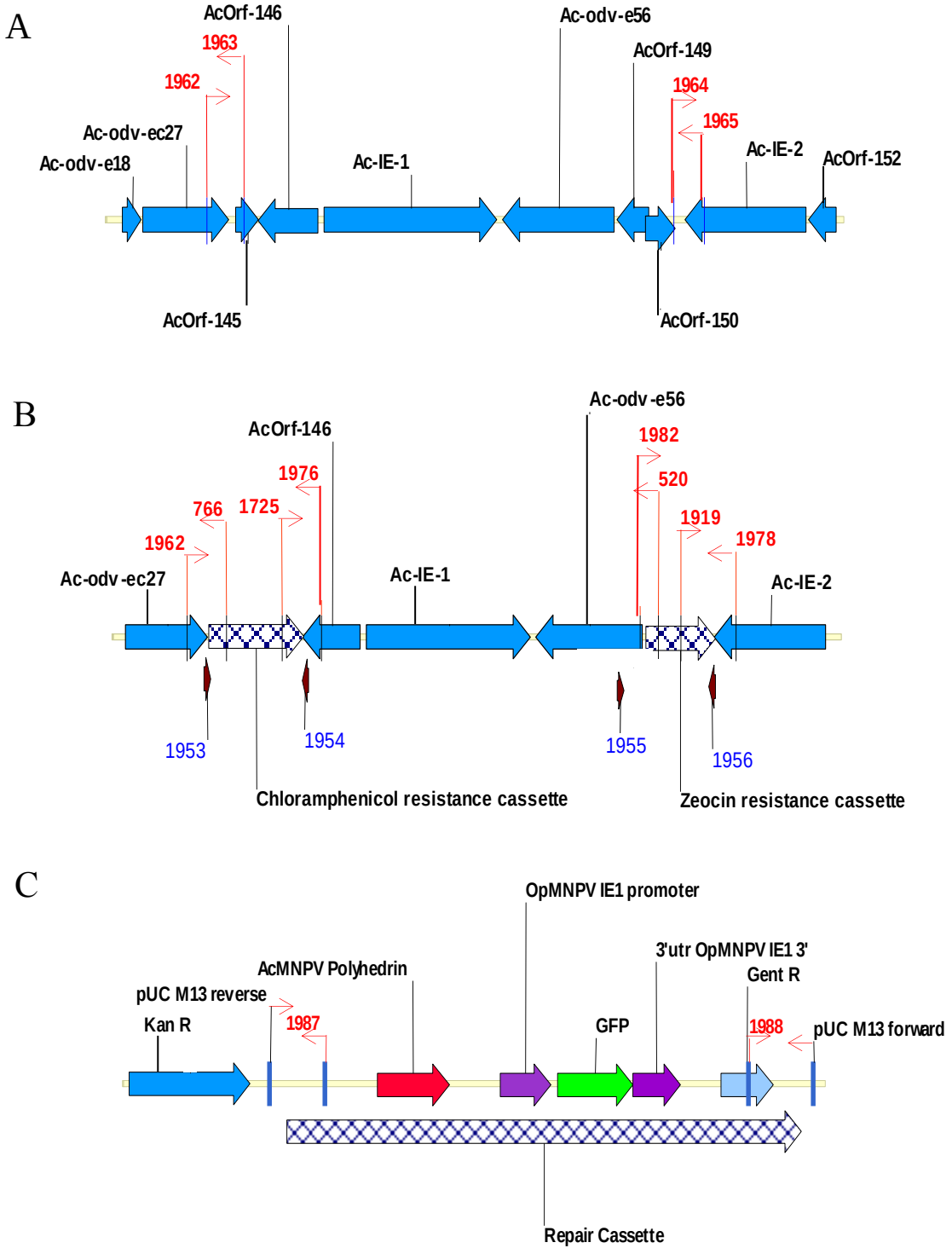

Figure 24. Location of primer pairs for confirming the knockout and repair constructs. Panel A: Wt Ac145 and Ac150, panel B: Ac145 and Ac150 double knockout, panel C: repair locus. Primer names in in red text. ORF names and regulatory regions are in black text.

Bacmid DNA from each knockout and repair construct was introduced into TnHi5 cells by transfection using the Cellfectin II reagent following the protocol described in Section 4.3.2. The flasks were incubated at 27^{o}C for 48 to 72 h until OB were visible in greater than 30% of the cells. The supernatant containing P1 BV and the cell pellet containing OB were collected as described in Section 4.3.2.

To confirm the validity of the P1 BV, viral DNA was extracted from 100 µL of P1 BV as described in Section 4.3.2. The viral DNA was diluted 1:10 in sterile distilled water and 1 µL used per PCR reaction. The PCR primers (Table 10), reaction mixtures, and reaction conditions were as described above.

The titre of the P1 BV stocks was determined using an end-point dilution assay, the tissue culture infectious dose 50% ($TCID_{50}$). Five microlitres of a 4.0 X 10^5 cells/mL stock of TnHi5 cells were dispensed into each well of a 60-well Nunclon microwell tissue culture plate (VWR Canlab) using a Hamilton repeating syringe. Serial dilutions of each BV preparation were made from 10^{-1} to 10^{-9} in 150 µL total volume of GIM. Five microlitres of GIM were added to the first well in each column of the 60-well plates as a negative control. Five microlitres of a BV dilution were added to the second through tenth well of a particular column. The assay was performed in duplicate. The plates were placed in a Tupperware container with several sheets of damp paper towel to reduce evaporation and the container incubated at 27^{o}C for 7 d.

Each well was monitored for the presence of OB using a Nikon phase contrast LWD 0.52 inverted microscope (10 X optical and 10 X objective power), as well as for GFP expression using a Zeiss Axiovert 100 fluorescent microscope (10 X optical, 40 X objective power). The number of infected wells was tallied and used to calculate the titre of the BV stock.

To increase the viral titre, an infection was set up in TnHi5 cells using the P1 BV collected from the transfection assay following the protocol described in Section 4.3.2. The flasks were incubated at 27^{o}C for 48 to 72 h. The supernatant containing the P2 BV and the cell pellet containing OB were harvested as described in Section 4.3.2. Viral DNA was extracted from the P2 BV, the validity of the construct was confirmed by PCR, and the titre of the P2 BV was determined by $TCID_{50}$ assay as described above.

6.3.3. Confirmation of knockout and repair constructs

Reverse transcriptase PCR (RT-PCR) was used to monitor the temporal transcription of *Ac145*, *Ac149*, and *Ac150*, as well as to confirm that transcription of non-target genes had not been affected during the creation of the knockout constructs.

Infections were set up using P2 BV stocks for each viral construct at a MOI of 5 in 25 cm^2 cell culture flasks using 1.0 X 10^6 TnHi5 cells as described in Section 4.3.2. Two flasks were set up per viral construct. The infected cells from one flask were harvested at 4 hpi, and were harvested from the second flask at 24 hpi following the method described in Section 4.3.2. Total RNA was extracted from the TnHi5 cells and converted to cDNA using the SuperScript III™ CellsDirect cDNA Synthesis System (Invitrogen Corporation). Briefly, the cells were gently scraped from the flask using a rubber scraper. The cells and media were transferred to a 15 mL Falcon tube and the cells were pelleted by centrifugation at 3000 rpm for 5 min in a bench top centrifuge. The supernatant was discarded and the cell pellet washed using 5 mL of cold PBS. The cells were washed once more and re-suspended in 1 mL of cold PBS. Two microlitres of the re-suspended cells were transferred to a 0.2 mL thin-walled PCR tube and mixed with 10 µL re-suspension buffer (provided in the CellsDirect Kit) and 40 U of RNase OUT™. The reaction mixture was incubated at 75°C for 10 min. Genomic DNA was removed from the reaction by treatment with 5 U of DNase1 in 1 X DNase1 buffer at RT for 5 min. EDTA was added to a final concentration of 1.5 mM and the reaction mixture incubated at 70°C for 5 min to inactivate the DNase1. An oligo $(dT)_{20}$ primer was added at a final concentration of 4.2 mM along with 0.42 mM of a dNTP mix. The reaction mixture was incubated at 70°C for 5 min and then immediately placed on ice for 2 min. 1 X RT Buffer, 40 U RNaseOUT™, 200 U SuperScript™ III RT, and 3 mM Dithiothreitol (DTT) were added and the reaction mixture, and it was incubated at 50°C for 50 min, followed by 85°C for 5 min. Two units of RNase H were added to each reaction and the tubes incubated at 37°C for 20 min, followed by 5 min on ice.

PCR reactions were performed for each sample using the primer pairs listed in Table 11. In a 25 µL reaction mixture, 1 X PCR buffer was mixed with 1.5 mM $MgCl_2$, 0.2 µM forward primer, 0.2 µM reverse primer, 300 ng of template cDNA, and 2.5 U Taq Polymerase. The reaction mixtures were incubated at 95°C for 2 min, followed by 35 cycles of 95°C for 30 s, 58°C for 30 s, and 72°C for 30 s. A final elongation step was carried out at 72°C for 10 min. The PCR amplicons were separated in a 1% agarose gel in TAE buffer at 80 V for 1 h.

Table 11. PCR primer pairs used to monitor transcript abundance of *Ac145*, *Ac149*, *Ac150*, *GP64*, *Chitinase*, *Polh*, *IE-0*, and *IE-0/IE-1*.

Primer Pair	Sequence	Amplifies	Amplicon Size
1991	AGGGTATTTTGGCCTCAACG	AcMNPV ORF 145	169 bp
1992	ATACATGCGAGCCGTACACC		
1993	TGCCGTCGTCAATACAACAC	AcMNPV ORF 149	153 bp
1994	TTGCTTCATACGTCGAGATACC		
1995	GAATCAGACGACGGGTTCAG	AcMNPV ORF 150	197 bp
1996	TTTTGGTTAGCGGTACATCC		
1997	GTTGGGCAATAAACGACCAG	AcMNPV ORF 128 (*GP64*)	243 bp
1998	ACGACACGTTTTTGCTGATG		
850	TTTGGCAAGGGAACTTTGTC	AcMNPV ORF 126 (*Chitinase*)	100 bp
851	ACAAACCTGGCAGGAGAGAG		
1999	CTTCTTAGCCAGGCTGATGC	AcMNPV ORF 8 (*Polh*)	156 bp
2000	AACATGCGTCCCACTAGACC		
1414	GGTGTACGACGCGTTAAAAT	AcMNPV ORF 141 (*IE-0*)	126 bp
1446	CCATATTCGTGCGAGGCAACG		
1505	GACAACAGCTATTCAGAGT	AcMNPV ORF 147 (*IE-0 and IE-1*)	144 bp
1523	CGAGTTGACGCTTGCCAAAAA		

Quantitative real-time PCR (qPCR) was used to monitor the rate of BV production for each construct to ensure that BV was being produced at a rate similar to that of the wt construct. This was done to ensure that the production and transmission of BV was not altered by any of the genetic manipulations done to the bacmid DNA.

A time course assay was set up in 6-well cell culture plates (Corning Incorporated) using 5.0 X 10^5 TnHi5 cells per well. P2 BV was used to inoculate each well at an MOI of 5 as described in Section 4.3.2. One 6-well plate was set up per construct. The cells from one well from each plate were harvested at 6, 12, 24, 48, 72, and 96 hpi following the protocol described in Section 4.3.2. The infected cell pellets were stored at -80^{o}C and the BV stocks stored at 4^{o}C. The experiment was performed in duplicate.

DNA was extracted from each BV sample as described in Section 4.3.2. Serial dilutions of a previously titred BV standard were prepared in GIM. DNA was extracted from these samples following the method described in Section 4.3.2. A qPCR reaction was set up in 96-well plates. In a 20 µL reaction, 1 X Finnzymes DyNAmo HS SYBR® Green master mix (Thermo Scientific) was mixed with 0.5 µM of primer 850, 0.5 µM primer 851 (Table 11), and 2 µL of diluted DNA. Each reaction was prepared in triplicate. The qPCR reaction was performed using a BioRad CFX96 thermal cycler using the following reaction profile: 15 min at 95^{o}C, followed by 40 cycles of 95^{o}C for 30 s, 58^{o}C for 24 s, and 72^{o}C for 30 s. The samples were then heated to 95^{o}C for 1 min and then held at 55^{o}C for 20 min. The samples were again heated to 95^{o}C and

then cooled to 65°C. The temperature was increased by 0.5°C every 5 s to 95°C to determine the melting temperature of the PCR amplicon. The data were analyzed using the BioRad CFX Manager 2.1 software using the standard curve method to determine the absolute titre of all samples.

The rate of viral DNA replication was monitored for each construct using the infected cell pellets from the time course assay described above. The cells were re-suspended in 1 mL of lysis buffer (10 mM Tris-Cl pH 8.0, 1 mM EDTA, 0.5% SDS, and 20 µg/mL RNase A) and incubated at 37°C for 30 min. Fifty microlitres of the cell lysate was added to 250 µL of Tris-HCl pH 8.0 with 80 µg/mL Proteinase K. The samples were incubated overnight at 50°C, followed by extraction with an equal volume of phenol:chloroform:isoamyl alcohol and then with chloroform:isoamyl alcohol as described in Section 4.3.2. The DNA was diluted 1:10 in sterile distilled water and 2 µL of the DNA preparation used in a qPCR reaction as described above.

To determine if the biological titre of the BV stocks from each viral construct was comparable to the absolute titre obtained using qPCR, an end-point-dilution assay was set up using the 6 and 96 hpi BV samples from the time course assay. The experiment was performed in duplicate following the $TCID_{50}$ protocol described in Section 6.3.2.

6.4. Results

6.4.1. Creation and confirmation of knockout and repair constructs

To confirm that each knockout and repair construct lacked the GOI and/or contained a repaired GOI at the *Polh* locus, a series of PCR reactions were performed on the bacmid DNA, P1 BV and P2 BV stocks. The results from the bacmid confirmation PCR are shown in Figure 25. The results for the P1 and P2 BV stocks were identical to the bacmid constructs.

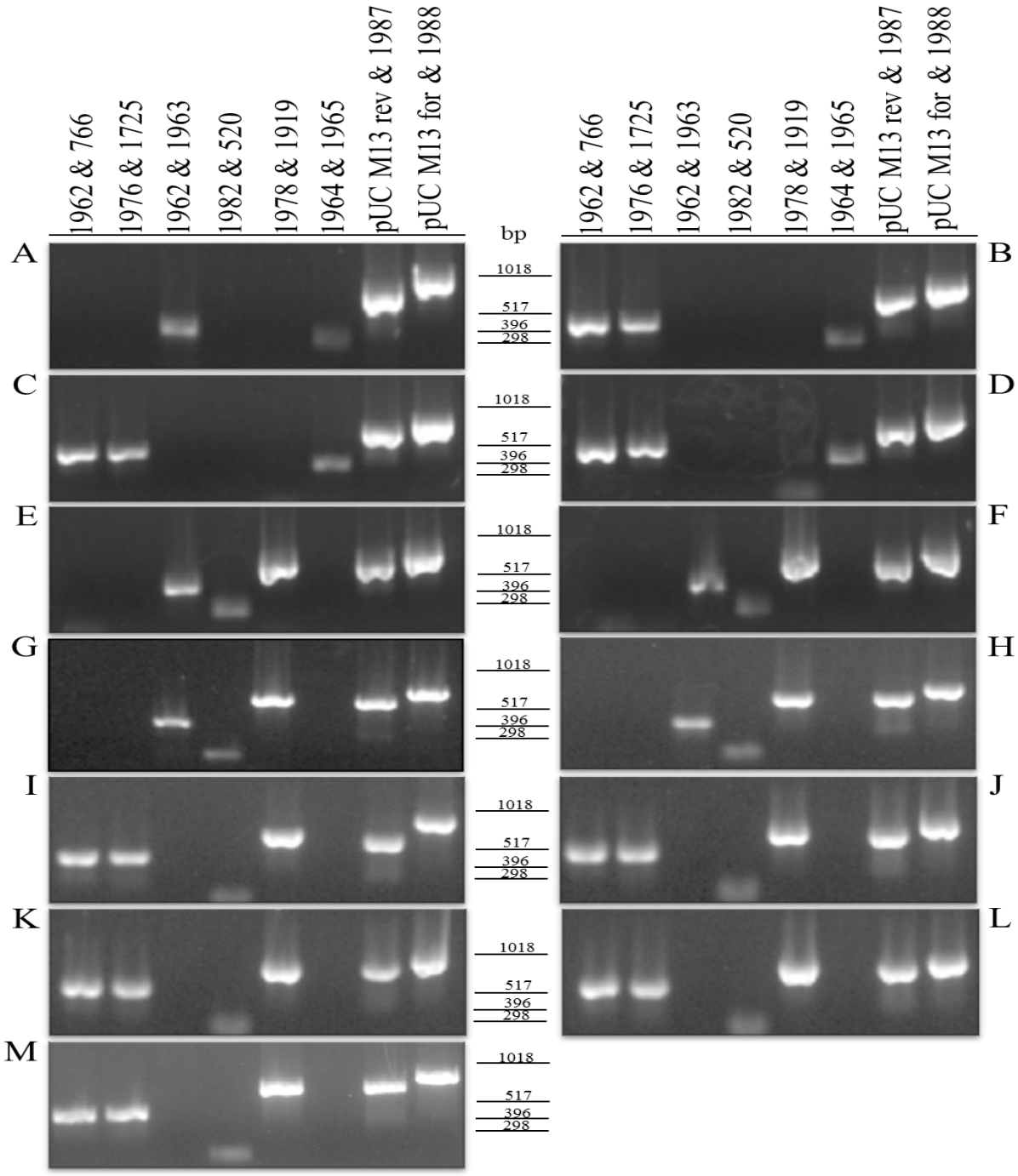

Figure 25. PCR confirmation of the knockout and repair bacmid constructs.
Each panel contains the PCR results for an individual knockout or repair construct. vAcBac 887(A), vAc^{145null} (B), vAc$^{145null\text{-}AC145\text{-}HA}$ (C), vAc$^{145null\text{-}MC164\text{-}HA}$ (D), vAc$^{149/150null}$ (E), vAc$^{149/150null\text{-}AC149\text{-}MYC+AC150\text{-}HA}$ (F), vAc$^{149/150null\text{-}AC149\text{-}MYC}$ (G), vAc$^{149/150null\text{-}MC118\text{-}HA+AC149\text{-}MYC}$ (H), vAc$^{145/149/150null}$ (I), vAc$^{145/149/150null\text{-}AC149\text{-}MYC}$ (J), vAc$^{145/149/150null\text{-}AC145\text{-}HA+AC149\text{-}MYC}$ (K), vAc$^{145/149/150null\text{-}AC149\text{-}MYC+AC150\text{-}HA}$ (L), vAc$^{145/149/150null\text{-}AC145\text{-}HA+AC149\text{-}MYC+AC150\text{-}HA}$ (M). Primer pairs are listed at the top of the figure. The expected size of each PCR amplicon, along with the region of the bacmid that is amplified is provided in Table 10.

Reverse transcriptase-PCR was performed to confirm the temporal transcriptional patterns of the GOI *Ac145*, *Ac149*, and *Ac150*, as well as non-target genes *GP64*, *Chitinase*, *Polh*, *IE-0*, and *IE0*/*IE-1*. At the 4 hpi time point, *Ac149*, *GP64*, *IE-0*, and *IE-1*were expected to be transcribed. As expected, *GP64* was transcribed at this time point for all constructs. Transcripts were detected for *IE-0* and *IE-1* at the 4 hpi time point for most, but not all of the constructs. The $vAc^{145/149/150null}$ series of knockout and repair constructs in particular showed variability in the temporal transcription of these genes. The *Ac149* transcript was not detected in any of the constructs at the early time point. At 24 hpi, *Ac145*, *Ac149*, *Ac150*, *GP64*, *Chitinase*, *Polh*, *IE-0*, and *IE-1* were expected to be transcribed. As expected, the reference genes, *GP64*, *Chitinase*, *Polh*, *IE-0*, and *IE-1*, were transcribed in all constructs. *Ac145* was not transcribed in $vAc^{145null}$, $vAc^{145null-MC164-HA}$, $vAc^{145/149/150null}$, $vAc^{145/149/150null-AC149-MYC}$, or $vAc^{145/149/150null-AC149-MYC+AC150-HA}$, but was transcribed in $vAc^{145null-AC145-HA}$, $vAc^{145/149/150null-AC145-HA+AC149-MYC}$, and $vAc^{145/149/150null-AC145-HA+AC149-MYC+AC150-HA}$, as expected. *Ac150* was not transcribed in $vAc^{149/150null}$ or $vAc^{145/149/150null}$ as expected, but was transcribed in $vAc^{149/150null-AC149-MYC}$, $vAc^{149/150null-MC118-HA+AC149-MYC}$, $vAc^{145/149/150null-AC149-MYC}$, and $vAc^{145/149/150null-AC145-HA+AC149-MYC}$. The results from this experiment are shown in Figure 26.

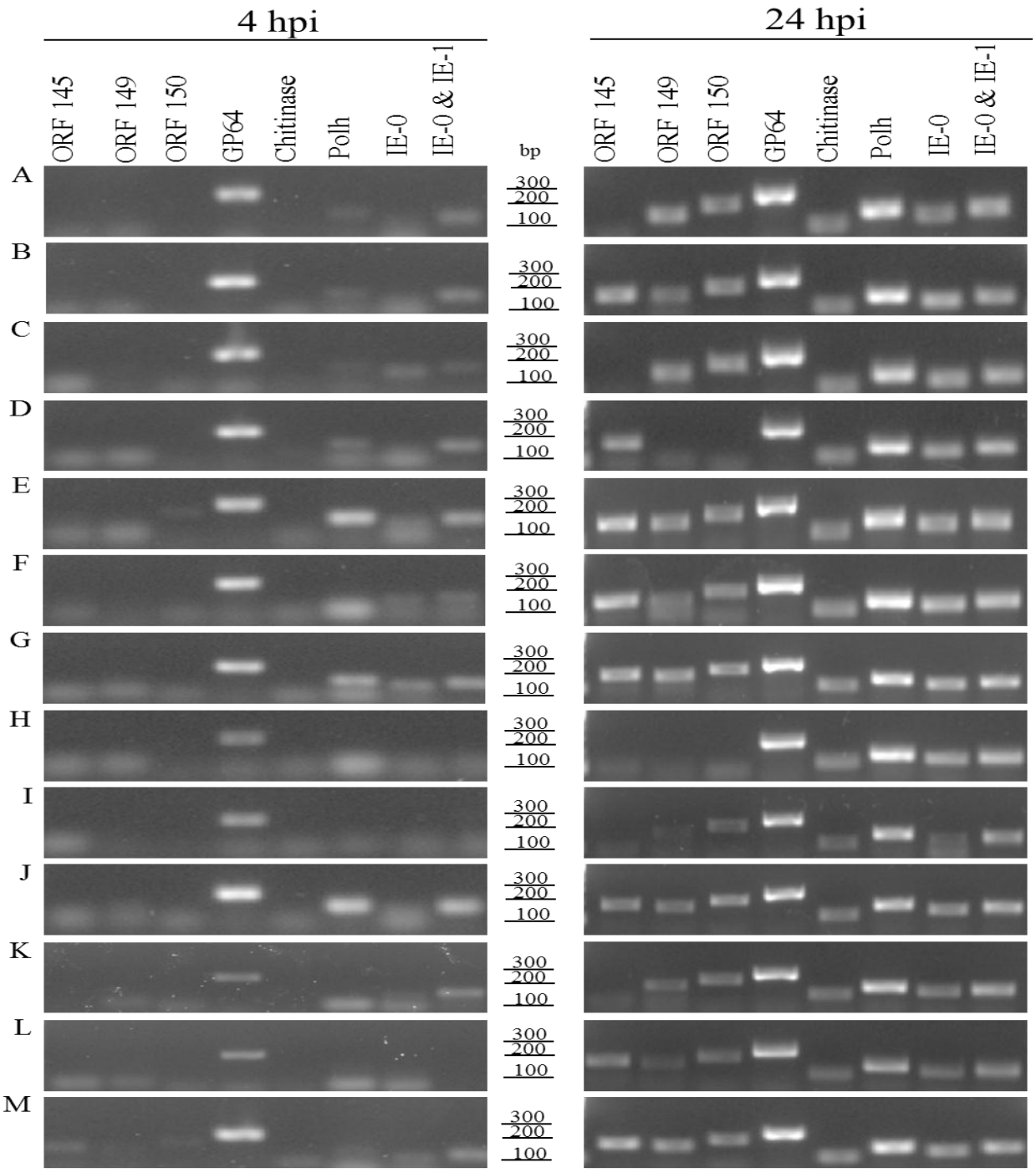

Figure 26. RT-PCR to monitor transcript abundance.
Each panel contains the RT-PCR results for an individual knockout or repair construct. vAc^{145null} (A), vAc$^{145null\text{-}AC145\text{-}HA}$ (B), vAc$^{145null\text{-}MC164\text{-}HA}$ (C), vAc$^{149/150null}$ (D), vAc$^{149/150null\text{-}AC149\text{-}MYC+AC150\text{-}HA}$ (E), vAc$^{149/150null\text{-}AC149\text{-}MYC}$ (F), vAc$^{149/150null\text{-}MC118\text{-}HA+AC149\text{-}MYC}$ (G), vAc$^{145/149/150null}$ (H), vAc$^{145/149/150null\text{-}AC149\text{-}MYC}$ (I), vAc$^{145/149/150null\text{-}AC145\text{-}HA+AC149\text{-}MYC}$ (J), vAc$^{145/149/150null\text{-}AC149\text{-}MYC+AC150\text{-}HA}$ (K), vAc$^{145/149/150null\text{-}AC145\text{-}HA+AC149\text{-}MYC+AC150\text{-}HA}$ (L), vAcBac 887 (M). The predicted temporal expression patterns for each gene are: ORF 145 (late/very late), ORF 149 (early and late/very late), ORF 150 (late/very late), GP64 (early and late/very late), chitinase (late/very late), Polh (late/very late), IE-0 (early and late/very late), IE-0/IE-1 (early and late/very late). Primer pairs used and expected product sizes are listed in Table 11.

The rate of viral DNA replication (Figure 27) and BV production (Figure 28) were monitored using quantitative PCR. The results shown are the average of two independent infection experiments. The supernatant samples from the time course infection (containing BV) were used for the qPCR to monitor BV production, and the infected cell pellet fraction (containing OB) were used for the qPCR to monitor viral DNA replication. The three *Ac145*-deletion and repair constructs, vAc^{145null}, vAc$^{145null\text{-}AC145\text{-}HA}$, and vAc$^{145null\text{-}MC164\text{-}HA}$, and the *Ac150*-deletion and repair constructs, vAc$^{149/150null}$, vAc$^{149/150null\text{-}AC149\text{-}MYC+AC150\text{-}HA}$, vAc$^{149/150null\text{-}AC149\text{-}MYC}$, and vAc$^{149/150null\text{-}MC118\text{-}HA+\ AC149\text{-}MYC}$, all replicate at the same rate as the wt and produce similar numbers of viral genomes (Figure 27 A and B). The vAc$^{145/149/150null\text{-}AC149\text{-}MYC}$, vAc$^{145/149/150null\text{-}AC149\text{-}MYC+AC150\text{-}HA}$, and vAc$^{145/149/150null\text{-}AC145\text{-}HA+AC149\text{-}MYC+AC150\text{-}HA}$ constructs also replicate at the same rate as the wt. Two constructs, vAc$^{145/149/150null}$ and vAc$^{145/149/150null\text{-}AC145\text{-}HA+AC149\text{-}MYC}$, replicate at a substantially slower rate than the wt (Figure 27 C). vAc$^{145/149/150null}$ replicate faster than the wt from 12 to 24 hpi before slowing to a rate similar to the wt. vAc$^{145/149/150null\text{-}AC145\text{-}HA+AC149\text{-}MYC}$ replicates slower than the wt, although the differences in starting quantity of virus make it difficult to confirm this.

The *Ac145* and *Ac150* single deletion and repair constructs produce BV at a similar rate to the wt construct (Figure 28 A and B), whereas the *Ac145*/*Ac149*/*Ac150* triple deletion constructs produced BV at a substantially slower rate than the wild type (Figure 28 C).

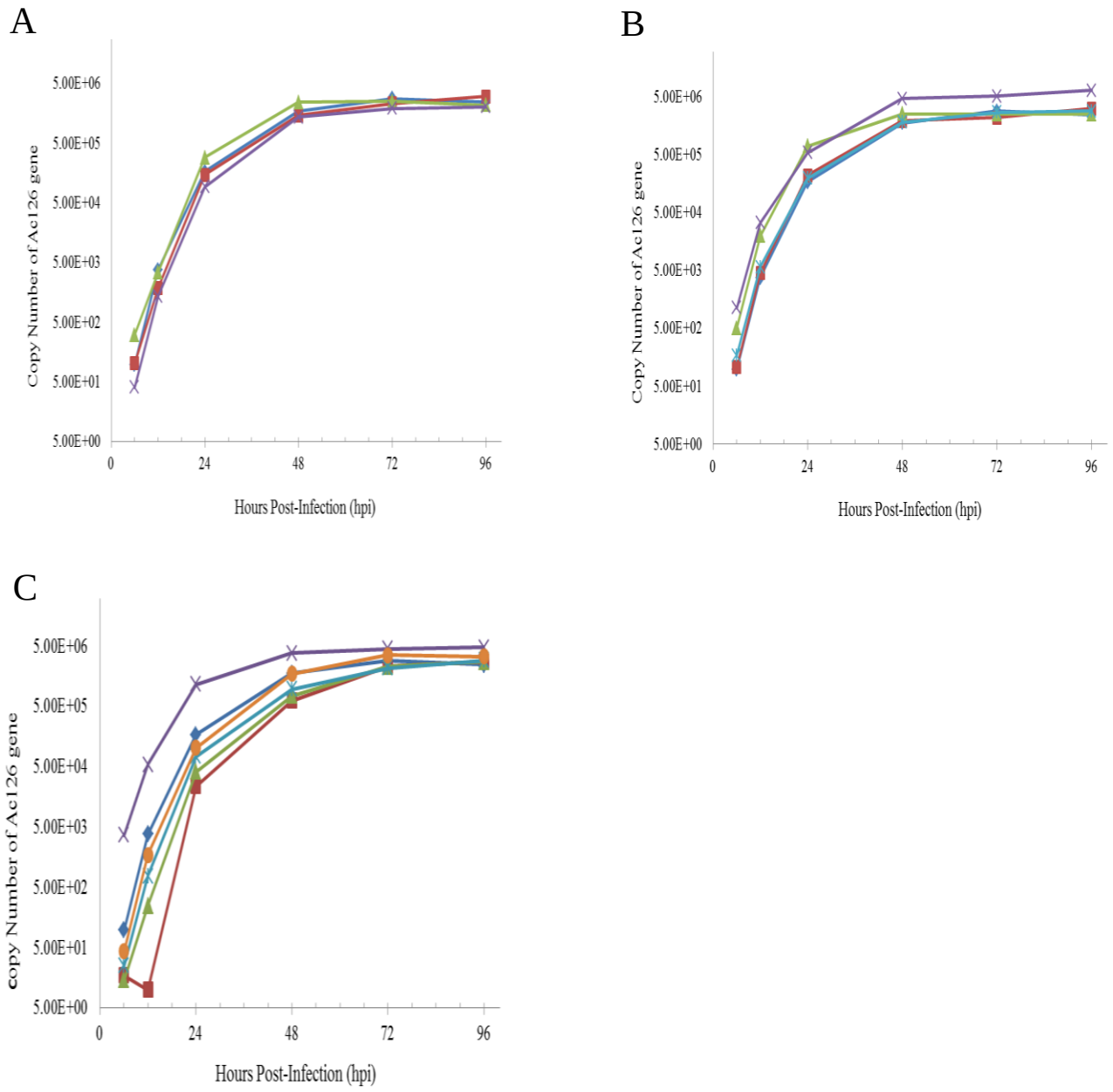

Figure 27. Rate of viral DNA replication as determined by qPCR.
The number of copies of the *Ac126* gene (*chitinase*) are measured. The averages of two independent biological replicates are shown. Technical replicates were performed in triplicate. **Panel A (ORF 145 knockout and repair constructs):** vAcBac 887 (wt; blue diamond), $vAc^{145null}$ (red square), $vAc^{145null\text{-}AC145\text{-}HA}$ (green triangle), $vAc^{145null\text{-}MC164\text{-}HA}$ (purple cross). **Panel B (ORF 150 knockout and repair constructs)**: vAcBac 887 (wt; blue diamond), $vAc^{149/150null}$ (red square), $vAc^{149/150null\text{-}AC149\text{-}MYC+AC150\text{-}HA}$ (green triangle), $vAc^{149/150null\text{-}AC149\text{-}MYC}$ (purple cross), $vAc^{149/150null\text{-}MC118\text{-}HA+AC149\text{-}MYC}$ (blue cross). **Panel C (ORF 145 and 150 double knockout and repair constructs)**: vAcBac 887 (wt; blue diamond), $vAc^{145/149/150null}$ (red square), $vAc^{145/149/150null\text{-}AC149\text{-}MYC}$ (green triangle), $vAc^{145/149/150null\text{-}AC145\text{-}HA+AC149\text{-}MYC}$ (purple cross), $vAc^{145/149/150null\text{-}AC149\text{-}MYC+AC150\text{-}HA}$ (blue cross), $vAc^{145/149/150null\text{-}AC145\text{-}HA+AC149\text{-}MYC+AC150\text{-}HA}$ (orange circle).

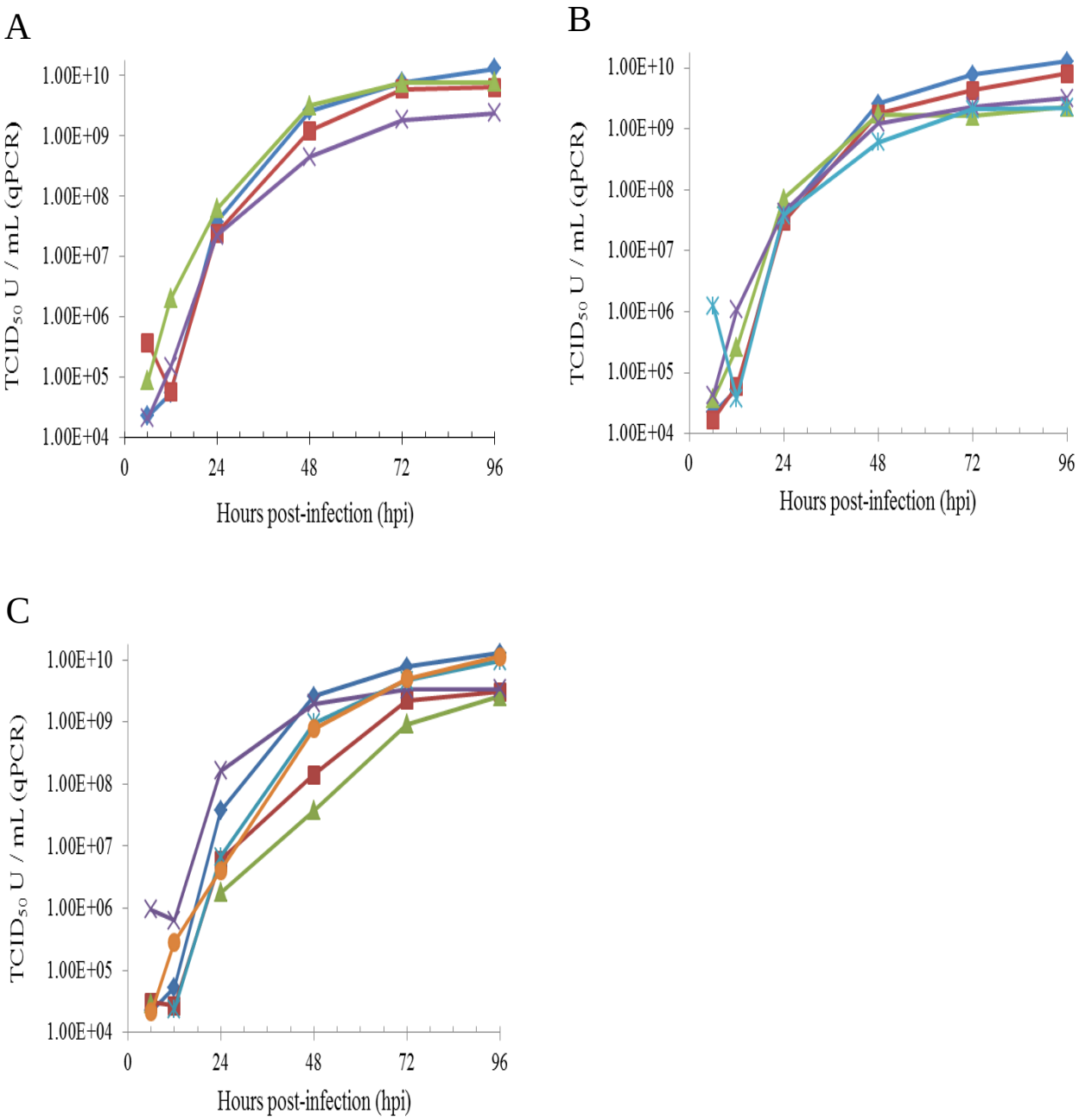

Figure 28. Rate of BV production as determined by qPCR.
These are the averages of two independent biological replicates of this experiment. Technical replicates were performed in triplicate.
Panel A (ORF 145 knockout and repair constructs): vAcBac 887 (wt; blue diamond), vAc^{145null} (red square), vAc$^{145null\text{-}AC145\text{-}HA}$ (green triangle), vAc$^{145null\text{-}MC164\text{-}HA}$ (purple cross). **Panel B (ORF 150 knockout and repair constructs)**: vAcBac 887 (wt; blue diamond), vAc$^{149/150null}$ (red square), vAc$^{149/150null\text{-}AC149\text{-}MYC+AC150\text{-}HA}$ (green triangle), vAc$^{149/150null\text{-}AC149\text{-}MYC}$ (purple cross), vAc$^{149/150null\text{-}MC118\text{-}HA+AC149\text{-}MYC}$ (blue cross). **Panel C (ORF 145 and 150 knockout and repair constructs)**: vAcBac 887 (wt; blue diamond), vAc$^{145/149/150null}$ (red square), vAc$^{145/149/150null\text{-}AC149\text{-}MYC}$ (green triangle), vAc$^{145/149/150null\text{-}AC145\text{-}HA+AC149\text{-}MYC}$ (purple cross),

vAc$^{145/149/150null\text{-}AC149\text{-}MYC+AC150\text{-}HA}$ (blue cross), vAc$^{145/149/150null\text{-}AC145\text{-}HA+AC149\text{-}MYC+AC150\text{-}HA}$ (orange circle).

As this qPCR reaction provided an estimate of the absolute numbers of BV particles, a $TCID_{50}$ assay was performed using the 6 and 96 hpi samples from the same time course experiments to determine if the biological titres for each of the constructs were similar. At 6 hpi, all constructs produced biological titres between 10^2 and 10^4 $TCID_{50}$ U / mL. At 96 hpi, all of the virus constructs produced biological titres of between 10^7 and 10^9 $TCID_{50}$ U / mL. At 6 hpi, vAc$^{145/149/150null}$ produced fewer infectious particles than the wt vAcBac 887 construct. At the 96 hpi time point, vAc$^{145null\text{-}MC164\text{-}HA}$, vAc$^{149/150null\text{-}MC118\text{-}HA+AC149\text{-}MYC}$, vAc$^{145/149/150null}$, vAc$^{145/149/150null\text{-}AC149\text{-}MYC}$, and vAc$^{145/149/150null\text{-}AC145\text{-}HA+AC149\text{-}MYC}$ produced fewer infectious particles than the wt construct. The results from this experiment are shown in Figure 29.

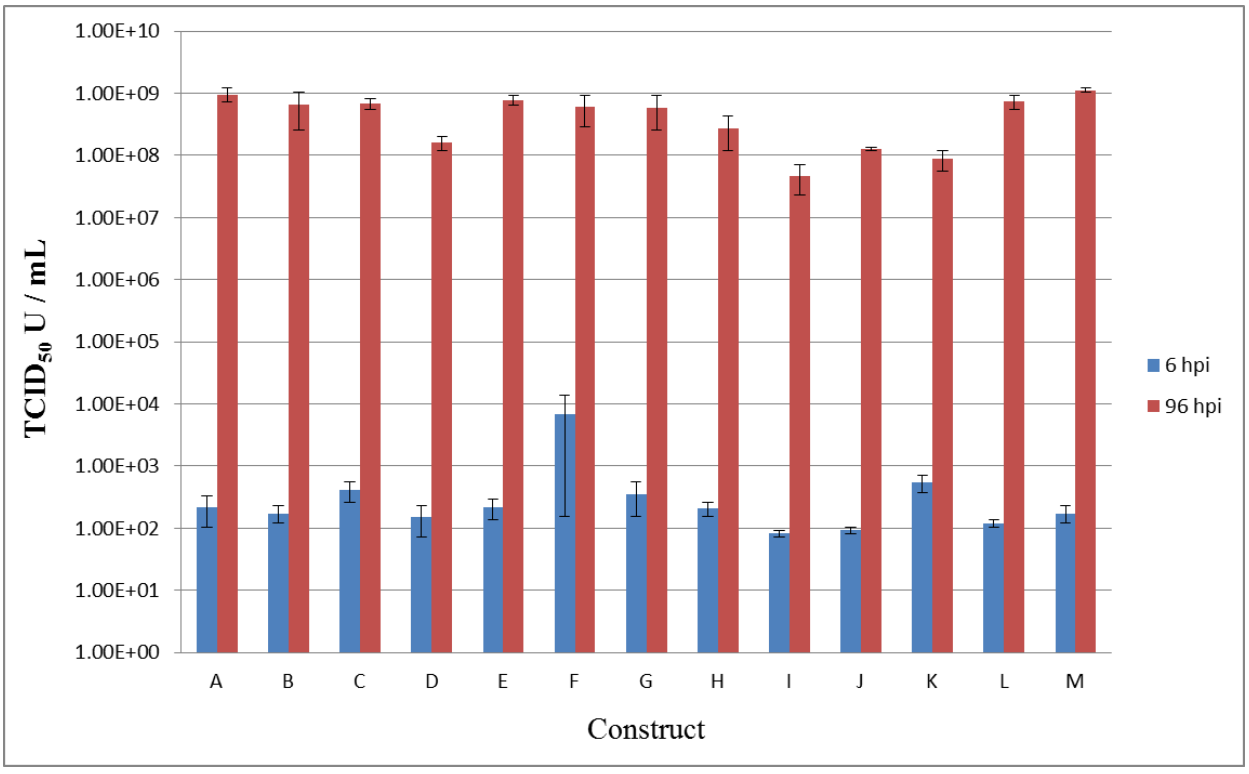

Figure 29. $TCID_{50}$ assay to determine biological titre of BV stocks at 6 and 96 hpi.
These results are the averages of two independent biological replicates. The error bars represent the standard error for the two biological replicates for each construct.
Lane A –vAcBac 887 (wt), lane B – vAc^{145null}, lane C – vAc$^{145null\text{-}AC145\text{-}HA}$, lane D – vAc$^{145null\text{-}MC164\text{-}HA}$, lane E – vAc$^{149/150null}$, lane F – vAc$^{149/150null\text{-}AC149\text{-}MYC+AC150\text{-}HA}$, lane G – vAc$^{149/150null\text{-}AC149\text{-}MYC}$, lane H – vAc$^{149/150null\text{-}MC118\text{-}HA+AC149\text{-}MYC}$, lane I – vAc$^{145/149/150null}$, lane J – vAc$^{145/149/150null\text{-}AC149\text{-}MYC}$, lane K – vAc$^{145/149/150null\text{-}AC145\text{-}HA+AC149\text{-}MYC}$, lane L – vAc$^{145/149/150null\text{-}AC149\text{-}MYC+AC150\text{-}HA}$, lane M – vAc$^{145/149/150null\text{-}AC145\text{-}HA+AC149\text{-}MYC+AC150\text{-}HA}$.

6.5. Discussion

Lapointe et al. (87) produced a series of knockout and repair virus constructs using a two-step homologous recombination process in insect cells. In order to keep all regulatory regions intact for the genes flanking *Ac145* and *Ac150*, only partial deletions of each gene were created. Their *Ac145* knockout construct kept the 31 bp at the 3′ end of *Ac145* intact to not disturb the native *Ac146* stop codon. Their Ac150 knockout construct kept 104 bp at the 5′ end of *Ac150* intact to not disturb the coding sequence for *Ac149*, and an additional 20 bp at the 3′ end of *Ac150* were kept intact to not disturb the native *IE-2* polyadenylation signal, resulting in approximately 57% of *Ac150* being deleted. Lapointe et al. produced repair constructs for each of the single deletion viruses as well as an *Ac145* single repair for the *Ac145*/*Ac150* double deletion virus. In a follow-up study, Zhang et al. (86) created *Ac150*-deletion and repaired virus constructs using a similar method to Lapointe et al. Their knockout and repair constructs deleted approximately 60% of *Ac150*, ensuring that the coding sequence for *Ac149* was not disturbed.

Both the Lapointe and Zhang groups produced their gene knockout constructs in insect cells. Each of their constructs was subjected to multiple manipulations, followed by several rounds of plaque purification to obtain pure virus stocks. This approach could be problematic, as baculoviruses that undergo multiple rounds of amplification and purification in insect cells may rapidly acquire mutations within the viral genome (130-133). Production of knockout constructs in bacterial cells reduces the likelihood of accumulating mutations by keeping the viral passage number low, decreasing the amount of time required to produce a knockout, and allowing for confirmation of the construct validity by PCR, sequencing, or restriction digest at several stages throughout the production. The knockout and repair constructs for this study were analyzed by PCR and sequencing at the bacmid stage, and by PCR at the P1 BV, P2 BV, and P2 OB stages to ensure that the GOI was deleted and that a repair construct was inserted into the *Polh* locus. At each stage in development, the expected PCR products were produced for each of the knockout and repair constructs. These results suggest that the expected changes to the virus backbone were produced.

Construct validity was further confirmed by RT-PCR to monitor transcript abundance. This was done to ensure that the GOI was not transcribed in the knockout construct and that transcription was restored in the repair construct. Several additional transcripts were monitored to ensure that undesired changes to the virus backbone had not occurred. At the 4 hpi time point,

Ac149, *GP64*, *IE-0*, and *IE-1*were expected to be transcribed. As expected, *GP64* was transcribed at this time point for all constructs. Transcripts were detected for *IE-0* and *IE-1* at the 4 hpi time point for most, but not all of the constructs. The vAc$^{145/149/150null}$ series of knockout and repair constructs in particular showed variability in the temporal transcription of these genes. Lack of transcription of *IE-0* or *IE-1* at this early time point for the triple knockout constructs could be a result of size differences in the bacmid backbone. The vAc$^{145/149/150null}$ series of constructs, which are larger in size than the single knockout constructs due to the presence of both a CAT and Zeo gene, could be uncoated more slowly, or transcription initiation could be delayed slightly compared to the other constructs. By 24 hpi, both *IE-0* and *IE-1* were transcribed for all constructs. The *Ac149* transcript was not detected in any of the constructs at the early time point. This was an interesting result, as *Ac149* was found to be an early gene, expressed as early as 4 hpi, by both RACE and northern blot. It is possible that only low levels of *Ac149* are required during the early phases of infection. It is also possible that at 4 hpi, the level of *Ac149* transcripts produced may be below the detection limit of this assay. By 24 hpi, *Ac149* was transcribed in all constructs except vAc$^{149/150null}$ and vAc$^{145/149/150null}$, as expected.

At 24 hpi, *Ac145*, *Ac149*, *Ac150*, *GP64*, *Chitinase*, *Polh*, *IE-0*, and *IE-1* were expected to be transcribed. As expected, all of the reference genes were transcribed in all constructs. *Ac145* was not transcribed in any of the Ac145 single or double knockout constructs, as expected. *Ac150* was not transcribed in vAc$^{149/150null}$ or vAc$^{145/149/150null}$ as expected, but was transcribed in vAc$^{149/150null\text{-}AC149\text{-}MYC}$, vAc$^{149/150null\text{-}MC118\text{-}HA+AC149\text{-}MYC}$, vAc$^{145/149/150null\text{-}AC149\text{-}MYC}$, and vAc$^{145/149/150null\text{-}AC145\text{-}HA+AC149\text{-}MYC}$. These four virus constructs were produced using the 1958/1959^{Mut} repair cassette. This cassette contains the coding region of *Ac149* and a mutated *Ac150* containing three stop codons at the *5′* end. This construct restores function of *Ac149*, but not *Ac150*. As the coding region for *Ac150* was not removed from the virus construct, it is not surprising that the *Ac150* transcript can still be detected. Due to the presence of the three stop codons, translation of *Ac150* will not occur in these constructs.

qPCR was used to confirm that neither the rate of BV production nor the rate of viral DNA replication was altered by any of the genetic manipulations made to the virus DNA. The *Ac145*-deletion and repair constructs, the *Ac150*-deletion and repair constructs, and some of the *Ac145*/*Ac149*/*Ac150*- deletion and repair constructs (vAc$^{145/149/150null\text{-}AC149\text{-}MYC}$, vAc$^{145/149/150null\text{-}AC149\text{-}MYC+AC150\text{-}HA}$, and vAc$^{145/149/150null\text{-}AC145\text{-}HA+AC149\text{-}MYC+AC150\text{-}HA}$) replicate at the same rate as

the wt. The vAc$^{145/149/150null}$ and vAc$^{145/149/150null\text{-}AC145\text{-}HA+AC149\text{-}MYC}$ constructs replicate slower than the wt. The *Ac145* and *Ac150* single knockout and repair constructs also produce BV at a similar rate to the wt construct, whereas the *Ac145*/*Ac149*/*Ac150* triple deletion constructs show more variability in the rate of BV production.

qPCR provides an absolute measurement of the number of viral genomes or $TCID_{50}$ U produced. All constructs produce between 10^5 to 10^6 viral genome copies and 10^9 to 10^{10} $TCID_{50}$ U / mL. The number of $TCID_{50}$ U estimated with this method is higher than is usually obtained from infection experiments, either *in vitro* or *in vivo*. Almost certainly, non-infectious virus particles are produced during the course of an infection and qPCR is not able to distinguish between infectious and non-infectious particles. A $TCID_{50}$ assay using the same 6 hpi and 96 hpi BV samples as used in the qPCR experiment was performed to determine if equivalent biological titres were obtained for each virus construct.

All constructs produced biological titres between 10^2 and 10^4 $TCID_{50}$ U / mL at 6 hpi when measured using a $TCID_{50}$ end-point dilution assay. At 6 hpi, vAc$^{145/149/150null}$ produced fewer infectious particles than the wt vAcBac 887 construct based on non-overlapping 95% confidence intervals. However, vAc$^{145/149/150null}$ produced the same number of infectious particles as vAc$^{145null\text{-}MC164\text{-}HA}$ and vAc$^{145/149/150null\text{-}AC149\text{-}MYC}$, which produced as many infectious particles as the wt construct, suggesting that there is no difference in the number of infectious particles produced by these constructs at 6 hpi. As BV is not expected to be produced by 6 hpi, these values likely represent BV originally bound to the cell membranes at the beginning of the infection but which did not enter the cell. At 96 hpi, all of the virus constructs produced biological titres of between 10^7 and 10^9 $TCID_{50}$ U / mL. These values are as much as an order of magnitude lower than the values obtained using qPCR, and support the hypothesis that non-infectious particles are produced during the infection and are detected using qPCR.

At 96 hpi, vAc$^{145null\text{-}MC164\text{-}HA}$, vAc$^{149/150null\text{-}MC118\text{-}HA+AC149\text{-}MYC}$, vAc$^{145/149/150null}$, vAc$^{145/149/150null\text{-}AC149\text{-}MYC}$, and vAc$^{145/149/150null\text{-}AC145\text{-}HA+AC149\text{-}MYC}$ produced fewer infectious particles than the wt construct. Each of these constructs produced similar numbers of infectious particles based on overlapping 95% confidence intervals, and produced the same number of infectious particles as Ac^{145null}, vAc$^{149/150null\text{-}AC149\text{-}MYC+AC150\text{-}HA}$, and vAc$^{149/150null\text{-}AC149\text{-}MYC}$, which were not significantly different from the wt construct.

Although the *Ac145*/*Ac149*/*Ac150*-deletion constructs replicate and produce BV at a slower rate than the wt, there is no clear pattern of rate reduction based on the presence or absence of a particular gene(s). From this data, it is difficult to determine which combination of these three genes is responsible for the change in BV production and/or viral DNA replication. It remains to be seen if the variations in DNA replication and BV production affect infectivity *in vivo*. The ability of each of the virus constructs to infect a susceptible host via the oral route and via intrahaemocelic injection will be assessed in Chapter 7 of this thesis.

6.6. Summary and conclusions

Knockout and repair constructs were produced for *Ac145*, *Ac150*, and *Ac145* and *Ac150* using an established bacmid system. The genetic backbone of the constructs was confirmed by PCR analysis of the knockout and repair regions. RT-PCR was employed to ensure that transcription of the GOI was interrupted in the knockout constructs and restored in the repair constructs. Several non-target transcripts were also monitored to ensure that their transcription had not been altered by any of the genetic manipulations made to the constructs. Together, these results suggest that the knockout and repair constructs produced in this study were generated correctly.

qPCR was used to monitor the rate of viral DNA replication, which was found to be consistent among the constructs. qPCR was also used to monitor the rate of BV production for each construct. The rate of BV production was more varied than the rate of viral DNA replication among the *Ac145*/*Ac149*/*Ac150* constructs, and a follow-up $TCID_{50}$ assay also indicated variation in number of infectious particles produced by these constructs. The variation in rate of DNA replication and BV production cannot be explained due to the presence or absence of any one particular gene or genes.

Chapter 7 of this thesis aims to assess the ability of each of the virus construct described above to infect a susceptible host, and to determine if the variations in the rate of BV production and/or viral DNA replication affect levels of infectivity *in vivo*.

7. ORAL AND INJECTION BIOASSAYS

7.1. Introduction

7.1.1. Review of the baculovirus infection cycle and the predicted role of the 11K gene products

The baculovirus infection cycle is biphasic with two types of virions, BV and ODV (35, 36). The BV and ODV are genetically identical, but phenotypically distinct and serve different roles in the infection cycle (35, 36). The ODV are released from viral OB and are responsible for initiating infection within the insect midgut (35, 36). The BV are released from infected cells and are responsible for sustaining a systemic infection within the host (35, 36).

OB are ingested by a susceptible host and dissolve and release the ODV in the alkaline midgut lumen (35, 36). Virus entry into the midgut cells is challenged by the presence of the PM, a chitin and protein meshwork that lines the midgut and protects the epithelial cells from abrasion and pathogens (35, 36). In some instances, the ODV are able to transit the PM and the ODV envelope fuses with the brush border of the columnar epithelial cells of the midgut (35, 36). The nucleocapsids are released into the epithelial cells and an infection occurs (35, 36).

The mechanism by which the ODV pass through the PM is unknown, but it has been suggested (86, 87) that the 11K genes, which encode proteins with a peritrophin A CBD, may be involved in facilitating an interaction between the baculovirus ODV envelope and the chitin of the PM or the chitin-secreting cells of the midgut epithelium. Therefore, it was expected that the 11K gene products may play a key role in initial oral infectivity of a host by a baculovirus.

7.2. Hypothesis

If the 11K gene products from AcMNPV, Ac145 and Ac150, facilitate an interaction between the ODV envelope and the chitin fibrils in the PM or chitin-secreting cells of the midgut, it is predicted that deleting one or both of the corresponding genes from the virus would reduce the ability of the virus construct to initiate infection in the midgut. It is predicted that the *Ac145*, *Ac150*, and *Ac145* and *Ac150* double-knockout constructs will have lower oral infectivity *in vivo* compared to the wt virus. Neither Ac145 nor Ac150 are predicted to play a role in systemic infection in the larval host, so it is predicted that each of the knockout constructs will be as infectious as the wt virus when BV is injected directly into the haemocoel.

7.3. Materials and methods

7.3.1. Rearing *Trichoplusia ni* larvae

T.ni larvae from two sources were used for the bioassays. Two batches of *T. ni* eggs were received from the Insect Production Services (IPS) lab at Natural Resources Canada in Sault Ste. Marie, Ontario. The eggs were incubated at 26.5^{o}C with a 14 h light: 10 h dark photoperiod for 5 d until all of the eggs had hatched and the larvae had moulted from the 1st to the 2nd instar. The larvae were transferred to cups with artificial diet (12.8% w/v pinto beans, 1.2% w/v agar, 1.01% w/v Wesson's salt mixture, 1.6% w/v alfalfa meal, 3.73% w/v brewer's yeast, 3.2% w/v wheat germ, 0.13% w/v linseed oil, 0.4% w/v corn oil, 0.32% w/v Tween 80, 0.11% w/v Nystatin, 0.03% w/v alpha-tocopherol, 0.08% w/v sorbic acid, 1.6% w/v ascorbic acid, 0.05% w/v Tet, 0.05% w/v Chl) and kept for an additional 2 d under the same temperature and photoperiod regimen.

A second population of *T.ni* larvae was obtained from the *T. ni* colony at AAFC Saskatoon Research Centre, Saskatoon, Saskatchewan. The eggs were surface sterilized in 0.06% Javex bleach for 3 min then in 1.45% (w/v) thiosulfate for 1 min. The eggs were rinsed in sterile distilled water and allowed to dry. The eggs were transferred to 6 oz. Lily cups with artificial diet and were incubated at 26.5^{o}C with a light: dark ratio of 14 h: 10 h until the larvae had emerged. The larvae were maintained on artificial diet following the same temperature and photoperiod regimen as described above. Larvae from IPS and AAFC were sorted based on their developmental stage and 4th instar larvae, approximately 1 d post-molt, were used for the oral and injection bioassay experiments.

7.3.2. Production and confirmation of OB stocks for oral bioassays

P1 BV stocks for each of the knockout and repair constructs as well as the wt construct, vAcBac 887, were titred by $TCID_{50}$ (see Section 6.3.2.). Each BV sample was diluted to 20 $TCID_{50}$ U /µL in 250 µL final volume of GIM.

Fourth instar *T. ni* larvae from the AAFC population were chilled on ice for 10 min to reduce their activity. A Micro4 MicroSyringe pump controller and micro-applicator (World Precision Instruments) with a 100 µL glass syringe (Hamilton Company) and 29 gauge needle (Hamilton Company) was used to dispense 5 µL of BV (100 $TCID_{50}$ U per larva) at a rate of 1 µL per s. Twelve larvae were injected per virus construct. The larvae were injected through the body wall

on the ventral surface, near the base of one of the prolegs. The needle was inserted into the insect until the tip was approximately one body segment past the insertion point. The larvae were held on the needle for approximately 5 s following the injection to ensure that the BV entered the haemocoel. The larvae were transferred to 12-well Costar plates (Corning Life Sciences) and kept on artificial diet at 25^{o}C. Any deaths within 3 d of the injection were assumed to have been caused by the injection and these cadavers were discarded. The remainder of the cadavers for each construct were pooled and homogenized in sterile distilled water using a small plastic pestle.

OB were harvested from the cadaver homogenate by filtering through four layers of cheesecloth and centrifugation at 4000 rpm for 15 min in a Megafuge 1.0R (Heraeus Instruments) to pellet the virus OB and cellular debris. The supernatant was discarded and the OB pellets re-suspended in purification buffer (0.12% w/v Tris, 0.04% w/v Na_2EDTA, 0.1% v/v Triton X-100) using 1 mL of buffer per homogenized cadaver. The suspension was incubated at 30^{o}C for 2 h with gentle shaking. The suspension was filtered through four layers of cheesecloth and centrifuged at 4000 rpm for 15 min to pellet the virus OB and any remaining cellular debris. The supernatant was discarded. The pellet was re-suspended in 15 mL of sterile distilled water and then centrifuged at 4000 rpm for 15 min. This wash step was repeated three times. The OB were then re-suspended in 1 mL of sterile distilled water for each homogenized cadaver. Dilutions of 1/1000 were prepared for each OB stock and were counted using a haemocytometer (Neubauer Improved DIN, Depth 0.100 mm, 0.0025 mm^2) and a Zeiss Standard 25 microscope at 10 X optical and 10 X objective powers.

The authenticity of each viral construct OB stock was confirmed by PCR prior to using the OB in oral bioassays. To extract DNA from the OB stocks, 50 μL of OB were dissolved by adding 1 μL of 1 M Na_2CO_3 and incubating at 37^{o}C for 15 min. The samples were checked microscopically to ensure that the majority of the OB had dissolved and ODV released. Five microlitres of 10% SDS were added to each sample and the reaction incubated at 37^{o}C for 30 min. The ODV DNA was extracted once using an equal volume of phenol:chloroform:isoamyl alcohol (25:24:1) and then once with an equal volume of chloroform:isoamyl alcohol (24:1) following the procedure in Section 4.3.2. The DNA was precipitated overnight at -20^{o}C in two volumes of 95% ethanol. Following the overnight precipitation, the DNA was pelleted by centrifugation at 14,000 rpm for 20 min at RT in a bench top microcentrifuge. The supernatant

was discarded and the DNA pellet allowed to dry for 5 min at RT. The pellet was re-suspended in 25 µL of 10 mM Tris, pH 7.5. One microlitre of this DNA preparation was used in a PCR reaction to confirm the presence of the antibiotic resistance genes at the knockout locus (or loci) and the repair construct at the *Polh* locus. The primer pairs, reaction mixes, and thermo profiles used for the confirmation PCR were as described in Section 6.3.2.

7.3.3. Oral bioassay

A dilution series constituting 5 OB/µL, 25 OB/µL and 125 OB/µL were prepared in sterile distilled water containing 0.05% Triton X-100 for each of the knockout and repair constructs. Twenty four-well NuTrend trays (Corrigan & Co., Jacksonville, FL) were set up with 1 mL per well of 1% laboratory grade agar (Fisher Scientific) prepared in sterile distilled water. The agar was allowed to set at RT for approximately 1 h. Canola (cv. AC Excel) leaf discs were prepared using a #1 cork borer. A single leaf disc was placed in each of the wells of the 24-well plates. Two microlitres of an OB preparation were pipetted onto each leaf disk, giving final OB doses of 10, 50, or 250 OB per leaf disk. The discs were allowed to dry overnight at 4^{o}C.

One larva per well was added to the NuTrend plates. A piece of polyester Mylar film was heat sealed to the plates using a hot iron. Small holes were punched into the Mylar film above each well to allow moisture to escape. The larvae were allowed to eat for 4 h at RT and all larvae that had completely consumed the leaf disk were transferred to 12-well Costar plates containing artificial diet. The larvae were kept at 25^{o}C and checked daily for mortality. Two replicates of the oral bioassay were performed with insects from the IPS population using 12 larvae per dose per construct.

7.3.4. Injection bioassay

P2 BV stocks of each knockout and repair construct were produced in TnHi5 cells and titred by end-point-dilution assay as described in Section 6.3.2. Each BV stock was diluted to 3 $TCID_{50}$ U/µL in GIM with 0.3% blue food colouring (McCormick Canada Inc, London, Ontario, Canada). Five microlitres of this diluted BV stock were injected into 4th instar *T. ni* larvae from the IPS population following the injection protocol described in Section 7.3.2., resulting in a final dose of 15 $TCID_{50}$ U per larva. Twenty-four larvae were injected per construct and the

experiment was performed in duplicate. The larvae were transferred to 12-well Costar plates containing artificial diet and kept at 25^{o}C. The larvae were monitored daily for mortality.

7.4. Results

7.4.1. Single dose injection bioassays (15 $TCID_{50}$ U/larva)

Percent mortality data (Table 12) from the injection bioassay were arcsine-transformed using Microsoft Excel (Microsoft Corporation) to normalize the data. This process removes the limitations imposed on percentage data, namely that the data points must be between 0% and 100%, and it allows the data points to vary around the mean. One-way analysis of variance (ANOVA) was performed using Microsoft Excel to determine if there was any significant difference in mortality when BV from each of the constructs was injected directly into the haemocoel of a susceptible host insect. The control sample was omitted from this analysis. An alpha level of 0.05 was used for all statistical tests.

Table 12. Percent mortality for each construct at a dose of 15 $TCID_{50}$ units per larva. All experiments were performed using 4th instar *T.ni* larvae (1 d post-molt). The sample size (n) is listed in brackets beside the percent mortality. Two replicate infection experiments (Rep 1 and Rep 2) were performed using two different cohorts of insects from the IPS population.

	Percent Mortality (n)	
Construct	**Rep 1**	**Rep 2**
Control	0.00 (23)	0.00 (17)
$vAc^{145null}$	91.3 (23)	95.0 (20)
$vAc^{145null\text{-}AC145\text{-}HA}$	100 (23)	100 (22)
$vAc^{145null\text{-}MC164\text{-}HA}$	86.7 (15)	85.0 (20)
$vAc^{149/150null}$	95.2 (21)	85.0 (20)
$vAc^{149/150null\text{-}AC149\text{-}MYC+AC150\text{-}HA}$	81.8 (22)	91.3 (23)
$vAc^{149/150null\text{-}AC149\text{-}MYC}$	95.5 (22)	100 (18)
$vAc^{149/150null\text{-}MC118\text{-}HA+AC149\text{-}MYC}$	95.2 (21)	91.3 (23)
$vAc^{145/149/150null}$	100 (19)	88.9 (18)
$vAc^{145/149/150null\text{-}AC149\text{-}MYC}$	82.6 (23)	100 (22)
$vAc^{145/149/150null\text{-}AC145\text{-}HA+AC149\text{-}MYC}$	100 (20)	100 (20)
$vAc^{145/149/150null\text{-}AC149\text{-}MYC+AC150\text{-}HA}$	86.4 (22)	81.0 (21)
$vAc^{145/149/150null\text{-}AC145\text{-}HA+AC149\text{-}MYC+AC150\text{-}HA}$	100 (20)	72.7 (22)
vAcBac 887	91.3 (23)	95.2 (21)

The results of the one-way ANOVA indicated that there was no statistical difference between mortality rates for insects injected with budded virus from the different virus constructs ($F_{(12, 13)} = 1.00$, $p = 0.496$).

7.4.2. Multiple dose oral bioassay (10, 50, 250 OB per larva)

Percent mortality for each construct at doses of 10, 50, and 250 OB are shown in Table 13. Data from two replicates from two different cohorts of insects from the IPS population were used to determine if there were any differences in oral infectivity between the virus constructs or at the various doses.

The statistical analysis program SAS (SAS Institute Inc.) was used to analyze the oral bioassay data. Percent mortality data were arcsine-transformed using SAS to normalize the data. The data was analyzed using a general linear model (PROC GLM) in SAS. Three constructs, $vAc^{149/150null\text{-}AC149\text{-}MYC+AC150\text{-}HA}$, $vAc^{149/150null\text{-}AC149\text{-}MYC}$, and $vAc^{149/150null\text{-}MC118\text{-}HA+AC149\text{-}MYC}$, were omitted from the analysis as these constructs gave 100% mortality at all three doses tested. A two-way ANOVA, with mortality as the dependent variable, indicated that construct ($F_{(9,59)} = 6.52$, $p = 0.0007$), dose ($F_{(2,59)} = 6.52$, $p = <0.0001$), and the construct-dose interaction, construct X dose ($F_{(18,59)} = 6.52$, $p = 0.0383$), each had a statistically significant effect on mortality. There was no statistically significant differences between the two replicates ($F_{(1,59)} = 6.52$, $p = 0.6626$). An analysis of covariance (ANCOVA) using dose as the covariate, was performed to evaluate if mortality levels were equivalent between constructs at a given dose. Construct ($F_{(9,59)} = 3.27$, $p = 0.0050$) and dose ($F_{(1,59)} = 3.27$, <0.0001) both had a statistically significantly effect on mortality, while the interaction between dose and construct ($F_{(9,59)} = 3.27$, $p = 0.3501$) was not significant. These results indicate that the linear relationship between dose and mortality is equivalent between the constructs (i.e., the lines are parallel). This suggests that the degree of increase in mortality observed with increasing dose is consistent between the constructs.

Table 13. Percent mortality for each construct at doses of 10, 50, and 250 OB per larva. All experiments were conducted using 4th instar *T.ni* larvae (1 d post-molt). The sample size (n) for all experiments is 10 – 12 larvae. Two replicate infection experiments (Rep 1 and Rep 2) were performed using two different cohorts of insects from the IPS population.

Construct	Dose (OB / larva)	Rep 1	Rep 2
Control	---	0.00	0.00
vAc^{145null}	10	50.0	41.7
	50	100	100
	250	100	100
vAc$^{145null\text{-}AC145\text{-}HA}$	10	16.7	80.0
	50	83.3	100
	250	100	100
vAc$^{145null\text{-}MC164\text{-}HA}$	10	66.7	66.7
	50	50.0	83.3
	250	100	91.7
vAc$^{149/150null}$	10	63.6	83.3
	50	100	91.7
	250	100	100
vAc$^{149/150null\text{-}AC149\text{-}MYC+AC150\text{-}HA}$	10	100	100
	50	100	100
	250	100	100
vAc$^{149/150null\text{-}AC149\text{-}MYC}$	10	100	75.0
	50	100	100
	250	100	100
vAc$^{149/150null\text{-}MC118\text{-}HA+AC149\text{-}MYC}$	10	100	91.7
	50	100	100
	250	100	100
vAc$^{145/149/150null}$	10	8.33	8.33
	50	81.8	33.3
	250	100	91.7
vAc$^{145/149/150null\text{-}AC149\text{-}MYC}$	10	60.0	63.6
	50	100	83.3
	250	100	100
vAc$^{145/149/150null\text{-}AC145\text{-}HA+AC149\text{-}MYC}$	10	41.7	33.3
	50	83.3	75.0
	250	100	100
vAc$^{145/149/150null\text{-}AC149\text{-}MYC+AC150\text{-}HA}$	10	50.0	41.7
	50	83.3	58.3
	250	100	100
vAc$^{145/149/150null\text{-}AC145\text{-}HA+AC149\text{-}MYC+AC150\text{-}HA}$	10	58.3	41.7
	50	100	91.7
	250	100	100
vAcBac 887	10	91.7	66.7
	50	100	91.7
	250	100	100

The results from the ANCOVA suggest that the relationship between dose and mortality is equivalent between the constructs, but that dose and construct still significantly affect mortality. A one-way ANOVA was performed using the arcsine-transformed mortality data (excluding $vAc^{149/150null\text{-}AC149\text{-}MYC+AC150\text{-}HA}$, $vAc^{149/150null\text{-}AC149\text{-}MYC}$, and $vAc^{149/150null\text{-}MC118\text{-}HA+AC149\text{-}MYC}$) at the 10 OB / larva dose. At this dose, the effect of construct on mortality ($F_{(12,25)} = 5.11$, $p = 0.0029$) was significant, suggesting that one or more of the constructs produced mortality levels different from that of the wt. A test of least significant differences (LSD) and a Tukey's Studentized Range Test were performed using this data set to determine which constructs produced significantly different mortality rates at this dose. The mean of the arcsine-transformed mortality data for $vAc^{145/149/150null}$ was significantly different from the other constructs with the LSD test, suggesting that this construct is less infectious than the wt; however, this finding was not supported by the Tukey's Studentized Range Test, which found that all constructs were equally as infectious (Table 14). One-way ANOVA using the 50 OB/larva dose revealed that at that dose, the effect of construct on mortality is no longer significant ($F_{(12,25)} = 1.95$, $p = 0.1160$), suggesting that all constructs were as infectious as the wt at that dose.

Table 14. LSD and Tukey's mean groups for the knockout and repair constructs at a dose of 10 OB/larva.
Means were calculated using the arcsine-transformed mortality data from the two oral bioassay bioreplicates. Constructs with the same mean group letter (A-E) or symbol (# or *) are not significantly different from one another (i.e., these constructs are equally as infectious in 4th instar *T.ni* larvae).

Construct	Mean	Mean Groups (LSD)				Mean Groups (Tukey's)	
vAc$^{149/150null-AC149-MYC+AC150-HA}$	0.10017	A				#	
vAc$^{149/150null-MC118-HA+AC149-MYC}$	0.09803	A				#	
vAc$^{149/150null-AC149-MYC}$	0.09344	A	B			#	
vAcBac 887	0.08882	A	B	C		#	
vAc$^{149/150null}$	0.08564	A	B	C	D	#	
vAc$^{145null-MC164-HA}$	0.08174	A	B	C	D	#	
vAc$^{145/149/150null-AC149-MYC}$	0.07870	A	B	C	D	#	
vAc$^{145/149/150null-AC145-HA+AC149-MYC+AC150-HA}$	0.07052		B	C	D	#	*
vAc$^{145/149/150null-AC149-MYC+AC150-HA}$	0.06768			C	D	#	*
vAc^{145null}	0.06768			C	D	#	*
vAc$^{145null-AC145-HA}$	0.06520			C	D	#	*
vAc$^{145/149/150null-AC145-HA+AC149-MYC}$	0.06118				D	#	*
vAc$^{145/149/150null}$	0.02887				E		*

7.5. Discussion

One-way ANOVA was performed to determine if there was a difference in mortality between the knockout, repair, and the wt constructs when they were injected directly into the haemocoel. The control construct was omitted from this analysis, as it produced 0% mortality across all replicates, as expected. The ANOVA indicated that there was no significant difference ($F_{(12,13)}$ = 1.00, p=0.496) in mortality rates between the constructs. This agrees with the hypothesis that Ac145 and Ac150 may be involved in oral infectivity by facilitating an interaction between the envelope of the baculovirus ODV and the chitin of the PM or chitin-secreting cells of the midgut epithelium, and are not likely to be involved in cell-to-cell spread of the virus. This also agrees with the findings of Lapointe et al. (87) and Zhang et al. (86) who found that there was no difference in mortality rates of their knockout and repair constructs compared to the wt construct when injected directly into the haemocoel. This finding is supported by the results provided in Chapter 6 of this thesis that indicate that deletion of *Ac145*, *Ac150*, or both together had a

minimal effect on the rate of BV production or viral DNA replication (Figures 27 and 28), both of which could affect the ability of the virus to propagate in the host.

The oral bioassays were performed using two independent cohorts of insects from the IPS population. Mortality data from the oral bioassays was analyzed using a general linear model in the statistical analysis program, SAS. Two-way ANOVA was performed, with mortality as the dependent variable, to determine if dosage or construct significantly affected mortality. The construct ($F_{(9,59)} = 6.52$, $p = 0.0007$), dose ($F_{(2,59)} = 6.52$, $p = <0.0001$), and the construct-dose interaction, construct X dose ($F_{(18,59)} = 6.52$, $p = 0.0383$), were all found to have significant effects on insect mortality. As the construct X dose interaction was found to have a significant effect on mortality, ANCOVA was performed, using dose as the covariate, to evaluate if mortality levels were equivalent between constructs at a given dose. This test controls for one of the independent variables (dose) and can determine if the linear relationship between mortality and dose is equivalent between constructs (i.e., determine if the lines are parallel). Construct ($F_{(9,59)} = 3.27$, $p = 0.0050$) and dose ($F_{(1,59)} = 3.27$, <0.0001) both had a significant effect on mortality, while the interaction term, dose X construct ($F_{(9,59)} = 3.27$, $p = 0.3501$) did not. These results suggest that the dose administered and the construct used have a significant effect on mortality and that the linear relationship between mortality and dose is equivalent between constructs (i.e., the lines are parallel).

One-way ANOVA was performed using the mortality data from the 10 OB per larva dose. At this dose, the construct used had a significant effect on mortality ($F_{(12,25)} = 5.11$, $p = 0.0029$). Two post-hoc statistical tests, LSD and Tukey's Studentized Range Test, were performed to determine which of the constructs produced mortality levels that were statistically different from the wt construct. The LSD test indicated that the $vAc^{145/149/150null}$ construct was less infectious than the other constructs at a dose of 10 OB per larva, but the Tukey's Studentized Range Test did not support this finding. The LSD test consists of multiple pairwise comparisons between sample means. This test controls for Type 1 (false-positive) comparisonwise errors, but not Type 1 experimentwise errors. The Tukey's Studentized Range Test controls for Type 1 experimentwise errors and is a more robust analysis. It takes into account the total number of comparisons made in the experiment and corrects for this in each of the pairwise comparisons made. This results in fewer Type 1 errors being made on an experiment-wide scale. The results from the Tukey's Studentized Range Test suggest that the statistical difference in mortality for

the vAc$^{145/149/150null}$ construct at a dose of 10 OB per larva is likely a false-positive result, caused by the multiple pairwise comparisons made in the LSD test. Based on these results, it does not appear that any of the constructs produce statistically different mortality rates than the wt construct at a dose of 10 OB per larva. At a dose of 50 OB per larva, a one-way ANOVA indicated that all of the constructs were statistically as infectious as the wt construct ($F_{(12,25)}$ = 1.95, p = 0.1160). An ANOVA was not performed using the 250 OB per larva dose as all constructs produced 100% mortality at this dosage.

As no reduction in infectivity was observed for the *Ac145* or *Ac150*-deletion viruses, it is impossible to determine at this point if the MacoNPV homologues were able to restore the function of the deleted AcMNPV gene. Further work is required to determine if the 11K genes in MacoNPV have overlapping functions with the 11K genes from AcMNPV.

The loss of *Ac149* does not appear to affect the ability of an AcMNPV-like virus to initiate or sustain infection. As *Ac149* is not highly conserved among baculovirus species (115), it is not surprising that virus constructs lacking *Ac149* were as infectious as the wt virus in *T. ni* larvae. The function of *Ac149* in the baculovirus infection cycle remains unclear.

Based on these results, deletion of *Ac145*, *Ac150*, or both together, has no effect on mortality in 4th-instar *T. ni* larvae when the virus construct is administered via the haemocoel or via the oral route. These results differ from the findings of both Lapointe et al. (87) and Zhang et al. (86). The Lapointe group determined that deletion of *Ac145* resulted in a 6-fold decrease in oral infectivity compared to the wt virus in *T. ni* larvae, but not in *H. virescens* larvae (two-way ANOVA, $p < 0.05$). Although there was a significant change in infectivity between the wt virus and the *Ac145*-deletion virus, all other virus constructs (*Ac145*-repaired, *Ac150*-deletion and -repaired, *Ac145/Ac150*-double deletion, and *Ac150*-deletion/*Ac145*-repaired), were as infectious as both the wt virus and as the *Ac145*-deletion virus. This suggests that as an isolated pairwise comparison, the *Ac145*-deletion virus is less infectious than the wt construct; however, when a comparison is made between all deletion and repair viruses, the *Ac145*-deletion virus is as infectious as all other viruses in *T. ni* neonate larvae. The Lapointe group also demonstrated that the *Ac145*/*Ac150*-double deletion virus was 39-fold less infectious than the wt in *H. virescens* larvae, but as infectious as the *Ac145*-deletion virus in *T. ni* larvae. This result is consistent with the findings of this study that suggest that the vAc$^{145/149/150null\text{-}AC149\text{-}MYC}$ construct, which is similar to an *Ac145*/*Ac150*-double deletion virus, is as infectious as the wt in *T. ni* larvae. The

significance of the 39-fold reduction in infectivity in *H. virescens* larvae is not clear, but suggests that Ac145 and Ac150 have overlapping roles in this host (87). Lapointe et al. also found no difference in oral infectivity with the *Ac150*-deletion virus in either *T. ni* or in *H. virescens* larvae, which is consistent with the results of this study.

The Zhang group, who did not produce an *Ac145*-single deletion or *Ac145*/*Ac150*-double deletion virus, determined that their *Ac150*-deletion virus was as infectious as the wt virus when BV was injected into the haemocoel of 4th-instar *Spodoptera exigua*, *H. virescens*, and *T. ni* larvae. An *Ac150*-repaired virus was also produced, but the infectivity of BV from this virus construct was not tested by intrahaemocoelic injection. Oral infectivity was monitored for both the *Ac150*-deletion and –repaired viruses. Purified OB from each virus construct were injected through the mouth, and directly into the larval midgut using a blunt needle. The infectivity of the *Ac150*-repaired virus was monitored at a dose of 10 OB per larva. Zhang et al. found that at this dose, the wt virus produced 48%, 39%, and 57% mortality in *H. virescens*, *T. ni*, and *S. exigua*, respectively, whereas the *Ac150*-repaired virus produced 50%, 47%, and 40% mortality, respectively. Based on this data, they suggest that the *Ac150*-repaired virus produces similar infectivity levels to the wt virus. Zhang et al. used a multi-dose oral assay to determine that the *Ac150*-deletion virus was 4.1-, 5.6-, and 18-fold less infectious than wt virus in 4th-instar *S. exigua*, *H. virescens*, and *T. ni* larvae, respectively. As a follow-up to this experiment, the Zhang group injected purified ODV from the wt or the *Ac150*-deletion virus directly into the midgut of *H. virescens* and *T. ni* larvae. They found that there was no difference in infectivity between the wt and deletion virus ODV. Zhang et al. suggest that Ac150 was lost from the wt ODV or inactivated during purification.

Proteomic analysis of the AcMNPV ODV (80) did not identify either Ac145 or Ac150 as ODV-associated proteins, but Lapointe et al. (87) identified both Ac145 and Ac150 as OB-associated. This difference in localization could explain why Zhang et al. found the *Ac150*-deletion virus was less infectious than the wt when OB were injected into the midgut, but as infectious as wt when purified ODV was injected. Further proteomic analysis is required to determine the localization of these proteins.

Feeding trials in lepidopteran larvae conducted by Zhang et al. (86), indicated that administering a 1% Calcofluor solution along with OB from an *Ac150*-deletion virus does not restore oral infectivity levels to that of wt AcMNPV. As Calcofluor is known to disrupt the

structure of the PM (110), this result, in combination with the chitin-binding studies presented in Chapter 4 of this thesis, suggests that although Ac145, Ac150, Maco118, and Maco164 are all able to interact with chitin they likely do not interact with the chitin in the PM.

Lapointe et al. and Zhang et al. suggest that *Ac145* and *Ac150* play a role in oral infection of a susceptible host by AcMNPV, and likely do so in a host-dependent manner. As the experiments conducted for this thesis only studied infectivity in *T. ni* larvae, it is possible that Ac145 and Ac150 are required for oral infectivity in other hosts, but neither appears to be required for infection to occur in *T. ni*.

7.6. Conclusions and future research

Neither *Ac145* nor *Ac150* are required for the initiation of an infection within the midgut cells of *T. ni* larvae, nor are they required for systemic infection to occur. The loss of *Ac149* in addition to *Ac150* also does not affect infectivity. As no reduction in infectivity was observed for the *Ac145*, *Ac150*, or *Ac145*/*Ac150*-double deletion virus, the function of the MacoNPV homologues cannot be determined at this time.

Further studies to determine the localization patterns of Ac145 and Ac150 are warranted. Discrepancies in infectivity between *Ac150*-deletion virus OB and ODV as determined by Zhang et al. suggests that Ac150 localizes to the OB calyx or other structure that is liberated from the ODV following alkali-treatment. Determining the localization patterns for these proteins within the OB or virions could provide insight into possible functions. In addition, localization studies using fluorescently tagged Ac145 and 150 could also be used to determine which structure these proteins interact with, within a susceptible host, during the infection cycle.

8. SUMMARY AND CONCLUSIONS

The 11K group of genes, which are highly conserved among insect-infecting viruses, produce small proteins, each of which contains a conserved 6 cysteine motif known as a peritrophin A CBD. It has been proposed that the 11K proteins may facilitate an interaction between a virus particle and the chitin fibrils of the PM or the chitin-secreting cells of the midgut epithelium and may therefore be required for infectivity.

The 11K proteins from two baculovirus species, Ac145 and Ac150 from AcMNPV, and Maco118 and Maco164 from MacoNPV, were expressed in a baculovirus expression system. *In vitro* binding studies using chitin beads indicated that all four of these proteins interact with chitin. The binding is mediated by hydrophobic interactions or hydrogen bonding, as some of the bound protein was released by the application of a 2% SDS solution. This is consistent with the binding patterns of a known chitin-binding protein, WGA. However, there appears to be other mechanism(s) involved in the interaction between the 11K proteins and the chitin beads, as the SDS solution does not liberate all of the bound protein.

To determine the function of the 11K genes in the infection cycle, gene knockout constructs were produced using a bacmid system. Deletion of *Ac145* or *Ac150* has no effect on the timing or level of transcription of other genes within the genome, nor does it effect on the rate of BV production or viral DNA replication. Deletion of *Ac145, Ac149,* and *Ac150* together had a minor effect on immediate early gene transcription, the rate of BV production, and the rate of viral DNA replication. These changes could not be attributed to the loss of any one particular gene.

Deletion viruses produced equivalent levels of mortality as the wt virus in *T. ni* larvae when the virus was injected directly into the haemocoel. This agreed with the findings of two independent laboratories that determined that neither of the AcMNPV 11K proteins affects infectivity when injected and agrees with the hypothesis that these proteins are not involved in cell-to-cell transmission. In oral feeding trials, there was no statistical difference between any of the knockout constructs and the wt virus, suggesting that loss of one or both of the 11K genes does not affect initial oral infection of *T. ni* larvae. Based on the results of this study and the accepted definition of a PIF gene, it is suggested that *Ac145* and *Ac150* not be classified as PIF genes. It is evident that they are not essential for, nor do they appear to mediate, the oral infectivity process in a susceptible insect host. Further work is required to determine the exact role of these proteins in the baculovirus infection cycle.

9. REFERENCES

1. Longtin, K. (2006) *An overview of the Canadian agriculture and agri-food system*, Government of Canada, Agriculture and Agri-Food Canada, Ottawa.

2. Salunkhe, D.K., Chavan, J.K., Adsule, R.N., and Kadam, S.S. (1992) *World Oilseeds: Chemistry, Technology, and Utilization*, Van Nostrand Reinhold, New York.

3. Gavloski, J., Carcamo, H., and Dosdall, L. (2011) Insects of canola, mustard, and flax in Canadian grasslands. In: Floate, K.D., ed. *Arthropods of Canadian Grasslands* Biological Survey of Canada, Ottawa.

4. Losey, J.E., and Vaughan, M. (2006) The economic value of ecological services provided by insects. *BioScience* 56, 311-323.

5. Gillott, C. (2005) *Entomology*, 3rd Ed., Springer, Dordrecht.

6. Dag, A. (2011) Crop polination in modern agriculture. In: Seckbach, J., and Dubinsky, Z., eds. *All Flesh Is Grass - Plant-Animal Interrelationships*, Springer, Dordrecht.

7. Pimentel, D. (2009) Pesticides and pest control. In: Peshin, R., and Dhawan, A.K., eds. *Integrated Pest Management: Innovation-Development Process*, Springer, Dordrecht.

8. Gerhardson, B. (2002) Biological substitutes for pesticides. *Trends in Biotechnology* 20, 338-343.

9. Metcalf, R.L. (1989) Insect resistance to insecticides. *Pesticide Science* 26, 333-358.

10. Lewis, W.J., van Lenteren, J.C., Phatak, S.C., and Tumlinson, J.H. (1997) A total system approach to sustainable pest management. *Proceedings of the National Academy of Science* 94, 12243-12248.

11. Luck, R.F., van den Bosch, R., and Garcia, R. (1997) Chemical insect control: a troubled pest management strategy. *BioScience* 27, 606-611.

12. Zehnder, G., Gurr, G.M., Kuhne, S., Wade, M.R., Wratten, S.D., and Wyss, E. (2007) Arthropod pest management in organic crops. *Annual Review of Entomology* 52, 57-80.

13. Kogan, M. (1998) Integrated pest management: historical perspectives and contemporary developments. *Annual Review of Entomology* 43, 243-270.

14. Rodriguez, V.A., Belaich, M.N., and Ghiringhelli, P.D. (2012) Baculoviruses: members of integrated pest management strategies. In: Larramendy, M.L., and Soloneski, S., eds. *Integrated Pest Management and Pest Control - Current and Future Tactics*, InTech - Open Access Company.

15. McEvoy, P.B. (1996) Host specificity and biological pest control. *BioScience* 46, 401-405.

16. Lapointe, R., Thumbi, D., and Lucarotti, C.J. (2012) Recent advances in our knowledge of baculovirus molecular biology and its relevance for the registration of baculovirus-based products for insect pest population control. In: Larramendy, M.L., and Soloneski, S., eds. *Integrated Pest Management and Pest Control - Current and Future Tactics*, InTech - Open Access Company.

17. Bale, J., van Lenteren, J.C., and Bigler, F. (2008) Biological control and sustainable food production. *Philosophical Transactions of the Royal Society B* 363, 761-776.

18. Thiem, S.M. (1997) Prospects for altering host range for baculovirus bioinsecticides. *Current Opinion in Biotechnology* 8, 317-322.

19. Mason, P.G., Arthur, A.P., Olfert, O.O., and Erlandson, M. (1998) The bertha armyworm (*Mamestra configurata*) (Lepidoptera: Noctuidae) in Western Canada. *The Canadian Entomologist* 130, 321-336.

20. Knodel, J., and Ganehiarachchi, M. (2008) Bertha armyworm in canola: biology and integrated pest management. North Dakota State University Extension Service. July 20, 2012, http://www.ag.ndsu.edu/pubs/plantsci/pests/e1347.htm.

21. Hartley, S., and Risula, D. (2008) Bertha armyworm. Government of Saskatchewan. July 20, 2012, http://www.agriculture.gov.sk.ca/Default.aspx?DN=defc273b-db17-48fd-a341-32a7c541fbe0.

22. Li, Q., Donly, C., Li, L., Willis, L.G., Theilmann, D.A., and Erlandson, M. (2002) Sequence and organization of the *Mamestra configurata* Nucleopolyhedrovirus genome. *Virology* 294, 106-121.

23. Erlandson, M. (1990) Biological and biochemical comparison of *Mamestra configurata* and *Mamestra brassicae* Nuclear Polyhedrosis Virus isolates pathogenic for the bertha armyworm, *Mamestra configurata* (Lepidoptera: Noctuidae). *Journal of Invertebrate Pathology* 56, 47-56.

24. Chapman, R.F. (1975) *The Insects: Structure and Function*, American Elsevier Publishing Company, Inc., New York.

25. Klowden, M.J. (2007) *Physiological Systems in Insects*, 2nd Ed., Elsevier, Burlington.

26. Smith, D.S. (1968) *Insect Cells: Their Structure and Function*, Oliver and Boyd, Edinburgh.

27. Lehane, M., and Billingsley, P.F. (1996) *Biology of the Insect Midgut*, Chapman and Hall, London.

28. Loeb, M.J., Clark, E.A., Blackburn, M., Hakim, R.S., Elsen, K., and Smagghe, G. (2003) Stem cells from midguts of lepidopteran larvae: clues to the regulation of stem cell fate. *Archives of Insect Biochemistry and Physiology* 53, 186-198.

29. Moffett, D.F., and Koch, A. (1992) Driving forces and pathways for H^+ and K^+ transport in insect midgut goblet cells. *Journal of Experimental Biology* 172, 403-415.

30. Hegedus, D., Erlandson, M., Gillott, C., and Toprak, U. (2009) New insights into peritrophic matrix synthesis, architecture, and function. *Annual Review of Entomology* 54, 285-302.

31. Lehane, M. (1997) Peritrophic matrix structure and function. *Annual Review of Entomology* 42, 525-550.

32. Terra, W.R. (1990) Evolution of digestive systems in insects. *Annual Review of Entomology* 35, 181-200.

33. Shao, L., Devenport, M., and Jacobs-Lorena, M. (2001) The peritrophic matrix of hematophagous insects. *Archives of Insect Biochemistry and Physiology* 42, 119-125.

34. Toprak, U., Erlandson, M., and Hegedus, D. (2010) Peritrophic matrix proteins. *Trends in Entomology* 6, 23-51.

35. Rohrmann, G.F. (2011) *Baculovirus Molecular Biology*, 2nd Ed., National Center for Biotechnology Information, Bethesda.

36. Bonning, B.C. (2005) Baculoviruses: biology, biochemistry, and molecular biology. In: Gilbert, L., and Iatrou, K., eds. *Comprehensive Molecular Insect Science*, Elsevier, Oxford.

37. Erlandson, M. (2008) Insect pest control by viruses. In: Mahy, B.W.J., and van Regenmortel, M.H.V., eds. *Encyclopedia of Virology*, 3rd Ed., Elsevier, Oxford.

38. Moscardi, F. (1999) Assessment of the application of baculoviruses for control of lepidoptera. *Annual Review of Entomology* 44, 257-289.

39. Federici, B.A. (1993) Viral pathobiology in relation to insect control. In: Beckage, N., Thompson, S., and Federici, B., eds. *Parasites and Pathogens of Insects*, Academic Press, San Diego.

40. Kamita, S., Kang, K., and Hammock, B. (2005) Genetically modified baculoviruses for pest insect control. In: Gilbert, L., and Iatrou, K., eds. *Comprehensive Molecular Insect Science*, Elsevier, Oxford.

41. Theilmann, D.A., Blissard, G.W., Bonning, B.C., Jehle, J.A., O'Reilly, D.R., Thiem, S.M., and Vlack, J. (2005) Family Baculoviridae. In: Fauquet, C.M., Mayo, M.A., Maniloff, J., Desselberger, U., and Ball, L.A., eds. *Virus Taxonomy, VIIIth Report of the International Committee on Virus Taxonomy*, Elsevier, London.

42. Herinou, E.A., Olszewski, J.A., Cory, J.S., and O'Reilly, D. (2003) The genome sequence and evolution of baculoviruses. *Annual Review of Entomology* 48, 211-234.

43. van Oers, M.M., and Vlack, J. (2007) Baculovirus genomics. *Current Drug Targets* 8, 1051-1068.

44. Hayakawa, T., Rohrmann, G.F., and Hashimoto, Y. (2000) Patterns of genome organization and content in lepidopteran baculoviruses. *Virology* 278, 1-12.

45. Possee, R.D., and Rohrmann, G.F. (1997) Baculovirus genome organization and evolution. In: Miller, L.K., ed. *The Baculoviruses*, Plenum Press, New York.

46. Friesen, P.D. (1997) Regulation of baculovirus early gene expression. In: Miller, L.K., ed. *The Baculoviruses*, Plenum Press, New York.

47. Jehle, J.A., Blissard, G.W., Bonning, B.C., Cory, J.S., Herniou, E.A., Rohrmann, G.F., Theilmann, D.A., Thiem, S.M., and Vlak, J.M. (2006) On the classification and nomenclature of baculoviruses: a proposal for revision. *Archives of Virology* 151, 1257-1266.

48. Herinou, E.A., and Jehle, J.A. (2007) Baculovirus phylogeny and evolution. *Current Drug Targets* 8, 1043-1050.

49. Herinou, E.A., Luque, T., Chen, X., Vlak, J.M., Winstanley, D., Cory, J.S., and O'Reilly, D. (2001) Use of whole genome sequence data to infer baculovirus phylogeny. *Journal of Virology* 75, 8117-8126.

50. Monsma, S., A, Oomens, A.G.P., and Blissard, G.W. (1996) The GP64 envelope fusion protein is an essential baculovirus protein required for cell-to-cell transmission of infection. *Journal of Virology* 70, 4607-4616.

51. Ayres, M.D., Howard, S.C., Kuzio, J., Lopez-Ferber, M., and Possee, R.D. (1994) The complete DNA sequence of *Autographa californica* Nuclear Polyhedrosis Virus. *Virology* 202, 585-605.

52. Vail, P., Hostetter, D.L., and Hoffmann, D.F. (1999) Development of the multi-nucleocapsid nucleopolyhedroviruses (MNPVs) infectious to loopers (Lepidoptera: Noctuidae: Plusiinae) as microbial control agents. *Integrated Pest Management Reviews* 4, 231-257.

53. Lacey, L.A., Frutos, R., Kaya, H.K., and Vail, P. (2001) Insect pathogens as biological control agents: do they have a future? *Biological Control* 21, 230-248.

54. Slack, J., and Arif, B.M. (2007) The baculoviruses occlusion-derived virus: virion structure and function. *Advances in Virus Research* 69, 99-165.

55. Funk, C.J., Braunagel, S.C., and Rohrmann, G.F. (1997) Baculovirus structure. In: Miller, L.K., ed. *The Baculoviruses*, Plenum Press, New York.

56. Braunagel, S.C., and Summers, M.D. (2007) Molecular biology of the baculovirus occlusion-derived virus envelope. *Current Drug Targets* 8, 1084-1095.

57. Federici, B. (1997) Baculovirus pathogenesis. In: Miller, L.K., ed. *The Baculoviruses*, Plenum Press, New York.

58. Blissard, G.W., Kogan, P.H., Wei, R., and Rohrmann, G.F. (1992) A synthetic early promoter from a baculovirus: roles of the TATA box and conserved start site CAGT sequence in basal levels of transcription. *Virology* 190, 783-793.

59. Passarelli, A.L., and Guarino, L.A. (2007) Baculovirus late and very late gene regulation. *Current Drug Targets* 8, 1103-1115.

60. Lu, A., and Miller, L.K. (1997) Regulation of baculovirus late and very late gene expression. In: Miller, L.K., ed. *The Baculoviruses*, Plenum Press, New York.

61. Lu, A., and Miller, L.K. (1995) The roles of eighteen baculovirus late expression factor genes in transcription and DNA replication. *Journal of Virology* 69, 975-982.

62. Todd, J.W., Passarelli, A.L., and Miller, L.K. (1995) Eighteen baculovirus genes, including *lef-11*, *p35*, *39K*, and *p47*, support late gene expression. *Journal of Virology* 69, 968-974.

63. Rapp, J.C., Wilson, J.A., and Miller, L.K. (1998) Nineteen baculovirus open reading frames, including LEF-12, support late gene expression. *Journal of Virology* 72, 10197-10206.

64. Vanarsdall, A.L., Mikhailov, V.S., and Rohrmann, G.F. (2007) Baculovirus DNA replication and processing. *Current Drug Targets* 8, 1096-1102.

65. Kool, M., Ahrens, C.H., Vlack, J., and Rohrmann, G.F. (1995) Replication of baculovirus DNA. *Journal of General Virology* 76, 2103-2118.

66. Lu, A., Krell, P.J., Vlak, J.M., and Rohrmann, G.F. (1997) Baculovirus DNA replication. In: Miller, L.K., ed. *The Baculoviruses*, Plenum Press, New York.

67. Ahrens, C.H., Leisy, D.J., and Rohrmann, G.F. (1996) Baculovirus DNA replication. In: Depamphilis, M.L., ed. *DNA Replication in Eukaryotic Cells*, Cold Spring Harbor Laboratory Press, Cold Spring Harbor.

68. Haas-Stapleton, E.J., Washburn, J.O., and Volkman, L.E. (2004) P74 mediates specific binding of *Autographa californica* M nucleopolyhedrovirus occlusion-derived virus to primary cellular targets in the midgut epithelia of *Heliothis virescens* larvae. *Journal of Virology* 78, 6786-6791.

69. Guiterrez, S., Kikhno, I., and Ferber, M.L. (2004) Transcription and promoter analysis of pif, an essential but low-expressed baculovirus gene. *Journal of General Virology* 85, 331-341.

70. Pijlman, G.P., Pruijssers, A.J.P., and Vlack, J. (2003) Identification of pif-2, a third conserved baculovirus gene required for per os infection of insects. *Journal of General Virology* 84, 2041-2049.

71. Fang, M., Nie, Y., Wang, Q., Deng, F., Wang, R., Wang, H., Wang, H., Vlak, J.M., Chen, X., and Hu, Z. (2006) Open reading frame 132 of *Heliocoverpa armigera nucleopolyhedrovirus* encodes a functional *per os* infectivity factor (PIF-2). *Journal of General Virology* 87, 2563-2569.

72. Ohkawa, T., Washburn, J.O., Sitapara, E.S., and Volkman, L.E. (2005) Specific binding of *Autographa californica* M nucleopolyhedrovirus occlusion-derived virus to midgut cells of *Heliothis virescens* larvae is mediated by products of *pif* genes *Ac119* and *Ac022* but not by *Ac115*. *Journal of Virology* 79, 15258-15264.

73. Li, X., Song, J., Jiang, T., Liang, C., and Chen, X. (2007) The N-terminal hydrophobic sequence of *Autographa californica* nucleopolyhedrovirus PIF-3 is essential for oral infection. *Archives of Virology* 152, 1851-1858.

74. Fang, M., Nie, Y., Harris, S., Erlandson, M., and Theilmann, D.A. (2009) *Autographa californica* multiple nucleopolyhedrovirus core gene *ac96* encodes a *per os* infectivity factor (*pif-4*). *Journal of Virology* 83, 12569-12578.

75. Sparks, W.O., Harrison, R.L., and Bonning, B.C. (2011) *Autographa californica* multiple nucleopolyhedrovirus ODV-E56 is a *per os* infectivity factor, but is not essential for binding and fusion of occlusion-derived virus to the host midgut. *Virology* 409, 69-76.

76. Nie, Y., Fang, M., Erlandson, M., and Theilmann, D.A. (2012) Analysis of the *Autographa californica* Multiple Nucleopolyhedrovirus overlapping gene pair *lef3* and *ac68* reveals that AC68 is a *per os* infectivity factor and that LEF3 is critical, but not essential for virus replication. *Journal of Virology* 86, 3985-3994.

77. Song, J., Wang, R., Deng, F., Wang, H., and Hu, Z. (2008) Functional studies of *per os* infectivity factors of *Helicoverpa armigera* single nucleocapsid nucleopolyhedrovirus. *Journal of General Virology* 89, 2331-2338.

78. Peng, K., van Lent, J.W.M., Boeren, S., Fang, M., Theilmann, D.A., Erlandson, M., Vlak, J.M., and Van Oers, M.M. (2012) Characterization of novel components of the baculovirus *per os* infectivity factor complex. *Journal of Virology* 86, 4981-4988.

79. Peng, K., Van Oers, M.M., Hu, Z., Van Lent, J.W.M., and Vlack, J. (2010) Baculovirus *per os* infectivity factors form a complex on the surface of occlusion-derived virus. *Journal of Virology* 84, 9497-9504.

80. Braunagel, S.C., Russell, W.K., Rosas-Acosta, G., Russell, D.H., and Summers, M.D. (2003) Determination of the protein composition of the occlusion-derived virus of *Autographa californica* nucleopolyhedrovirus. *Proceedings of the National Academy of Science* 100, 9797-9802.

81. Deng, F., Wang, R., Fang, M., Jiang, Y., Xu, X., Wang, H., Chen, X., Arif, B.M., Guo, L., Wang, H., and Hu, Z. (2007) Proteomics analysis of *Helicoverpa armigera* single nucleocapsid

nucleopolyhedrovirus identified two new occlusion-derived virus-associated proteins, HA44 and HA100. *Journal of Virology* 81, 9377-9385.

82. Perera, O., Green, T.B., Stevens, S.M., White, S., and Becnel, J.J. (2007) Proteins associated with *Culex nigripalpus* nucleopolyhedrovirus occluded virions. *Journal of Virology* 81, 4585-4590.

83. Lungh, O.Y., Cruz-Alvarez, M., and Blissard, G.W. (2003) Ac23, an envelope fusion protein homolog in the baculovirus *Autographa californica* multicapsid nucleopolyhedrovirus, is a viral pathogenicity factor. *Journal of Virology* 77, 328-339.

84. Peng, K., Wu, M., Deng, F., Song, J., Dong, C., Wang, H., and Hu, Z. (2010) Identification of protein-protein interactions of the occlusion-derived virus-associated proteins of *Helicoverpa armigera* nucleopolyhedrovirus. *Journal of General Virology* 91, 659-670.

85. Dall, D., Luque, T., and O'Reilly, D. (2001) Insect-virus relationships: sifting by informatics. *Bioessays* 23, 184-193.

86. Zhang, J.-H., Ohkawa, T., Washburn, J.O., and Volkman, L.E. (2005) Effects of Ac150 on virulence and pathogenesis of *Autographa californica multiple nucelopolyhedrovirus* in noctuid hosts. *Journal of General Virology* 86, 1619-1627.

87. Lapointe, R., Popham, H.J.R., Straschil, U., Goulding, D., O'Reilly, D.R., and Olszewski, J.A. (2004) Characterization of two *Autographa californica* nucleopolyhedrovirus proteins, Ac145 and Ac150, which affect oral infectivity in a host-dependent manner. *Journal of Virology* 78, 6439-6448.

88. Tellam, R.L., Wijffels, G., and Willadsen, P. (1999) Peritrophic matrix proteins. *Insect Biochemistry and Molecular Biology* 29, 87-101.

89. Ciccarone, V.C., Polayes, D.A., and Luckow, V.A. (1997) Generation of recombinant baculovirus DNA in *E.coli* using a baculovirus shuttle vector. In: Reischl, U., ed. *Methods in Molecular Medicine*, Humana Press Inc, Totowa.

90. Luckow, V.A., Lee, S.C., Barry, G.F., and Olins, P.O. (1993) Efficient generation of infectious recombinant baculoviruses by site-specific transposon-mediated insertion of foreign genes into a baculovirus genome propagated in *Escherichia coli*. *Journal of Virology* 67, 4566-4579.

91. Invitrogen (2009) *Bac-to-Bac Baculovirus Expression System*, Version E, Carlsbad.

92. Shen, Z., and Jacobs-Lorena, M. (1999) Evolution of chitin-binding proteins in invertebrates. *Journal of Molecular Evolution* 48, 341-347.

93. Arnold, K., Bordoli, L., Kopp, J., and Schwede, T. (2006) The SWISS-MODEL workspace: a web-based environment for protein structure homology modelling. *Bioinformatics* 22, 195-201.

94. Kiefer, F., Arnold, K., Kunzli, M., Bordoli, L., and Schwede, T. (2009) The SWISS-MODEL repository and associated resources. *Nucleic Acids Research* 37, D387-D392.

95. Peitsch, M.C. (1995) Protein modeling by e-mail - from amino acid sequence to protein structure: a free one-hour service. *Bio/Technology* 13, 658-660.

96. Sambrook, J., Fritsch, E.F., and Maniatis, T. (1989) *Molecular Cloning: A Laboratory Manual*, 2nd Ed., Cold Spring Harbor Laboratory Press, Plainview.

97. Yi, S.-X., and Gillott, C. (1999) Purification and characterization of an oviposition-stimulating protein of the long hyaline tubules in the male migratory grasshopper, *Melanoplus sanguinipes*. *Journal of Insect Physiology* 45, 143-150.

98. Allen, A.K., Neuberger, A., and Sharon, N. (1973) The purification, composition and specificity of wheat-germ agglutinin. *Journal of Biochemistry* 131, 155-162.

99. Privat, J.-P., Delmotte, F., Mialonier, G., Bouchard, P., and Monsigny, M. (1974) Fluorescence studies of saccharide binding to wheat-germ agglutinin (lectin). *European Journal of Biochemistry* 47, 5-14.

100. Nielsen, H., Brunak, S., and von Heijne, G. (1999) Machine learning approaches for the prediction of signal peptides and other protein sorting signals. *Protein Engineering* 12, 3-9.

101. Emanuelsson, O., and von Heijne, G. (2001) Prediction of organellar targeting signals. *Biochemica et Biophysica Acta* 1541, 114-119.

102. Hao, B., Huang, J., Sun, X., Deng, F., Zhang, Y., Wang, H., Chen, H., and Hu, Z. (2009) Variants of open reading frame *Bm126* in wild-type *Bombyx mori* nucleopolyhedrovirus isolates exhibit functional differences. *Journal of General Virology* 90, 153-161.

103. Kawabata, S.-i., Nagayama, R., Hirata, M., Shigenaga, T., Agarwala, K.L., Saito, T., Cho, J., Nakajima, H., Takagi, T., and Iwanaga, S. (1996) Tachycitin, a small granular component in horseshoe crab hemocytes, is an antimicrobial protein with chitin-binding activity. *Journal of Biochemistry* 120, 1253-1260.

104. Boraston, A.B., Bolam, D.N., Gilbert, H.J., and Davies, G.J. (2004) Carbohydrate-binding modules: fine-tuning polysaccharide recognition. *Journal of Biochemistry* 382, 769-781.

105. Zeltins, A., and Schremph, H. (1997) Specific interaction of the *Streptomyces* chitin-binding protein CHB1 with alpha chitin: the role of individual tryptophan residues. *European Journal of Biochemistry* 246, 557-564.

106. Qin, G., Lapidot, S., Numata, K., Hu, X., Meirovitch, S., Dekel, M., Podoler, I., Shoseyov, O., and Kaplan, D. (2009) Expression, cross-linking, and characterization of recombinant chitin binding resilin. *Biomacromolecules* 10, 3227-3234.

107. Hardt, M., and Laine, R.A. (2004) Mutation of active site residues in the chitin-binding domain $ChBD_{ChiA1}$ from chitinase A1 of *Bacillus circulans* alters substrate specificity: use of a green fluorescent protein binding assay. *Archives of Biochemistry and Biophysics* 426, 286-297.

108. Hashimoto, M., Ikegami, T., Seino, S., Ohuchi, N., Fukada, H., Sugiyama, J., Shirakawa, M., and Watanabe, T. (2000) Expression and characterization of the chitin-binding domain of chitinase A1 from *Bacillus circulans* WL-12. *Journal of Bacteriology* 182, 3045-3054.

109. Wijffels, G., Eisemann, C., Riding, G., Pearson, R., Jones, A., Willadsen, P., and Tellam, R.L. (2001) A novel family of chitin-binding proteins from insect Type 2 peritrophic matrix. *The Journal of Biological Chemistry* 276, 15527-15536.

110. Wang, P., and Granados, R.R. (2000) Calcofluor disrupts the midgut defense system in insects. *Insect Biochemistry and Molecular Biology* 30, 135-143.

111. Baneyx, F. (1999) Recombinant protein expression in *Escherichia coli*. *Current Opinion in Biotechnology* 10, 411-421.

112. Verma, R., Boleti, E., and George, A.J.T. (1998) Antibody engineering: Comparison of bacterial, yeast, insect and mammalian expression systems. *Journal of Immunological Methods* 216, 165-181.

113. Sahdev, S., Khattar, S.K., and Saini, K.S. (2008) Production of active eukaryotic proteins through bacterial expression systems: a review of the existing biotechnology strategies. *Molecular Cell Biochemistry* 307, 249-264.

114. Georgiou, G., and Valax, P. (1996) Expression of correctly folded proteins in *Escherichia coli*. *Current Opinion in Biotechnology* 7, 190-197.

115. Cohen, D.P.A., Marek, M., Davies, B.G., Vlak, J.M., and Van Oers, M.M. (2009) Encyclopedia of *Autographa californica* nucleopolyhedrovirus genes. *Virologica Sinica* 24, 359-414.

116. Jarvis, D.L., and Garcia, A. (1994) Biosynthesis and processing of the *Autographa californica* nuclear polyhedrosis virus gp64 protein. *Virology* 205, 300-313.

117. Garrity, D.B., Chang, M.-J., and Blissard, G.W. (1997) Late promoter selection in the baculovirus *gp64* envelope fusion protein gene. *Virology* 231, 167-181.

118. Theim, S.M., and Miller, L.K. (1989) Identification, sequence, and transcriptional mapping of the major capsid protein gene of the baculovirus *Autographa californica* nuclear polyhedrosis virus. *Journal of Virology* 63, 2008-2018.

119. Hultmark, D., Klemenz, R., and Gehring, W. (1986) Translational and transcriptional control elements in the untranslated leader of the heat-shock gene *hsp22*. *Cell* 44, 429-438.

120. Pirrotta, V., Manet, E., Hardon, E., Bickel, S., and Benson, M. (1987) Structure and sequence of the *Drosophila* '*zeste*' gene. *The European Molecular Biology Organization (EMBO) Journal* 6, 791-799.

121. Hertzog, P.J., and Kola, I. (2001) Overview: gene knockouts. In: Yymms, M.J., and Kola, I., eds. *Gene Knockout Protocols*, Humana Press Inc., Totowa.

122. Dai, X., Stewart, T.M., Pathakamuir, J.A., Li, Q., and Theilmann, D.A. (2004) *Autographa californica* multiple nucleopolyhedrovirus *exon0* (*orf141*), which encodes a RING finger protein, is required for efficient production of budded virus. *Journal of Virology* 78, 9633-9644.

123. Chisholm, G.E., and Henner, D.J. (1988) Multiple early transcripts and splicing of the *Autographa californica* nuclear polyhedrosis virus IE-1 gene. *Journal of Virology* 62, 3193-3200.

124. Braunagel, S.C., He, H., Ramamurthy, P., and Summers, M.D. (1996) Transcription, translation, and cellular localization of three *Autographa californica* Nuclear Polyhedrosis Virus structural proteins: ODV-E18, ODV-E35, and ODV-EC27. *Virology* 222, 100-114.

125. Dickison, V.L. (2010) Deletion and Functional Analysis of AC146 of the Baculovirus *Autographa californica* Nucleopolyhedrovirus (Master's Thesis). Department of Biology, University of British Columbia - Okanagan, Kelowna.

126. Braunagel, S.C., Elton, D.M., Ma, H., and Summers, M.D. (1996) Identification and analysis of an *Autographa californica* Nuclear Polyhedrosis Virus structural protein of the occlusion-derived virus envelope: ODV-E56. *Virology* 217, 97-110.

127. Carson, D.D., Summers, M.D., and Guarino, L.A. (1991) Molecular analysis of a baculovirus regulatory gene. *Virology* 182, 279-286.

128. Datsenko, K.A., and Wanner, B.L. (2000) One-step inactivation of chromosomal genes in *Escherichia coli* K-12 using PCR products. *Proceedings of the National Academy of Science* 97, 6640-6645.

129. Sharma, R.C., and Schimke, R.T. (1996) Preparation of electrocompetent *E.coli* using salt-free growth medium. *Biotechniques* 20, 42-44.

130. Zwart, M.P., Erro, E., Van Oers, M.M., de Visser, J., and Vlak, J.M. (2008) Low multiplicity of infection *in vivo* results in purifying selection against baculovirus deletion mutants. *Journal of General Virology* 89, 1220-1224.

131. Kool, M., Voncken, J., van Lier, F., Tramper, J., and Vlak, J.M. (1991) Detection and analysis of *Autographa californica* nuclear polyhedrosis virus mutants with defective interfering properties. *Virology* 183, 739-746.

132. Pijlman, G.P., van den Born, E., Martens, D.E., and Vlak, J.M. (2001) *Autographa californica* baculoviruses with large genomic deletions are rapidly generated in infected insect cells. *Virology* 283, 132-138.

133. Wickham, T.J., David, T., Granados, R.R., Hammer, D.A., Shuler, M.L., and Wood, H.A. (1991) Baculovirus defective interfering particles are responsible for variations in recombinant protein production as a function of multiplicity of infection. *Biotechnology Letters* 13, 483-488.

10.APPENDICES

A. pKD3 plasmid. For amplification of the chloramphenicol acetyl transferase (CAT) gene (blue arrow). Construct map kindly provided by Dr. David Theilmann, AAFC, Summerland, B.C.

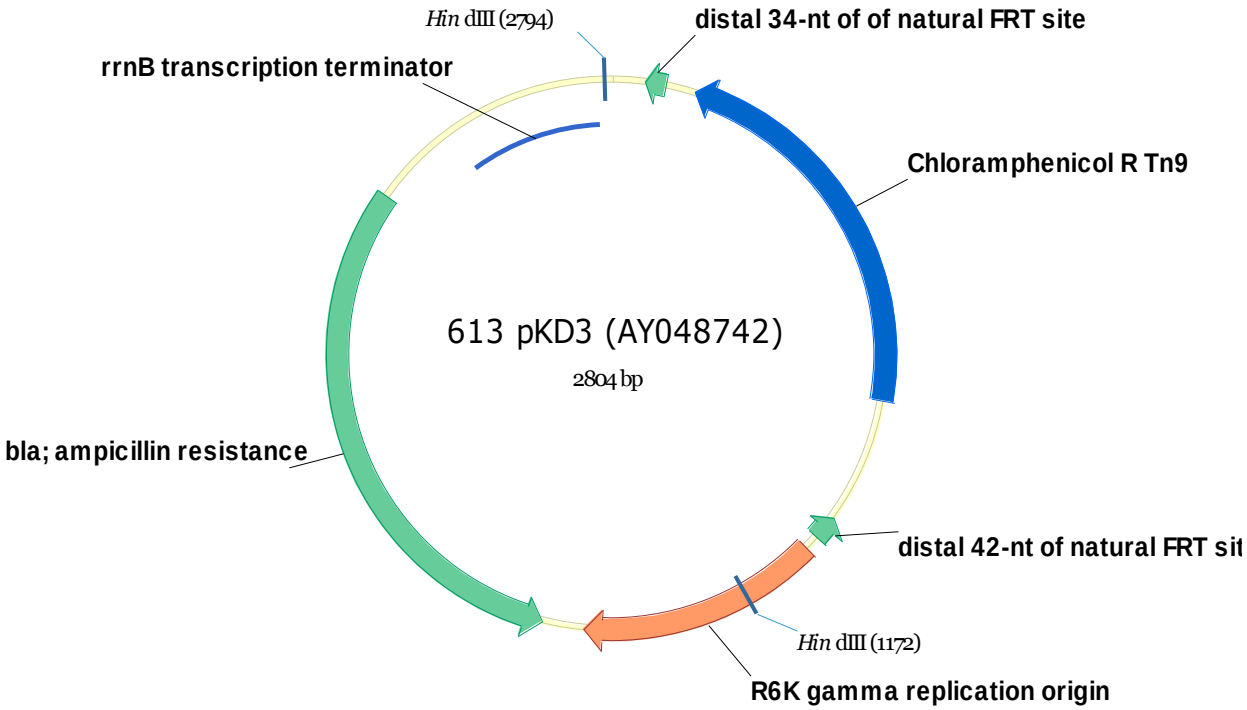

B. p2ZOp-2F plasmid. For amplification of the Zeocin resistance gene (orange arrow). Construct map kindly provided by Dr. David Theilmann, AAFC, Summerland, B.C.